AMRL-TR-67-62

CONFIGURATION INVESTIGATION FOR LITHIUM OXIDE CARBON DIOXIDE CONTROL SYSTEMS

DANIEL A. BORYTA
EUGENE W. DEZMELYK

FOREWORD

This study was initiated by the Biomedical Laboratory of the Aerospace Medical Research Laboratories, Aerospace Medical Division, Wright-Patterson Air Force Base, Ohio. The research was conducted by the Foote Mineral Company, Research and Engineering Center, Exton, Pennsylvania, under Contract No. AF33(615)-3382. Mr. Eugene W. Dezmelyk was the principal investigator for Foote Mineral Company and Mr. Daniel A. Boryta was the project supervisor. Mr. Clemens M. Meyer of the Biotechnology Branch, Life Support Division, was the contract monitor for the Aerospace Medical Research Laboratories. The work was performed in support of project 6373, "Equipment for Life Support in Aerospace," and task 637302, "Respiratory Support Equipment." The research sponsored by this contract was conducted between December 1965 and December 1966.

This technical report has been reviewed and is approved.

WAYNE H. McCANDLESS
Technical Director
Biomedical Laboratory
Aerospace Medical Research Laboratories

ABSTRACT

The bulk density of lithium oxide shapes and granules has been increased substantially while retaining good reactivity. Absorbent forms of the oxide can be prepared in the bulk density range of 0.18 to 0.28 g/cc. For granular oxide, results indicate a reasonable compromise between reactivity and absorbent volume efficiency is about 0.20 g/cc in passive systems and 0.26 to 0.28 g/cc in semipassive or dynamic systems. The improvement results from use of high (about 18 m^2/g) surface area lithium peroxide raw material and techniques in processing the peroxide to oxide. Tests indicate the oxide forms developed can equal (passive exposure) or exceed (semipassive or dynamic exposure) the 0.8 g CO_2/g LiOH capacity of granular lithium hydroxide before 2% breakthrough. Dusting of the granular oxide form was reduced by controlled abrasion and fabric encasement techniques. Tests at one-third and normal atmospheres indicated higher carbon dioxide absorption rates at the lower pressure. A marked improvement was found in oxygen-helium as compared to oxygen and oxygen-nitrogen atmospheres. Atmospheric moisture conditions required for efficient absorption were defined. Exploratory work indicates partial hydration of the oxide is one method for initiating absorption under low humidity conditions. Gravimetric analysis work, which confirmed that density limitations are presently imposed by reaction product-substrate molar volume relations, should provide useful guidelines for absorbent design and further experimentation.

TABLE OF CONTENTS

Section	Page
I. Introduction	1
1. General Considerations	1
2. Lithium Oxide Preparation	4
a. Lithium Peroxide	5
b. Lithium Peroxide Decomposition	5
3. Processes For Lithium Oxide Configurations	7
4. Li_2O and Reaction Product Analysis	10
a. Lithium Oxide	10
b. Reaction Products	10
c. Lithium Peroxide	10
II. Preliminary Screening Tests	13
1. Experimental Approach	13
2. Passive Tests - Gravimetric Analysis	13
a. Supported Bed Forms	17
(1) Granules from Li_2O_2 Powder	17
(2) Granules from Packed Li_2O Tablets	19
(3) Tablets from Li_2O_2 Tablets	23
(4) Granules from Pelletized Li_2O Powder	23
(5) Granules from Li_2O_2 Pellets	26
(6) Granules from Granular LiOH	26
(7) Comparative LiOH Granules	29
b. Self-supported Shapes	29
(1) From Pressed Li_2O Powder	29
(2) Sintered Shapes from Li_2O_2 Powder	32
(3) Sintered Shapes from Granular Li_2O_2	32
c. Gas Velocity Effect	32
d. Reaction Product Composition	35
e. Analysis of Results	35
3. Dynamic Tests	38
a. Apparatus and Procedure	38
b. Test Data	40
c. Analysis of Results	40

Section Page

III. Configuration Tests with Low Moisture Availability 52

1. Apparatus and Procedures 52

2. Exploratory Runs 54

3. Passive Tests 54

4. Dynamic Tests 70
   a. Dynamic Test Unit 70
   b. Tests 70
   c. Analysis of Results 74

IV. Absorber Development and Testing at 1-Atmosphere 77

1. Apparatus 77

2. Granular Li_2O Development 80
   a. Granule Coating 80
   b. Dedusting 81
   c. Fabric Encasement 83

3. Solid Li_2O Configuration Development 87

4. Configuration Testing 90

5. Analysis of Results 110

V. Tests at One-Third Atmosphere 120

1. General Considerations 120

2. Apparatus 120

3. Configuration Tests 122
   a. Dynamic Exposure, Packed Granular Bed 122
   b. Passive Exposure, Granular Belt 123
   c. Semipassive Exposure, Pierced Cylinder 126

4. Analysis of Results 129

VI. Effect of Atmosphere Composition 130

1. General Considerations 130

2. Apparatus 130

3. Experimental Data 131

4. Analysis of Results 131

Section Page

VII. Conclusions 137

1. Lithium Oxide Preparation and Performance 137
2. Effect of Atmosphere Variations 138
3. Configuration Design 139

References 143

LIST OF ILLUSTRATIONS

Figure		Page
1.	Lithium Peroxide Decomposer	6
2.	Gravimetric Analysis Absorption Chamber	14
3.	Gravimetric Curves; Samples 349-9-5, 349-11-2, 349-13-2	16
4.	Gravimetric Curves; Samples 349-16-2, 349-18-2, 349-21-2	16
5.	Gravimetric Curve, Sample 349-23-2	20
6.	Gravimetric Curves; Samples 358-7-1, 349-35-3, 349-42-1C	20
7.	Gravimetric Curves; Samples 349-42-4, 358-2-3, 358-7-3	22
8.	Li_2O_2 Tablets After Decomposition	24
9.	Gravimetric Curves; Samples 349-42-1B, 349-42-3, 358-2-1	22
10.	Gravimetric Curves; Samples 358-11-1, 358-10-1, 358-21-1	28
11.	Gravimetric Curves; Samples 358-24-1, 358-21-1, 358-31-1	28
12.	Gravimetric Curves; Granular LiOH	30
13.	Porous Solid Li_2O Shapes	30
14.	Gravimetric Curves; Samples 349-11-1, 359-13-1, 349-18-1	33
15.	Bulk Density of Li_2O versus Time for Complete Carbonation	37
16.	Dynamic Screening Test Apparatus	39
17.	Bulk Density of Granular Li_2O versus CO_2 Absorption in a Single Pass	43
18.	Log 4- by 10-mesh Bulk Density versus % CO_2 Input Absorbed in a Single Pass	45
19.	Dynamic Test, Effluent Gas Temperature and Relative Humidity, 1% CO_2 and 50% R.H. Input	46

Figure Page

20. Dynamic Test, Effluent Gas Temperature and Relative Humidity, 50% and 88% R.H. Input 51

21. Apparatus For 1-Atmosphere Tests 53

22. Passive Test Profiles, Granule Rectangular Bed (Run 368-39) 56

23. Passive Cylindrical Bed Configuration 60

24. Passive Test Profiles, Granule Cylindrical Bed (Run 368-45) 62

25. Passive Test Profiles, Granule Cylindrical Bed (Run 376-11) 63

26. Passive Test Profiles, Granule Cylindrical Bed (Run 376-13) 65

27. Passive Test Profiles, Granule Cylindrical Bed (Run 376-15) 66

28. Granule Belt Configuration 67

29. Granule Belt Configuration in Test Apparatus 67

30. Passive Test Profiles, Granule Belt (Run 376-16-1) 68

31. Passive Test Profiles, Granule Belt (Run 376-17-1) 69

32. Dynamic Absorption Unit 71

33. Dynamic Absorber in Test Apparatus 72

34. Dynamic Test Profiles (Run 376-19) 73

35. Dynamic Test Profiles (Run 376-38-1) 75

36. Apparatus For 1-Atmosphere Tests 79

37. Dedusting Apparatus 82

38. Microphotograph, Li_2O Granule Before Dedusting 84

39. Microphotograph, Li_2O Granule After Dedusting 85

40. Pierced Cylinder Configuration, Decomposed Li_2O Powder 88

41. Pierced Cylinder Configuration, Decomposed Li_2O_2 Granules 89

Figure | Page

42. Test Profiles (Runs 361-26 and 361-30) 92

43. Apparatus Arrangement, Pierced Cylinder Configuration 93

44. Test Profiles (Run 361-21) 95

45. Apparatus Arrangement, Passive Belt Configuration 97

46. Test Profiles (Run 361-29 and 361-34) 98

47. Test Profiles (Run 361-43) 101

48. Test Profiles (Run 361-46) 102

49. Test Profiles, Passive 8-Hour Mission (Run 397-1) 105

50. Apparatus Arrangement, Dynamic Granular Bed 106

51. Test Profiles (Runs 361-48 and 390-6) 108

52. Semipassive Configuration 111

53. Granular Li_2O Bed For Semipassive Configuration 112

54. Apparatus Arrangement, Semipassive Test 114

55. Test Profiles, Semipassive 8-Hour Mission (Run 397-3) 116

56. Apparatus Arrangement, One-third Atmosphere Tests 121

57. Test Profiles, Passive 8-Hour Mission at One-Third Atmosphere (Run 390-46) 125

58. Cross-section of Pierced Cylinder Configuration 127

59. Test Profiles, Semipassive 8-Hour Mission at One-Third Atmosphere (Run 397-19) 128

60. Gravimetric Curves For O_2, O_2-N_2, and O_2-He Atmospheres at 50% Relative Humidity 133

61. Gravimetric Curves For O_2 and O_2-N_2 Atmospheres at 25, 50, and 75% Relative Humidity 134

62. Gravimetric Curves for Partially Hydrated Li_2O 135

LIST OF TABLES

Table		Page
I	Maximum Reactant Densities	4
II	Process For Supported Bed Li_2O Forms	8
III	Processes For Self-supported Li_2O Forms	9
IV	Gravimetric Test Data, Process 2a-(2)	18
V	Gravimetric Test Data, Process 2a-(1)	21
VI	Gravimetric Test Data, Process 2a-(3)	25
VII	Gravimetric Test Data, Process 2a-(4) and 2a-(5)	27
VIII	Gravimetric Test Data, Porous Solid Li_2O	31
IX	Gravimetric Tests, Gas Velocity Effect	34
X	Gravimetric Tests, Reaction Product Analyses	36
XI	Dynamic Test Data at 50% R.H. Input	41
XII	Reaction Product Molar Ratios	48
XIII	Dynamic Test Results	49
XIV	Passive Test Data, Granule Rectangular Bed	55
XV	Test Data At 1 Atmosphere	57
XVI	Chamber Gas Velocities With Fan Operating	78
XVII	Chamber CO_2 Concentration With Zero Absorption	80
XVIII	Dedusting of 4- by 10-Mesh, Granular Li_2O	83
XIX	Dusting Tests With Fabric Encasement	86
XX	Test Data, Runs 361-26 and 361-30	91
XXI	Test Data, Run 361-21	96
XXII	Test Data, Runs 361-29 and 361-24	99
XXIII	Test Data, Runs 361-43 and 361-46	103
XXIV	Test Data, Passive 8-Hour Mission, Run 397-1	104
XXV	Test Data, Runs 361-48 and 390-6	109

Table		Page
XXVI	Configuration Dimensions and Gas Velocities, Run 397-3	113
XXVII	Test Data, Semipassive 8-Hour Mission, Run 397-3	115
XXVIII	Comparison of Passive Belt and Dynamic Bed	118
XXIX	Test Data, Runs 390-46 and 397-19	124
XXX	Absorption Tests in Various Atmospheres	132

SECTION I

INTRODUCTION

1. GENERAL CONSIDERATIONS

Previous comparisons of the carbon dioxide absorption capacity of nonregenerable chemical absorbents have indicated that lithium oxide is theoretically unsurpassed (references 1, 2,12). CO_2 absorption with high (0.32 g/cc) and low (0.10 g/cc) bulk density forms of Li_2O has been demonstrated with nearly complete utilization of the oxide's capacity. One obstacle in the practical application of Li_2O has been the low CO_2 absorption rate of high density forms of the oxide. A principal aim of this investigation was to establish the optimum bulk density and configuration for absorbing 45 g CO_2/hr while maintaining CO_2 concentration below 7.6 mm Hg partial pressure in an atmosphere at 50% relative humidity and 18 to 29°C temperature.

From a weight and volume efficiency standpoint (weight of CO_2 removed per unit weight and volume of Li_2O), the ideal form of Li_2O would be a single solid shape at its true density. However, there are two requirements for reasonable absorption rate and utilization which preclude use of this form. The gas must: (1) contact large absorbent surface areas for reasonable rate, and (2) have access to fresh absorbent for continued reaction. To meet these requirements, three types of void spaces can be visualized:

a. Channel voids or passages of regular geometric form.

Typical examples are free space between slabs or holes through blocks of absorbent.

b. Bulk voids or passages of irregular geometric form. The voids occurring in powdered or granular beds of absorbent illustrate this type.

c. Pore voids or passages of irregular form in the discrete particles of absorbent.

Providing gas-solid contact by any of the above techniques necessarily increases the gross volume occupied by the absorbent, with a corresponding decrease in volume efficiency. Thus, an important step in developing Li_2O absorbent configurations is evaluating void types, or combinations of them, which maximize volume efficiency. The selection of the macroscopic void types, bulk and channel voids, also involves consideration of gas pressure loss in flow-through systems. The characteristics of channel voids (such as gas-flow area, exposed absorbent area, and total void volume) can be readily controlled by fabricating to suitable dimensions, but channel voids have the inherent limitation of low exposed absorbent surface area. The characteristics of bulk voids can be controlled by altering particle size and packing, and larger surface areas can be provided than with channel voids. Pore voids are the only means for providing truly large absorbent surface areas. Their production and control is more difficult than providing macroscopic void types, since pore voids are governed by Li_2O preparation techniques.

The theoretical maximum bulk density of the absorbent, consistent with CO_2 absorption, can be approximately predicted from molar volume relations (reference 4). If the molar volume of the reaction product is greater than the equivalent molar volume of the reactive substrate, the reaction product can completely coat the substrate. If this coating is not disrupted during density changes, it is nonporous and shields the substrate from further reaction. Therefore, the reaction product to substrate molar volume ratio is a measure of the coating effect on the reaction, with ratios exceeding unity indicating the presence of potentially protective coatings. Molar volume ratios related to lithium oxide and intermediates in the CO_2 absorption process are given below. These indicate Li_2CO_3 is marginally protective on a LiOH substrate and nonprotective on $LiOH \cdot H_2O$. Also significant is the indication that LiOH and $LiOH \cdot H_2O$ can be quite protective on a Li_2O substrate. Since both forms of the hydroxide are necessary intermediates in the carbonation of Li_2O, it is essential to minimize their protective effect by void and density adjustment techniques.

Substrate Compound	True Density g/cc	Molar Volume cc/g Mol	Molar Volume Ratio		
			Li_2CO_3 Coat.	LiOH Coat.	$LiOH \cdot H_2O$ Coat.
Li_2O	2.01	14.87	2.355	2.253	3.737
LiOH	1.43	16.75	1.045	---	1.659
LiOH H_2O	1.51	27.79	0.635	---	---

NOTE: Li_2CO_3 specific gravity 2.11; molar volume 35.02

The volume ratio concept can be extended to predicting density limitations and is therefore useful in guiding experimental work. For example, the molar volume ratio of a granule of Li_2O, at its true density of 2.01 g/cc, reacting with water to yield

$LiOH \cdot H_2O$ is 3.74. The ratio, and protective effect of the $LiOH \cdot H_2O$, can be reduced by decreasing the Li_2O density. Thus, a porous granule of Li_2O at 0.53 g/cc apparent density yields a calculated ratio of unity. Since this ratio is borderline between a protective and nonprotective $LiOH \cdot H_2O$ coating, an upper limit has been defined for the apparent density of a Li_2O granule under the stated conditions. Table I gives apparent density limits for porous reactants yielding various nonporous products at a molar volume ratio of unity. For given granule sizes, the apparent density of the single granules can be translated to the bulk densities of beds of such granules. Thus, table I predicts for the stated reactions the maximum density attainable for configurations containing only pore voids and configurations based on 4- by 10-mesh granules containing both pore and bulk voids.

TABLE I

MAXIMUM REACTANT DENSITIES

Porous Reactant	Nonporous Product	Reactant Density- g/cc Single Granule	 4- by 10-Mesh Bulk Bed
Li_2O	$LiOH \cdot H_2O$	0.537	0.32
Li_2O	$LiOH$	0.912	0.54
Li_2O	Li_2CO_3	0.853	0.51
$LiOH$	$LiOH \cdot H_2O$	0.861	0.51

2. LITHIUM OXIDE PREPARATION

Lithium oxide can be prepared via two procedures, the dehydration of LiOH and the decomposition of Li_2O_2. In the former process, granular LiOH is dehydrated at high temperature and under vacuum. For CO_2 absorption applications, slow dehydration and careful temperature control are required to obtain the oxide in a porous and reactive form. The product is typically hard, white, 4- by 14-mesh granules with a bulk density of 0.35 g/cc and surface area of 0.94 m^2/g. The low surface area is a prime disadvantage of this process. For comparison purposes in the reported work a few experimental runs were made using LiOH based oxide. The major effort was concentrated on Li_2O_2 based oxide with preparation as outlined below.

a. Lithium Peroxide

The Li_2O_2 used for experimental work was obtained from Foote Mineral Company production facility. The Li_2O_2 was obtained in the form of a white powder with 0.28 g/cc bulk density. Typical analysis was 97.9% Li_2O_2 with 0.7% LiOH and 1.1% Li_2CO_3. Surface area ranged from 16.2 to 19.7 m^2/g.

b. Lithium Peroxide Decomposition

The atmospheric pressure decomposition apparatus (see figure 1) consisted of a glass beaker housed within an aluminum vessel, the assembly being set in a muffle furnace. Since the Li_2O product density is critical and varies with decomposition temperature, several precautions were taken to insure uniform and reproducible temperatures within the decomposer. The beaker containing the Li_2O_2 was supported to avoid glass to metal contact and resulting hot spots, and temperatures on the aluminum vessel and within the beaker were correlated. The aluminum vessel was continuously flushed with dry heated nitrogen

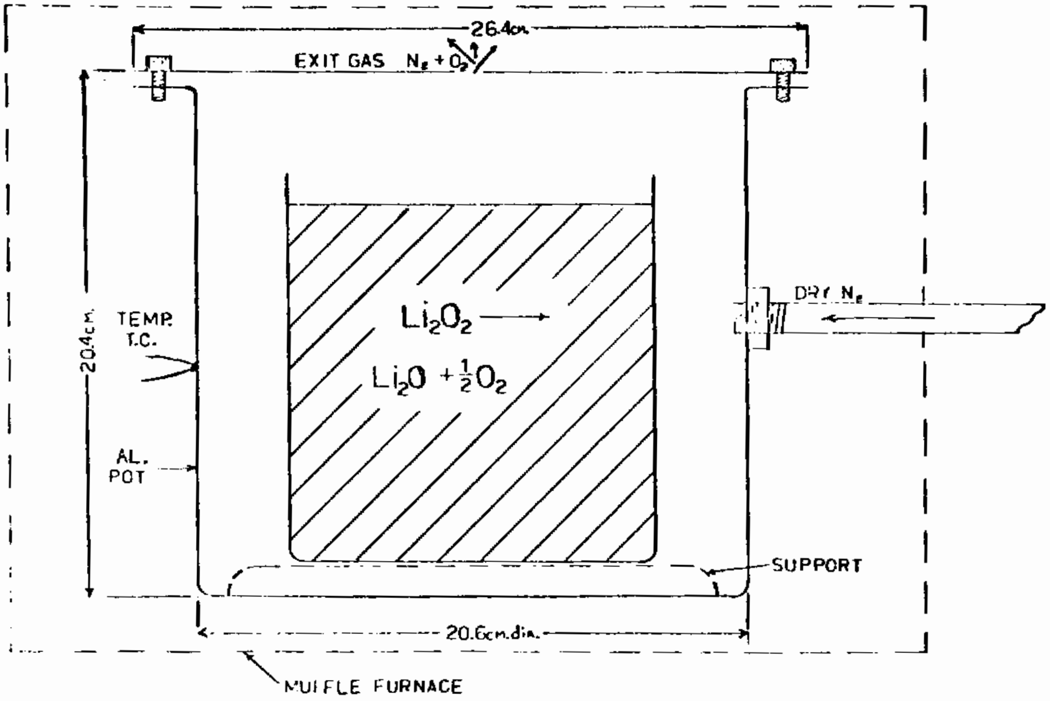

Fig. 1. Lithium Peroxide Decomposer

during operation. Peroxide decompositions under vacuum were conducted in a metal autoclave, and temperature uniformity did not equal that of the atmospheric pressure decomposer. Li_2O that was prepared by this method did not indicate any advantage in vacuum decomposition, therefore, no effort was spent in refining this apparatus.

3. PROCESSES FOR LITHIUM OXIDE CONFIGURATIONS

Two general methods can be used for presenting Li_2O surfaces to a carbon dioxide-containing atmosphere. In the first method, the oxide is displayed in the form of supported beds composed of relatively loosely packed particles or granules. The advantages of this technique are the possibility of fabricating configurations of virtually any shape, and the ability to alter oxide density (bulk and particulate) over a wide range. Potential penalties of the supported bed approach are weight of the support media and relatively high overall volume. The second method involves fabricating the oxide into self-supporting shapes, with required mechanical strength developed through interlocking or sintering of the oxide particles or granules. The potential advantages are weight and volume reduction. A major drawback is reduced ability to alter oxide density, since density and mechanical strength become interrelated in self-supported shapes. In the reported work, supported and self-supported configurations were prepared by a number of processes. Steps in the various processes are summarized in tables II and III. More detailed descriptions, process observations, and

TABLE II

PROCESSES FOR SUPPORTED BED Li_2O FORMS

			Decomposition		Post-Decomposition Processing				
Process No.	Raw Matl	Treatment	Li_2O_2 Feed Form	Li_2O Product Form					Final Product
2a-(1)	Li_2O_2 Powder	None	Powder	Sintered Cake	---	---	Crushed	Sieved	Li_2O Granules
2a-(2)	Li_2O_2	Tabletted	Packed Tablets	Sintered Cake	---	---	Crushed	Sieved	Li_2O Granules
2a-(3)	Li_2O_2	Tabletted	Loose Tablets	Loose Tablets	---	---	---	---	Li_2O Tablets
2a-(4)	Li_2O_2 Powder	None	Powder	Sintered Cake	Pulverized	Pelletized	Crushed	Sieved	Li_2O Granules
2a-(5)	Li_2O_2 Powder	Pelletized	Pellets	Sintered Pellets	---	---	Crushed	Sieved	Li_2O Granules
2a-(6)	LiOH Granules	None	LiOH Granules	Li_2O Granules	---	---	---	---	Li_2O Granules
2a-(7)	LiOH Granules	None	---	---	---	---	---	---	LiOH Granules

Note: Process details and test results are given in section II, under paragraphs corresponding to process numbers.

TABLE III

PROCESSES FOR SELF-SUPPORTED Li_2O FORMS

Process No.	Raw Matl	Treatment	Li_2O_2 Feed Form	Li_2O Product Form	Post-Decomposition Processing			Final Product
2b-(1)	Li_2O_2 Powder	None	Powder	Sintered Cake	Pulverized	Pelletized		Li_2O Cylinders
2b-(2)	Li_2O_2 Powder	None	Powder	Sintered Cake	---	---	Carved to Shape	Li_2O Cylinders
2b-(3)	Li_2O_2 Powder	Pelletized & Crushed	Granules	Sintered Cake				Li_2O Cylinders

Note: Process details and test results are given in section II, under paragraphs corresponding to process numbers.

the corresponding results in CO_2 absorption screening tests are reported in section II.

4. Li_2O AND REACTION PRODUCT ANALYSIS

All chemical analyses were conducted at the Foote Mineral Company, under the following procedures:

a. Lithium Oxide

Samples were prepared in a dry box and titrated with 1 normal HCl to the modified methyl orange endpoint for total alkalinity. This includes Li_2O, LiOH, Li_2CO_3 and Li_2O_2. Another portion of the sample was then titrated with 1 normal HCl after addition of neutral 15-percent $BaCl_2$ to the cresol red endpoint for total hydroxide which included Li_2O, LiOH and Li_2O_2 but excluded Li_2CO_3. For Li_2O_2 content, Li_2O_2 samples were acidified with 1:1 H_2SO_4 and titrated immediately with 0.1 normal $KMnO_4$ to a pink endpoint. The final results are obtained with appropriate calculations and corrections programmed for a computer.

b. Reaction Products

Samples were prepared with minimum atmospheric exposure. A Knorr Alkalimeter (reference 13) was used to selectively analyze for Li_2CO_3. Another portion was then titrated for total alkalinity with 1 normal HCl to the modified methyl orange endpoint which includes Li_2CO_3, Li_2O, LiOH and $LiOH \cdot H_2O$. Water was determined by difference.

c. Lithium Peroxide

Lithium peroxide samples were dissolved in 1:1 H_2SO_4

solution and titrated immediately with 0.1 normal $KMnO_4$ to a permanent pink endpoint.

SECTION II

PRELIMINARY SCREENING TESTS

1. EXPERIMENTAL APPROACH

Two preliminary CO_2 absorption screening tests were used to expedite selection of the most promising forms of Li_2O for further evaluation. The first was basically a passive test, with small Li_2O samples being continuously weighed while exposed to a controlled atmosphere. The second was a dynamic test with gas flowing through sample beds. The tests yielded data on the effect of Li_2O surface area, bulk density, and shape as related to reactivity and absorption rate.

2. PASSIVE TESTS - GRAVIMETRIC ANALYSIS

Passive tests were made using the recording balance of a thermogravimetric analysis apparatus (reference 6) to continuously weigh a sample of Li_2O suspended in a gas-filled tube. The absorption section of the apparatus is shown in figure 2. Oxygen containing 1% (vol) CO_2, before humidifying to 50% relative humidity at 22 C, was passed through the tube. Gas velocity, based on the cross-sectional area of the tube, was 81 cm/min at 500 cc/min gas flow rate. Under these conditions (0.54 g CO_2 feed/hr) the minimum time required to completely carbonate 1 g of pure Li_2O would be 2.7 hours, assuming 100% CO_2 removal from the feed stream.

Reaction mechanisms can be ascribed to various sections of the gravimetric analysis curves (cumulative weight gain versus time) derived in these tests. Initial CO_2 absorption, reaction

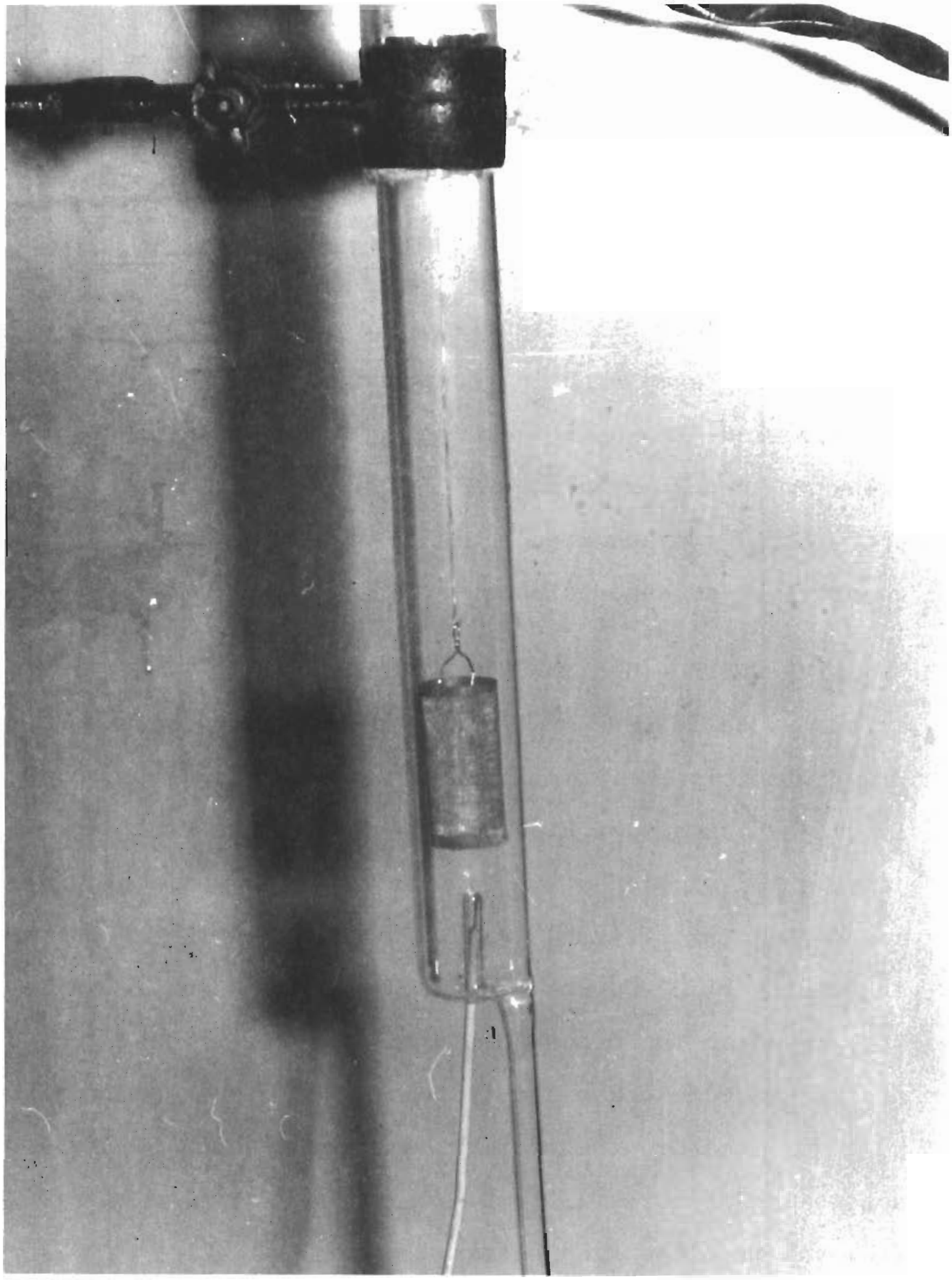

Fig. 2. Gravimetric Analysis Absorption Chamber

Tube: 2.8 cm inside diameter

Sample suspension basket: 400-mesh, stainless steel, screen cloth; 43.5% open area; 1.9 cm diameter by 4.2 cm deep.

(1) below, results from reactions (2), (3), and (4):

$2Li_2O + CO_2 + H_2O \rightarrow Li_2CO_3 + 2LiOH$ (1).*

$Li_2O + H_2O \rightarrow 2LiOH$ (2).

$2LiOH + CO_2 \rightarrow Li_2CO_3 + H_2O$ (absorbed) (3).

$Li_2O + H_2O$ (absorbed) $\rightarrow 2LiOH$ (4).

The rate of reaction (2) governs reaction (3). Therefore, a molar ratio of H_2O/CO_2 exceeding unity should be provided to maximize the rate of reaction (3). The theoretical weight gain resulting from reaction (1) is 1.038 g/g Li_2O and the heat of reaction and free energy change per mole Li_2O are:

ΔH^{25} -43.39 kcal

ΔF^{25} -29.28 kcal

Subsequent reactions in the CO_2 absorption process are given below. A weight loss occurs in reaction (7) because the weight of water evolved exceeds the weight of CO_2 absorbed.

$2LiOH + CO_2 \rightarrow Li_2CO_3 + H_2O$ (absorbed) (3)

$2LiOH + CO_2 \rightarrow Li_2CO_3 + H_2O$ (gas) (5)

$LiOH + H_2O$ (gas or absorbed) $\rightarrow LiOH \cdot H_2O$ (6)

$2LiOH \cdot H_2O + CO_2 \rightarrow Li_2CO_3 + 3H_2O$ (7)

The foregoing reaction mechanisms are illustrated by gravimetric curves developed for samples 349-11-2 and 349-13-2 (figure 3) and sample 349-16-2 (figure 4). In each case, constant rate weight gain occurs up to about 1.1 g gain/g Li_2O followed by a decreasing rate and then a weight loss as the secondary reactions proceed.

---

*Such numbers refer to reactions throughout this report.

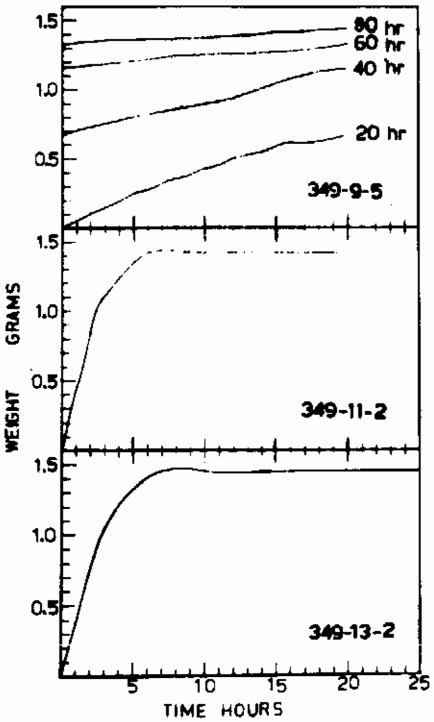

Fig. 3. Gravimetric Curves

Samples 349-9-5, 349-11-2, 349-13-2

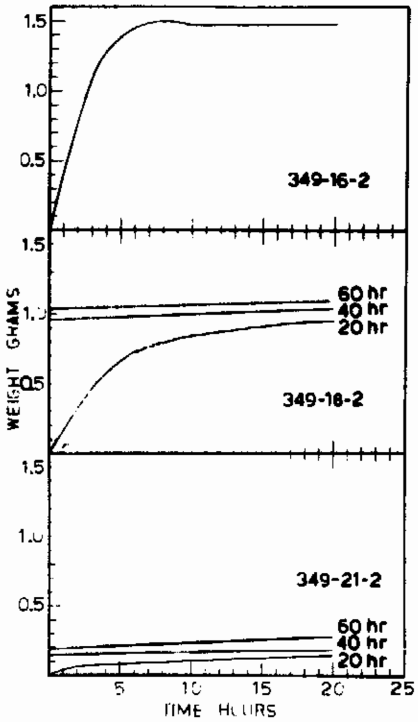

Fig. 4. Gravimetric Curves

Samples 349-16-2, 349-18-2, 349-21-2

Li_2O was prepared by a variety of processes in forms applicable to supported beds and self-supported shapes. Gravimetric CO_2 absorption tests were then run on the various forms. The processes and observations on them, and information developed in absorption screening tests are outlined as follows:

a. Supported Bed Forms

(1) Granules From Li_2O_2 Powder

High surface area (16.2 to 19.7 m^2/g) Li_2O_2 powder was thermally decomposed at atmospheric pressure and various temperatures. The material sintered during decomposition, and the resulting cake was crushed and sieved to 4- by 10-mesh Li_2O granules. Generally, increasing decomposition temperature raised bulk density and hardness but reduced surface area (see table IV). Samples which were decomposed below 325 C swelled and compressed against the vessel walls before sintering (suggesting a possible technique for preparing self-supporting shapes as subsequently reported). Decreasing conversion to Li_2CO_3 with increasing bulk density is evident in the results in table IV. The approximate times for reactions

$$2Li_2O + CO_2 + H_2O \rightarrow Li_2CO_3 + 2LiOH \qquad (1)$$

and $$2LiOH + CO_2 \rightarrow Li_2CO_3 + H_2O \qquad (3)$$

are indicated by inflection points in the gravimetric curves of figure 3 (samples 349-11-2 and 349-13-2) and figure 4 (sample 349-16-2). The curves also illustrate the rate reduction occurring at bulk densities of about 0.34 g/cc as typified by samples 349-9-5 and 349-18-2. These samples contained Li_2O, LiOH, and $LiOH \cdot H_2O$ in their reaction products as indicated by x-ray

TABLE IV

GRAVIMETRIC TEST DATA, PROCESS 2a-(1)

1 Gram 4- by 10-Mesh Granular Li_2O exposed to Oxygen Gas, 1% (Vol) CO_2, 50% R.H.

Preparation: Li_2O_2 Powder decomposed, Sintered Cake crushed and sieved

Sample No. 349-	Decomp. Temp. C	Bulk Density g/cc	Surf. Area m^2/g	Hard-ness No.	Reaction Times		Constant Wt. hr	Exposure Time hr	Product Li_2CO_3 %
					(b) hr	(c) hr			
11-2	285	0.100	14.70	66.3	2.5	5.5	8	20	99.9
13-2	325	0.124	13.35	59.3	3.0	7.0	10	25	97.7
16-2	325	0.123	13.80	54.6	2.8	6.3	10	20	97.6
18-2	350	0.341	3.85	93.1	---	---	(d)	190	85.1
21-2	385	0.573	0.28	98.2	---	---	(d)	64	22.9
23-2	430	0.630	----	92.6	---	---	(d)	95	26.6
9-5(a)	644	0.341	0.94	89.2	---	---	(d)	80	90.0

Notes: (a) Sample 349-9-5 prepared from LiOH at variable decomposition temperature, 644 C being maximum

(b) For reaction $2Li_2O + CO_2 + H_2O \rightarrow Li_2CO_3 + 2LiOH$

(c) For reaction $2LiOH + CO_2 \rightarrow Li_2CO_3 + H_2O$

(d) Constant weight not attained during total exposure diffraction analysis. This thermodynamically unstable condition (references 7,8) can only be explained by kinetic factors such as the formation of a nonporous coating of $LiOH \cdot H_2O$ on the LiOH and Li_2O. The remaining samples with even higher bulk density were virtually unreactive as illustrated by the gravimetric curve of figure 5 (sample 349-23-2).

(2) Granules From Packed Li_2O_2 Tablets

Li_2O_2 powder was pressed into small tablets, each 6.35 mm diameter by 3.3 mm thick, weighing 0.08 g, and compressed to 31% of true Li_2O_2 density. Loosely packed tablets, in 100 g quantities, were decomposed at various temperatures to explore the preparation of Li_2O tablets and void-containing shapes. The decompositions were run in the low temperature range as suggested by earlier results with the Li_2O_2 powder. In all cases, the entire mass swelled, compressed itself into a cake containing few bulk voids, and then became sintered. The mass shrunk away from the vessel walls during sintering, the amount of shrinkage varying with decomposition temperature. The cakes were crushed and sieved to 4- by 10-mesh Li_2O granules. Granule characteristics and absorption test results are given in table V. Bulk density increased with decomposition temperature while surface area remained relatively constant over the temperature range studied. All samples exhibited relatively high conversion is evident as bulk density increases. The gravimetric curves of figures 7 and 9 illustrate the declining trend in reaction rate with density increase. This particular preparation technique was a more complex route to granular Li_2O than decomposing

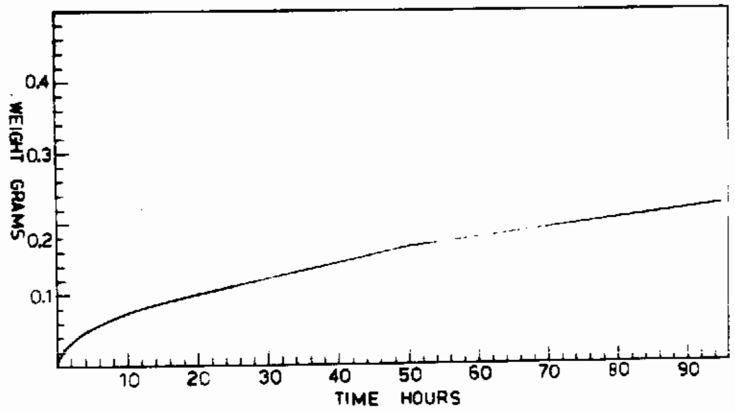

Fig. 5. Gravimetric Curve
Sample 349-23-2

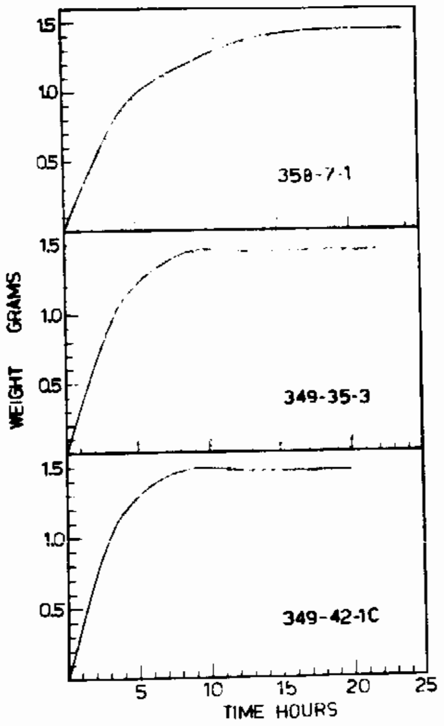

Fig. 6. Gravimetric Curves
Samples 358-7-1, 349-35-3, 349-42-1C

TABLE V

GRAVIMETRIC TEST DATA, PROCESS 2a-(2)

1 Gram 4- by 10-Mesh Granular Li_2O exposed to Oxygen Gas, 1% (Vol) CO_2, 50% R.H.

Preparation: Loosely packed Li_2O_2 Tablets decomposed, sintered, crushed, and sieved

Sample No.	Decomp. Temp. C	Bulk Density g/cc(a)	Surf. Area m^2/g	Reaction Times (b) hr	Reaction Times (c) hr	Constant Wt. hr	Exposure Time hr	Product Li_2CO_3 %
349-35-3	250	0.139	12.6	3.8	8.2	12	22	96.5
349-42-1C	275	0.134	12.8	3.2	10.8	14	20	97.9
349-42-4	300	0.145	13.8	3.6	14.4	18	22	97.2
358-2-3	318	0.186	13.3	5.0	17.0	22	22	96.6
358-7-3	325	0.231	12.7	5.0	15.0	20	22	95.0

Notes: (a) Bulk densities are approximate, being based on 1 g samples.

(b) For reaction $2Li_2O + CO_2 + H_2O \rightarrow Li_2CO_3 + 2LiOH$

(c) For reaction $2LiOH + CO_2 \rightarrow Li_2CO_3 + H_2O$

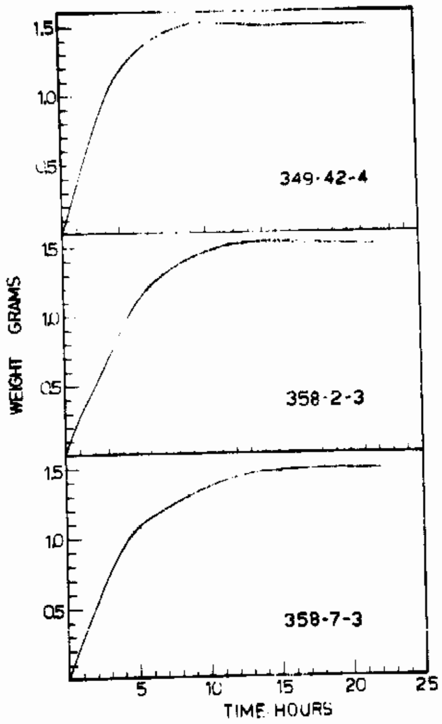

Fig. 7. Gravimetric Curves
Samples 349-42-4, 358-2-3, 358-7-3

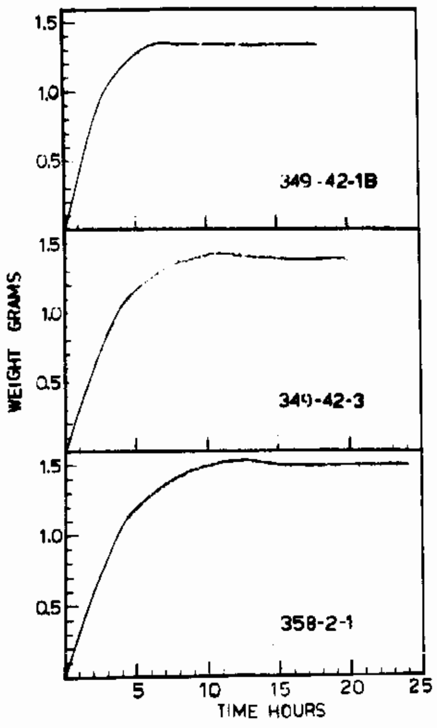

Fig. 9. Gravimetric Curves
Samples 349-42-1B, 349-42-3, 358-2-1

larger pellets and offered no apparent compensating advantage in granule performance.

(3) Tablets From Li_2O_2 Tablets

A few loose Li_2O tablets which had decomposed without sintering to the mass were obtained from the foregoing experiments. Figure 8 shows an original Li_2O_2 tablet and the resulting Li_2O tablets produced at various decomposition temperatures. The tablet sizes illustrate the swelling which occurs during decomposition and the subsequent increasing shrinkage as decomposition temperature exceeds about 275 C. As shown in table VI which gives tablet characteristics and test data, the density of individual Li_2O tablets increased with decomposition temperature. The bulk density of loosely packed tablets increased similarly. Gravimetric curves are shown in figure 6 (sample 358-7-1) and figure 9 (samples 349-42-1B, 349-42-3, 358-2-1). The results parallel earlier experience with reactivity declining as tablet density increases.

(4) Granules From Pelletized Li_2O Powder

A 270 g charge of Li_2O_2 powder, bulk density 0.28 g/cc was decomposed at 265 C under atmospheric pressure. On charging, the powder occupied a volume 10.4 cm in diameter by 11.8 cm deep. The sintered Li_2O cake following decomposition was 9.5 cm diameter by 13.5 cm deep, weighed 180 g, and had a bulk density of 0.188 g/cc. The Li_2O cake was pulverized and the powder was pressed into pellets 6.2 cm in diameter with a pellet density of 0.5 g/cc. The pellets were then crushed and sieved, yielding about 90 g of 4- by 10-mesh Li_2O granules.

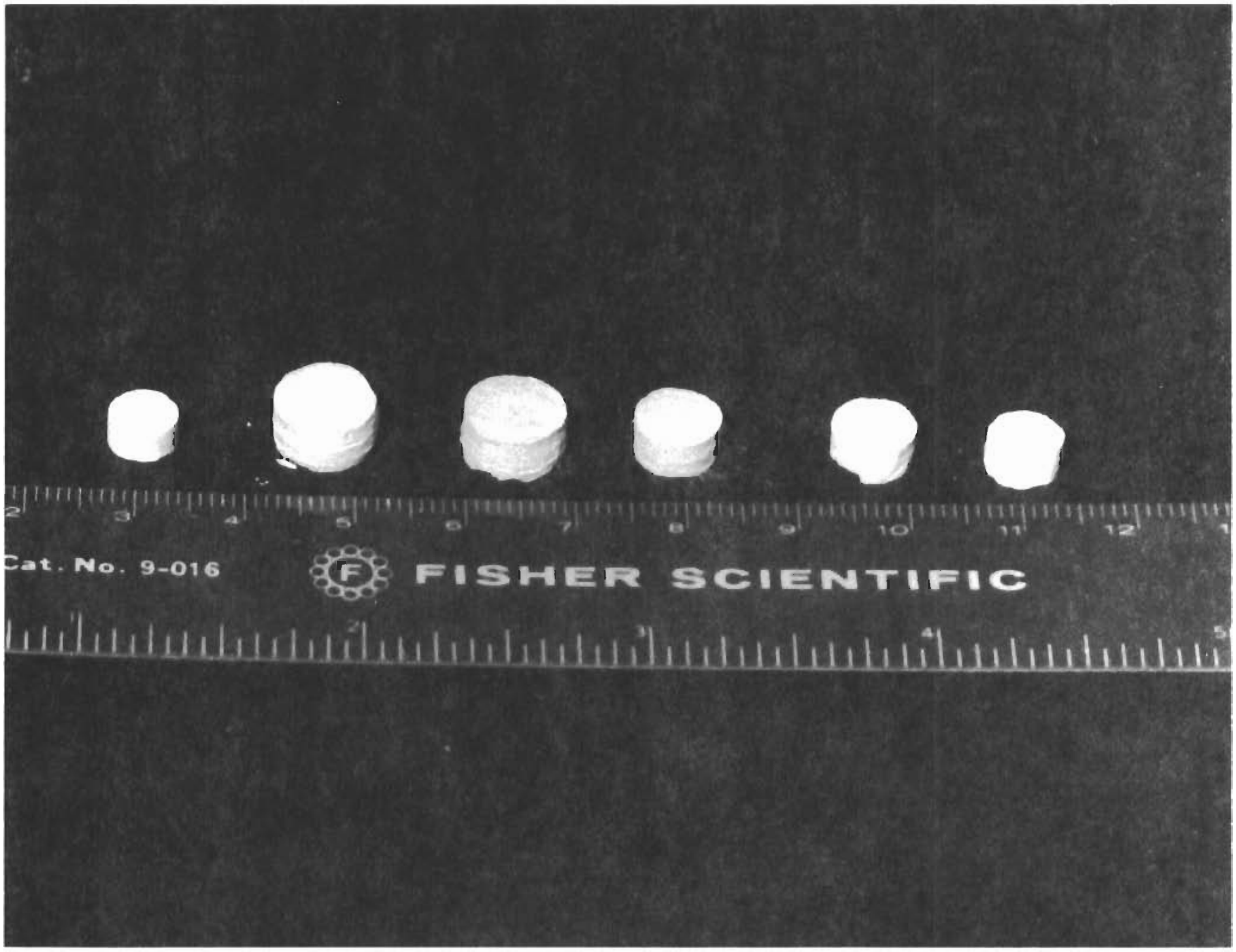

Fig. 8. Li_2O_2 Tablets After Decomposition

From left to right:

Tablet No.	Decomposition Temp. C	Sample No.
1	original Li_2O_2 tablet	
2-3	250-275	349-42-1B
4	300	349-42-3
5	318	358-2-1
6	325	358-7-1

TABLE VI

GRAVIMETRIC TEST DATA

1 Gram loosely packed Li_2O tablets exposed to Oxygen.Gas, 1% (Vol) CO_2, 50% R.H.

Preparation: Li_2O_2 tablets decomposed to Li_2O tablets

Sample No.	Li_2O Tablet Size Diam. cm	Li_2O Tablet Size Height cm	Tablet Density g/cc
349-42-1B	0.95	0.50	0.172
349-42-3	0.78	0.44	0.260
358-2-1	0.75	0.42	0.285
358-7-1	0.63	0.37	0.372

Sample No.	Decomp. Temp. C	Bulk Density g/cc	Reaction Times (a) hr	Reaction Times (b) hr	Constant Wt. hr	Exposure Time hr	Product Li_2CO_3 %
349-42-1B	250-275	0.085	3.2	4.8	8	18	97.9
349-42-3	300	0.147	4.0	12.0	16	20	84.6
358-2-1	318	0.169	4.0	14.0	18	24	97.0
358-7-1	325	0.238	5.8	17.2	23	23	93.1

Notes: (a) For reaction $2Li_2O + CO_2 + H_2O \rightarrow Li_2CO_3 + 2LiOH$

(b) For reaction $2LiOH + CO_2 \rightarrow Li_2CO_3 + H_2O$

Results are given in table VII and figure 10 (sample 358-21-1).

(5) Granules From Li_2O_2 Pellets

Li_2O_2 powder was pressed into pellets 6.2 cm in diameter and in thickness ranging from 3 to 4 cm to yield pellet densities of 0.77 and 0.97 g/cc. Pellets of a given density were then stacked three deep and decomposed at atmospheric pressure. During decomposition the pellets first swelled, then cracked, and finally sintered. The resulting Li_2O pellets were crushed and sieved into 4- by 10-mesh granules. Table VII (samples 358-24-1, 358-28-1, and 358-31-1) gives granule characteristics and test results. Gravimetric curves are given in figure 11. Several points are noteworthy in the data of table VII. This granular product is considerably harder than the granular material prepared by pressing Li_2O powder and crushing to size (as described in (4) above). It is also harder than granules prepared by decomposing Li_2O_2 powder and crushing the resulting sintered cake (table IV, reactive low-density range). Compaction plus sintering is superior to either step alone in terms of mechanical strength. The two-step process yields hardness about equal to that of standard LiOH granules shown in table VII for comparison. The anhydrous LiOH was also subjected to CO_2 absorption testing and conforms to bulk density-reactivity considerations as will be subsequently shown.

(6) Granules from Granular LiOH

A sample of high density Li_2O granules, prepared by dehydrating 4- by 14-mesh LiOH, was obtained from Foote Mineral Company inventory. This material was evaluated to

TABLE VII

GRAVIMETRIC TEST DATA, PROCESSES 2a-(4) AND 2a-(5)

1 Gram 4- by 10-mesh granular Li_2O exposed to Oxygen Gas, 1% (Vol) CO_2, 50% R.H.

Preparation: Li_2O_2 powder decomposed, pulverized, pressed into Li_2O pellets, pellets crushed and sieved

Li_2O_2 powder pelletized, decomposed, sintered Li_2O pellets crushed and sieved

Sample No.	Decomp. Temp. C	Densities Pellet g/cc	Densities Bulk Granules g/cc	Hardness No.	Surf. Area m^2/g	Reaction Times (c) hr	Reaction Times (d) hr	Constant Wt. hr	Exposure Time hr	Product Li_2CO_3 %
Pressed Li_2O:										
358-21-1	265	0.50	0.210	66.68	28.0	4.4	15.6	20	22	96.5
Pressed Li_2O_2:										
358-24-1	315	0.77	0.120	90.56	15.8	3.0	17.0	20	24	98.0
358-28-1	315	0.97	0.180	94.50	14.8	3.8	16.2	20	22	97.3
358-31-1	325	0.77	0.190	96.46	12.9	4.2	11.8	16	44	96.6
Granular LiOH:										
402-11-3 (a)	---	---	0.460	95	3.4	---	35	35	45	96.5
409-2 (b)	---	---	0.412	95.8	---	---	26	26	26	93.7

Notes:
(a) Granular anhydrous LiOH, 4 x 14 mesh, amount equivalent to 1 g Li_2O
(b) Granular anhydrous LiOH, 10 x 30 mesh, amount equivalent to 1 g Li_2O
(c) For reaction $2Li_2O + CO_2 + H_2O \rightarrow Li_2CO_3 + 2LiOH$
(d) For reaction $2LiOH + CO_2$ / $Li_2CO_3 + H_2O$

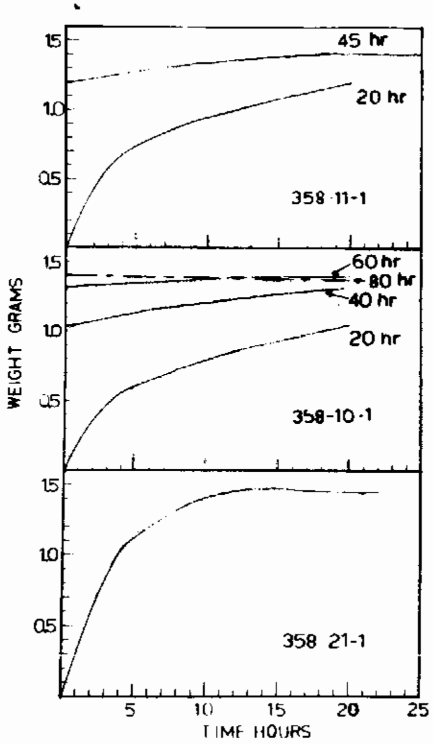

Fig. 10. Gravimetric Curves
Samples 358-11-1, 358-10-1, 358-21-1

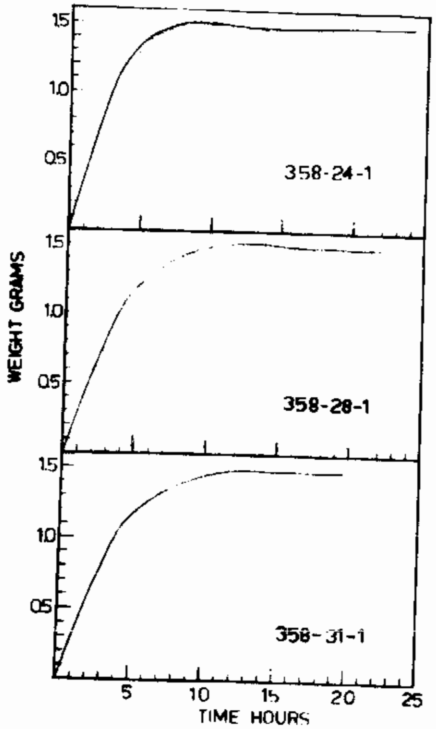

Fig. 11. Gravimetric Curves
Samples 358-24-1, 358-28-1, 358-31-1

provide Li_2O density versus performance data in the high-density range. The gravimetric curve of figure 3 (sample 349-9-5) illustrates the low reactivity of this high density, low-surface-area material.

(7) Comparative LiOH granules

Two samples of granular anhydrous LiOH, one 4- by 14-mesh and one 16- by 30-mesh, were tested to provide comparisons with Li_2O. Gravimetric curves are shown in figure 12 and in the data of table VII.

b. Self-supported Shapes

(1) From Pressed Li_2O Powder

Li_2O powder was prepared by decomposing Li_2O_2 powder and pulverizing the sintered cake. The oxide powder was then double-end pressed into 1.27 cm diameter pellets of 1 g each. Compaction pressures of less than 72 kg/cm^2 (200 psi) yielded pellets with virtually no strength. Higher pressures improved strength somewhat, but the resulting pellets tended to crack (as shown in figure 13) and remained weaker than desired. Table VIII gives characteristics of the pellets (samples 358-10-1 and 358-11-1) and shows the long reaction times encountered in absorption tests. The corresponding gravimetric curves of figure 10 reconfirm the effect of density on absorption rate. While the direct compaction of Li_2O powder offers process simplicity, the conflicting requirements of high density for strength and low density for reactivity probably cannot be compromised by mechanical pressing alone.

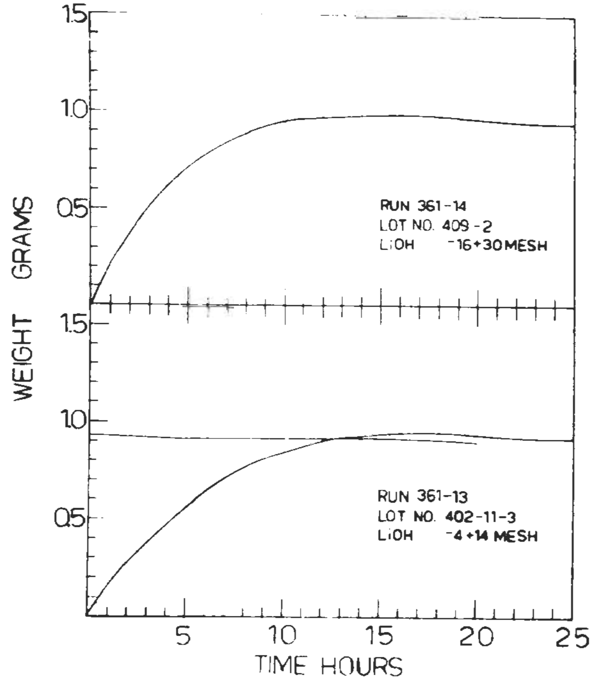

Fig. 12. Gravimetric Curves
Granular LiOH

Fig. 13. Porous Solid Li_2O Shapes
Left: Compressed Li_2O powder
Right: Decomposed, sintered Li_2O_2 powder

TABLE VIII

GRAVIMETRIC TEST DATA, POROUS SOLID Li_2O

1 Gram Cylindrical Li_2O Shape exposed to Oxygen Gas, 1% (Vol) CO_2, 50% R.H.

Preparation: Pressed Li_2O-Li_2O_2 Powder decomposed, pulverized, mechanically pressed
Sintered Li_2O-Li_2O_2 Powder decomposed, sintered cake carved into cylinders

Sample No.	Press Load kg/cm²	Shape Size Diam. cm	Shape Size Height cm
Pressed:			
358-11-1	72	1.27	1.72
358-10-1	144	1.27	1.60
Sintered:			
349-11-1	--	1.53	3.43
349-13-1	--	1.20	2.82
349-18-1	--	1.50	1.00

Sample No.	Decomp. Temp. C	Shape Density gm/cc	Reaction Times (a) hr	Reaction Times (b) hr	Constant Wt. hr	Exposure Time hr	Product Li_2CO_3 %
Pressed:							
358-11-1	285	0.475	15	25	40	47	90.0
358-10-1	285	0.487	20	70	90	98	97.9
Sintered:							
349-11-1	285	0.165	4	12	16	18	97.0
349-13-1	325	0.220	4	14	18	18	97.0
349-18-1	350	0.548	67	--	No	105	85.2

Notes: (a) For reaction $2Li_2O + CO_2 + H_2O \rightarrow Li_2CO_3 + 2LiOH$
(b) For reaction $2LiOH + CO_2 \rightarrow Li_2CO_3 + H_2O$

(2) Sintered Shapes From Li_2O_2 Powder

Li_2O shapes were prepared by carving cylinders from the lightly sintered cakes of oxide resulting from the decomposition of loosely packed Li_2O_2 powder. The cylinders (see figure 13) were fragile but appeared stronger than the mechanically compacted pellets reported above. Table VIII (samples 349-11-1, 349-13-1, and 349-18-1) gives characteristics of the sintered shapes. The first two samples demonstrated that porous, low-density shapes would allow active diffusion of CO_2 through depths of at least 7 mm. The low reactivity of high-density (0.548 g/cc) sample 349-18-1 conforms to earlier findings. Figure 14 shows the corresponding gravimetric curves.

(3) Sintered Shapes From Granular Li_2O_2

Li_2O_2 powder was pressed into large pellets which were then crushed and sieved to yield granules. The granules were decomposed in molds at normal packing density and atmospheric pressure. Swelling was observed at low decomposition temperatures (about 285 C), and the material filled the mold shape as decomposition proceeded. The swelling was more pronounced than in process (2) above, and the shapes were harder and more substantial. The process, considered the best of the alternates studied, is further reported in section III.

c. Gas Velocity Effect

In the foregoing screening tests, atmospheric conditions were held constant, and all samples were exposed to a nominally passive (81 cm/min velocity) gas. Only the oxide sample form and density were varied. To explore the effect of

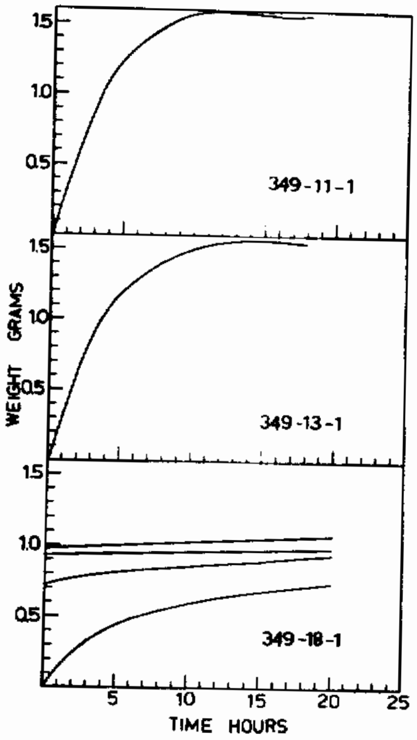

Fig. 14. Gravimetric Curves

Samples 349-11-1, 349-13-1, 349-18-1

gas velocity, granules and tablets were tested in the gravimetric apparatus at double the standard velocity. Table IX, which compares corresponding samples at standard and higher velocity, indicates CO_2 absorption rate increased significantly. The higher velocity apparently induced some circulation within the sample bed and increased CO_2 partial pressure at its face.

TABLE IX

GRAVIMETRIC TESTS, GAS VELOCITY EFFECT

1 Gram 4- by 10-Mesh Granular Li_2O exposed to Oxygen Gas, 1% (Vol) CO_2, 50% R.H.

Preparation:
349-42-1b: Li_2O_2 Tablets decomposed to Li_2O tablets
358-24-1: Li_2O_2 powder pelletized, decomposed, sintered Li_2O crushed and sieved
358-31-1: As above

Sample No.	Bulk Density g/cc(1)	Gas Velocity cm/min	Reaction Time (2) hr	Exposure Time hr	Product Li_2CO_3 %
Tabletted Li_2O_2					
349-42-1B	0.085	81	3.2	18	97.9
349-42-1B	0.107	162	2.5	7	96.0
Pressed Li_2O_2					
358-24-1	0.120	81	3.0	24	98.0
358-24-1	0.127	162	2.3	7	91.4
Pressed Li_2O_2					
358-31-1	0.199	81	4.2	44	96.6
358-31-1	0.199	162	3.3	7	85.6

Notes: (1) Bulk densities are approximate, being based on 1 g samples

(2) For reaction $2Li_2O + CO_2 + H_2O \rightarrow Li_2CO_3 + 2LiOH$

d. Reaction Product Composition

All reacted samples from the gravimetric runs were analyzed by the procedures outlined in section I. Reported total alkalinity was mathematically translated into the compound pairs which are theoretically in equilibrium with each other (i.e.-- Li_2O and LiOH; LiOH and $LiOH \cdot H_2O$; $LiOH \cdot H_2O$ and H_2O). Kinetically a Li_2O-LiOH-$LiOH \cdot H_2O$ mixture is possible and was detected by x-ray diffraction. Reaction product compositions, based on the equilibrium pairs, are given in table X.

e. Analysis of Results

In figure 15, the density of the various Li_2O samples is plotted against the corresponding time required for each to attain constant weight during passive gravimetric testing. Two curves are shown, one represents supported bed samples (granules or loose tablets) and one represents self-supported samples. Also shown are calculated limiting densities for 4- by 10-mesh granules and for self-supported shapes, based on formation of a nonporous protective coating of $LiOH \cdot H_2O$ on the Li_2O. In both cases, the experimental data substantiate the density limitations (0.32 g/cc bulk density for 4- by 10-mesh granules and 0.54 g/cc for self-supported shapes) estimated from the molar volume relations of section I. The curves also provide a more rational basis for performance prediction and absorbent design than heretofore available.

The curves intersect, indicating equivalent CO_2 absorption rate; at about 0.16 g/cc density. For the 4- by 10-mesh granular bed, this value represents bulk density; whereas the

TABLE X

GRAVIMETRIC TESTS, REACTION PRODUCT ANALYSES

Table No.	Sample No.	% Li_2O	% Li_2CO_3	% LiOH	% $LiOH \cdot H_2O$	% H_2O
IV	349-11-2	0	99.9	0	0	0
	349-13-2	0	97.7	0	0	2.2
	349-16-2	0	97.6	0	0	2.3
	349-18-2	0	85.1	14.9	0	0
	349-21-2	52.0	22.9	25.2	0	0
	349-23-2	63.1	26.6	10.3	0	0
	349-9-5	0	90.0	2.6	7.4	0
VIII	349-11-1	0	97.0	0	2.9	0
	349-13-1	0	97.0	0	2.1	0.8
	349-18-1	2.7	85.2	12.1	0	0
	358-11-1	0	90.05	0	8.5	1.5
	358-10-1	0	97.96	0	0.5	1.5
V	349-35-3	0	96.50	0	1.0	2.5
	349-42-1C	0	97.98	0	0	2.0
	349-42-4	0	97.20	0	1.0	1.8
	358-2-3	0	96.66	0	1.3	2.0
	358-7-3	0	95.07	0	3.7	1.2
VI	349-42-1B	0	97.90	0	0.2	1.9
	349-42-3	0	84.60	1.8	13.6	0
	358-2-1	0	97.0	0	0.4	2.6
	358-7-1	0	93.1	0	6.1	0.8
VII	358-21-1	0	96.49	0	1.6	1.9
	358-24-1	0	98.04	0	0.3	1.7
	358-28-1	0	97.37	0	0.8	1.8
	358-31-1	0	96.6	0	2.0	1.4
	402-11-3	0	96.5	0	2.4	1.1
	409-2	0	93.7	0	4.5	1.8
IX	349-42-1B(a)	0	96.0	0	2.1	1.9
	358-24-1(a)	0	91.4	0	6.6	2.0
	358-31-1(a)	0	85.6	4.5	9.9	0

(a) at 162 cm/min gas velocity

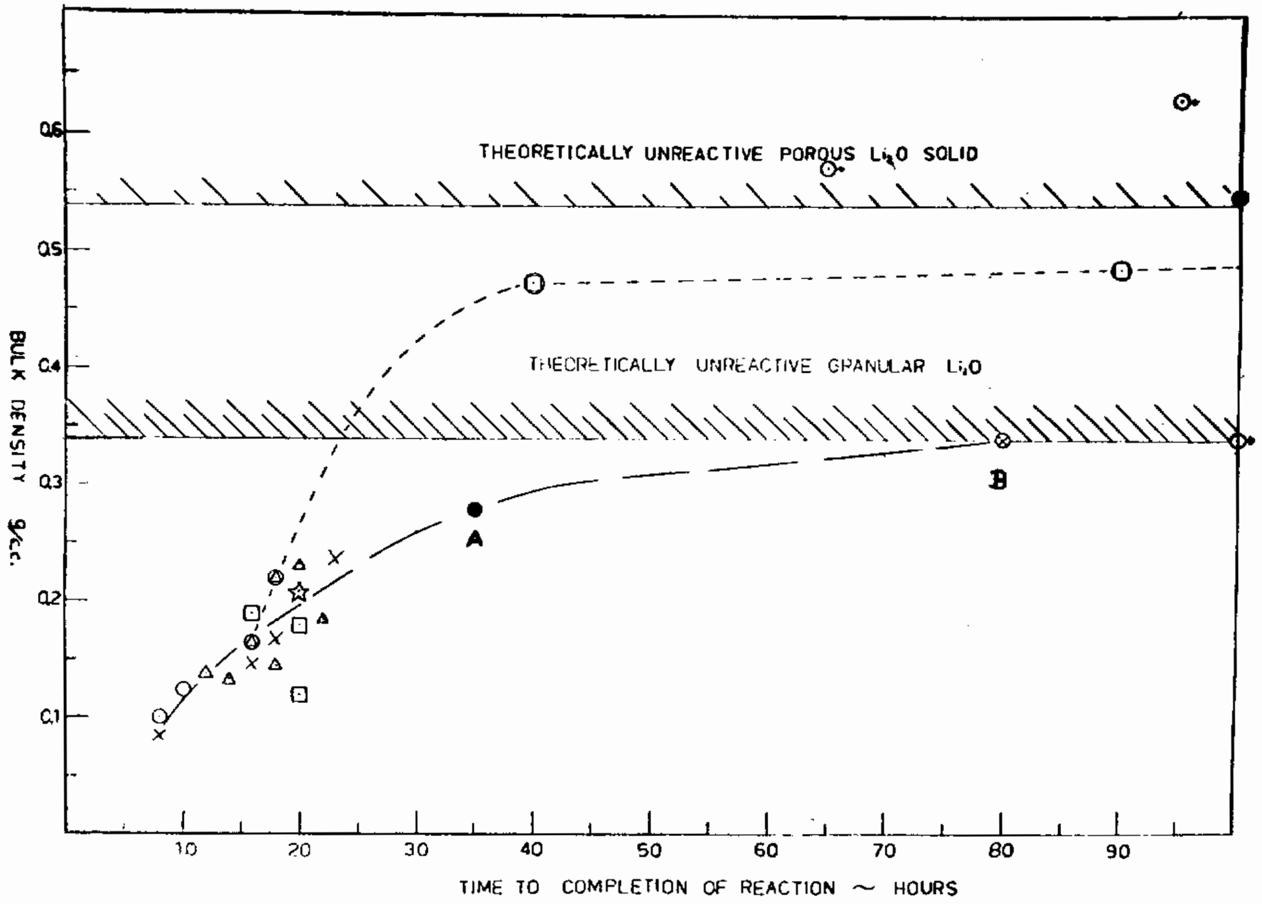

Fig. 15. Bulk Density of Li_2O versus Time for Complete Carbonation

Symbol	Li_2O Preparation Process No.	
○	2a - (1)	granular
△	2a - (2)	granular
×	2a - (3)	granular
☆	2a - (4)	granular
□	2a - (5)	granular
⊗	2a - (6)	granular
◯	2b - (1)	self-supported
◬	2b - (2)	self-supported
●	4- by 14-mesh, granular LiOH	
→	reaction incomplete	

Notes: (1) Processes are described in tables II and III
(2) Plotted LiOH bulk density adjusted to equivalent Li_2O basis
(3) Atmosphere 1% CO_2 in oxygen, 50% R.H., 81 cm/min gas velocity.

density of a single granule itself would be on the order of 0.26 g/cc (i.e., bulk voids between granules occupy about 38.5% of the bed volume). Several other points on the supported bed curve illustrate the general utility of the density-reactivity relation. Point A designates the reaction time for 4- by 14-mesh granular LiOH (sample 402-11-3) with the hydroxide density expressed on a Li_2O basis (i.e., LiOH bulk density x $Li_2O/2LiOH$). This represents a theoretical LiOH dehydration to Li_2O. The point conforms with other experimental points for Li_2O. Point B designates results obtained with Li_2O granules prepared by actually dehydrating 4- by 14-mesh LiOH. The sintering and volume shrinkage that occur in this dehydration increases bulk density and causes long reaction time.

3. DYNAMIC TESTS

a. Apparatus and Procedure

For screening tests under dynamic conditions, gas was passed directly through beds of Li_2O, using the apparatus shown in figure 16. The test was based on measuring per cent of CO_2 input absorbed by the sample in a single gas pass over a period of about one-half hour. Feed gas composition and flow rate and sample charge weights were held constant. The only pertinent variables were sample bulk density and bed depth. Gas flow rate was 28.9 liters/min, the gas being oxygen containing 1% (vol) CO_2 and water vapor equivalent to 50% relative humidity at 22 C. Relative humidity was controlled by bubbling the gas through a series of sulfuric acid solutions. A direct-reading, calibrated

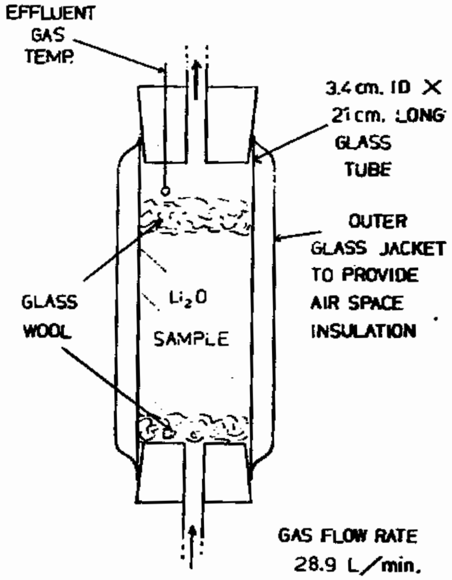

Fig. 16. Dynamic Screening Test Apparatus

hygrometer was used to check relative humidity before, during, and after each test run. Checks indicated the moisture input consistently ranged between 48 and 52% R.H. CO_2 flow was measured by a dry test gas meter with volume being adjusted to fix CO_2 input rate at 17 grams per half-hour. Sample quantities were fixed at 12.6 g Li_2O, which were larger than actually required (it required only 11.54 g pure Li_2O to absorb 17.02 g CO_2), to allow for impurity and moisture content.

b. Test Data

Granular samples were drawn from the same lots of material used in gravimetric testing and bear identical sample numbers for comparison. Information gathered in dynamic testing is listed below, and corresponding data are given in table XI.

Sample characteristics - analysis, bulk density, surface area, hardness, and decomposition temperature in preparation

Bed characteristics - depth and average pressure loss

Absorption performance - product analysis, fraction of input CO_2 absorbed, effluent gas temperature

c. Analysis of Results

In figure 17, sample bulk density is plotted against per cent of CO_2 input absorbed. Samples at a number of points, designated by identical symbols, were prepared by the same general process steps but with conditions varied to change density. As shown by the curve, bulk density was the prime factor in determining diffusion rate and CO_2 absorption regardless of preparation method. Point A (sample 402-11-3) designating granular LiOH with its density expressed on a Li_2O basis conforms with the other experimental points for Li_2O. This was also true in gravimetric testing. Point B (sample 349-9-5) designating Li_2O actually prepared by dehydrating LiOH is well off the experimental curve.

The granule volume shrinkage accompanying dehydration is illustrated by the bulk density change from point A to point B. However, the low CO_2 absorption at point B cannot be

TABLE XI

DYNAMIC TEST DATA AT 50% R.H. INPUT

Exposure of 4- by 10-mesh Li_2O to equivalent amount of 1% CO_2 in Oxygen at 50% relative humidity with 28.9 liters-per-minute gas flow.

Sample No.	Decomp. Temp. C	Bulk Density g/cc	Surface Area m^2/g	Hardness No.	Analysis Before Exposure			
					Li_2O %	$LiClO_3$ %	LiOH %	Li_2O_2 %
349-11-2	285	0.10	14.70	66.3	88.9	2.7	8.4	0.2
349-13-2	325	0.12	13.35	59.3	89.5	0.6	9.8	0.1
349-16-2	325	0.12	13.80	54.6	92.5	2.2	5.3	0.1
349-18-2	350	0.34	3.85	93.1	94.6	5.1	0.3	0.02
349-21-2	385	0.57	0.28	98.2	94.4	2.4	3.2	0.005
349-23-2	430	0.63	---	92.6	94.8	4.7	0.5	0.004
349-9-5	644	0.34	0.94	89.2	97.1	2.6	0.3	0.00
349-35-3	250	0.13	12.65	---	85.3	1.1	10.8	2.8
349-42-1C	275	0.13	12.85	---	93.9	3.0	2.6	0.5
349-42-4	300	0.16	13.84	---	92.7	1.5	5.8	0.1
358-2-3	318	0.18	13.34	---	89.6	2.0	8.4	0.08
358-7-3	325	0.23	12.75	---	93.1	1.8	5.1	0.06
358-21-1	265	0.21	28.03	66.6	91.0	2.5	6.5	0.13
358-24-1	315	0.13	15.77	90.56	93.1	1.2	5.7	0.09
358-28-1	315	0.15	14.82	94.5	91.4	1.6	7.0	0.07
358-31-1	325	0.20	12.97	96.4	93.5	1.3	5.2	0.05
402-11-3	---	0.47	3.44	95	---	---	99.5	---

TABLE XI (Continued)

Bed Depth (d) cm	Press. Loss (c) Mm Hg	Analysis After Exposure				Input CO_2 Absorbed %	Gas Temp. (e) C
		Li_2O %	LiOH %	$LiOH \cdot H_2O$ %	Li_2CO_3 %		
13.8	11.8	0	8.0	5.1	86.8	86.0	136
10.8	6.2	0	26.8	1.5	71.7	65.8	105
11.4	8.4	0	24.5	0.6	74.9	68.5	140
4.2	2.8	35.2	27.48	0	37.3	21.7	80
2.5	2.25	87.2	5.4	0	7.4	2.35	34
2.2	1.87	91.8	2.6	0	5.5	0.51	31
3.7	2.8	87.2	3.8	0	9.1	3.12	37
10.0	5.6	14.0	24.1	0	60.3	46.6	94
10.8	4.7	5.2	23.0	0	71.8	60.4	114
9.4	3.4	2.5	36.2	0	61.4	51.4	131
7.6	---	9.1	26.1	0	64.8	51.0	124
5.6	1.8	20.2	22.0	0	57.6	41.7	94
6.1	1.87	10.3	30.6	0	59.1	45.5	107
10.3	3.0	4.4	42.6	0	53.0	45.1	96
9.0	2.4	6.1	30.5	0	63.4	52.7	115
6.5	2.2	14.1	32.9	0	53.0	39.7	78
3.9	1.31	0	50.0	13.3	36.7	28.65	42

Notes:
(a) Li_2O preparation processes described in table II.
(b) Sample 402-11-3 is 4- by 14-mesh granular LiOH and weighed 18.5 grams.
(c) Pressure loss through bed is average value at 28.9 liters/min. gas flow.
(d) Bed diameter 3.4 cm in all cases.
(e) Gas temperatures listed are maximum temperature of gas leaving bed.

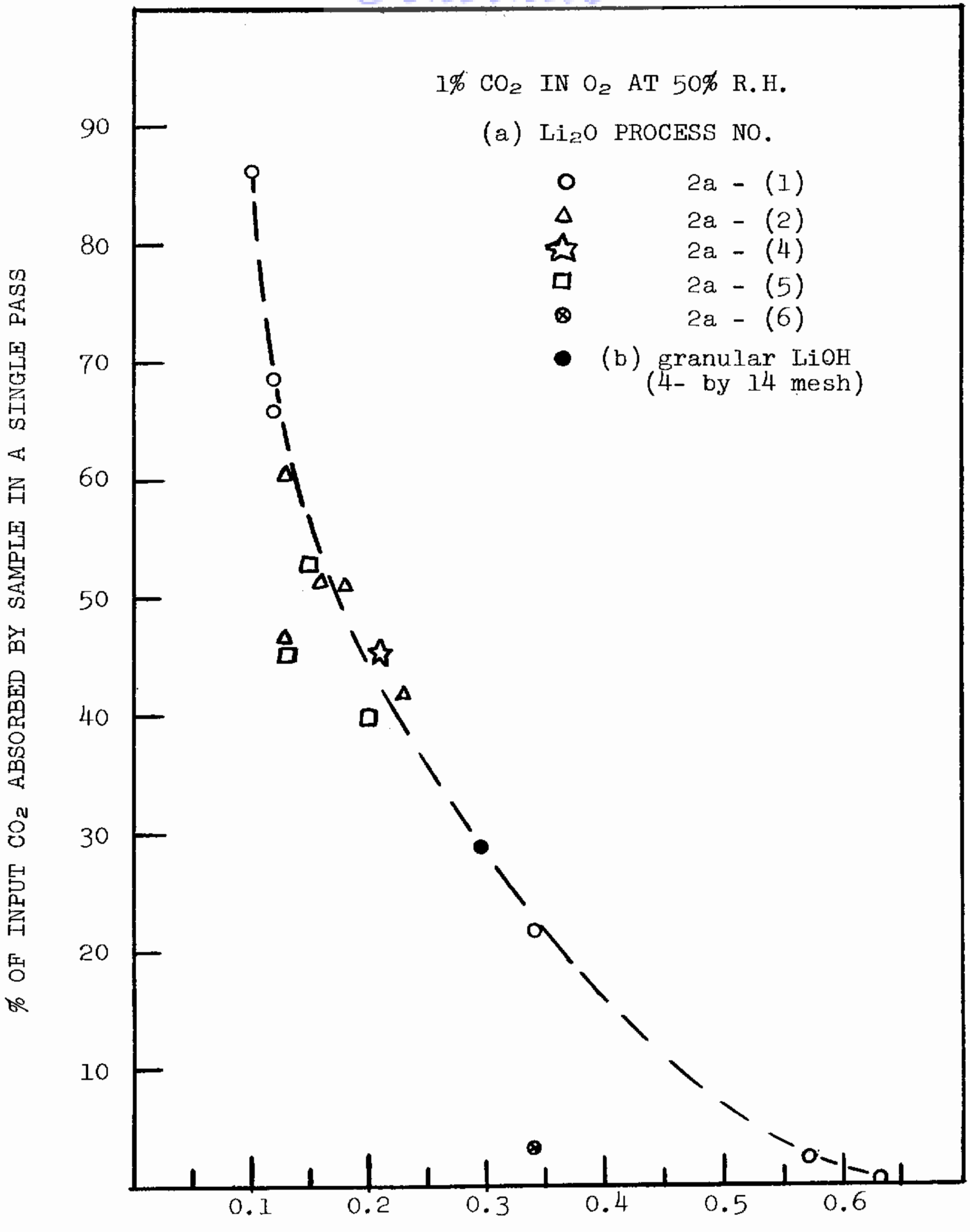

Fig. 17. Bulk Density of Granular Li_2O versus CO_2 Absorption in a Single Pass

Notes: (a) Processes are described in table II
(b) Plotted LiOH bulk density adjusted to equivalent Li_2O basis
(c) Atmosphere 1% CO_2 in oxygen, 50% R.H.

attributed to density increase alone. Very probably, a Li_2O granule prepared under the relatively high temperatures required for dehydration has a sintered surface and nonuniform density which greatly affects CO_2 diffusion in a short-run test.

A semi-logarithmic plot of the preceding results (figure 18) yields the following relation applicable to granular Li_2O under the stated test conditions--

$$\% \text{ Input } CO_2 \text{ absorbed} = \frac{\log 0.5968 - \log \text{bulk density}}{0.010671}$$

The zero intercept at 0.59 g/cc bulk density is of interest since the molar volume relations (table I) indicate formation of a nonporous LiOH coating on 4- by 10-mesh Li_2O at 0.54 g/cc bulk density. If LiOH is formed as a nonporous coating on the Li_2O, any subsequent reaction products (i.e. Li_2CO_3 or $LiOH \cdot H_2O$) amplify its protectiveness, since these products are protective on LiOH. In contrast, a $LiOH \cdot H_2O$ coating on Li_2O does not produce this double-barrier effect, since the Li_2CO_3 reaction product is porous relative to $LiOH \cdot H_2O$.

Figure 19 shows effluent gas relative humidity and temperature profiles for a number of samples. The correspondence between CO_2 removal ability and initial absorption of moisture is evident. The profile of sample 349-11-2 is noteworthy since it demonstrates that reaction

$$2LiOH + CO_2 \rightarrow Li_2CO_3 + H_2O \text{ (gas)} \qquad (5)$$

is proceeding toward the end of this run as evidenced by effluent humidity rising above feed moisture level.

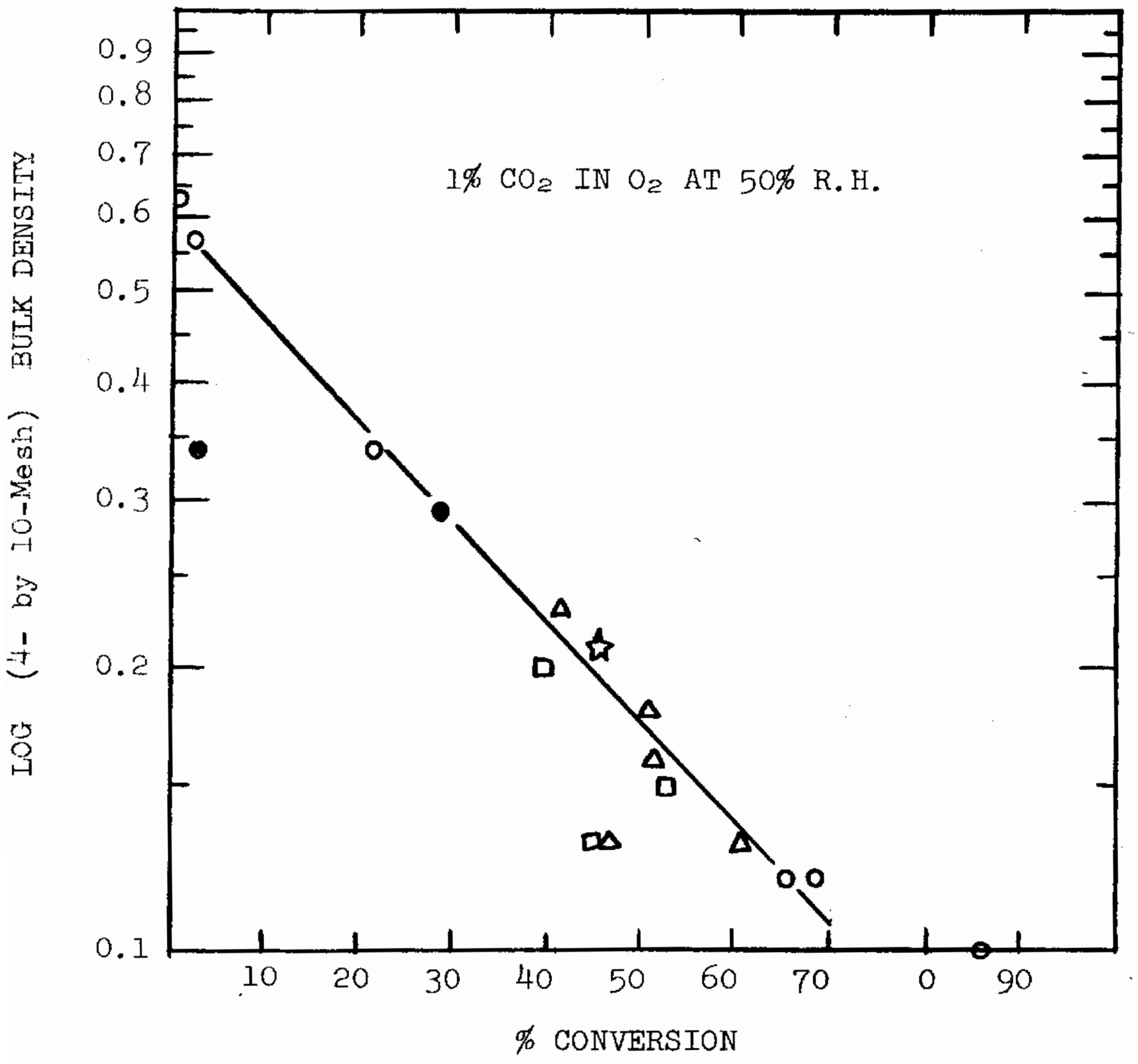

Figure 18

Log 4- by 10-mesh Bulk Density vs. % of CO_2 Input (1% CO_2 in Oxygen at 50% R.H.) Absorbed during a single pass.

Key same as in figure 16.

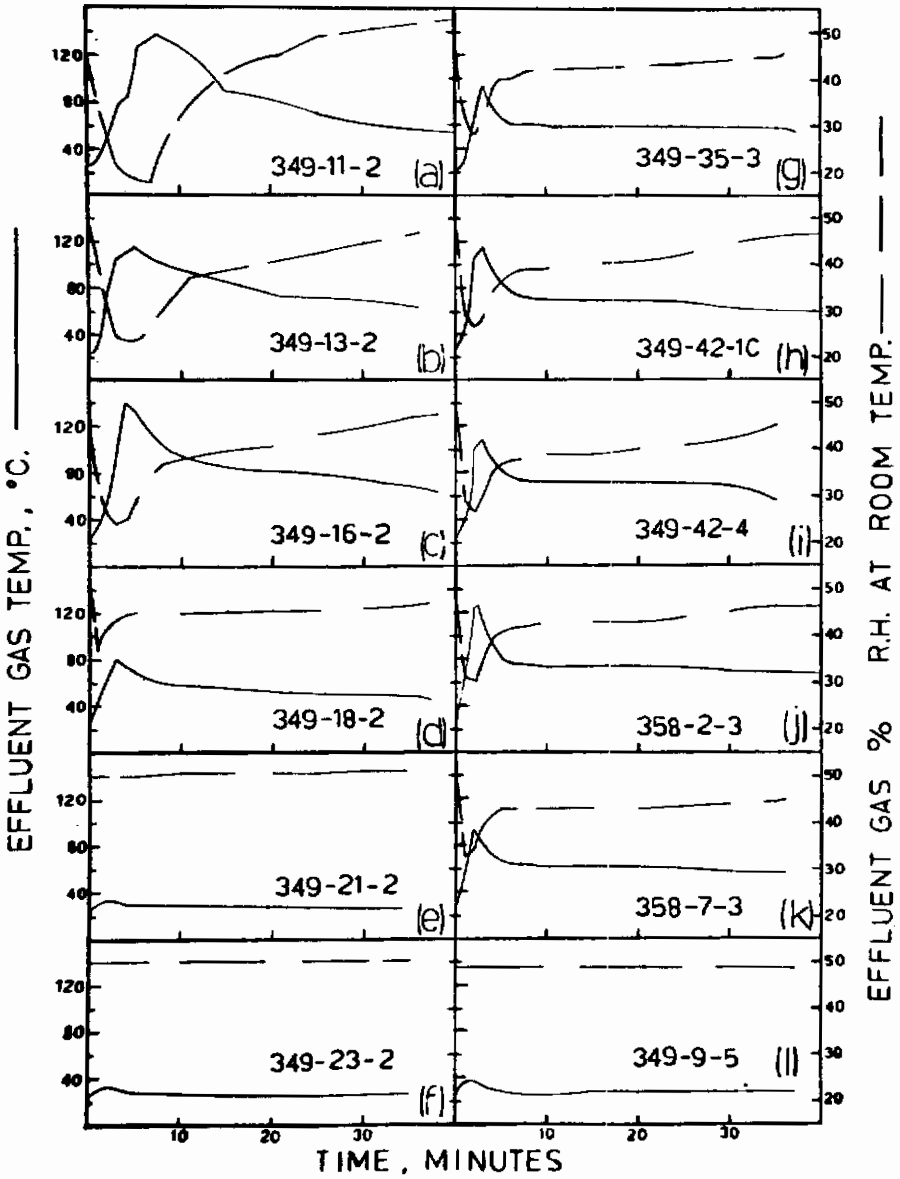

Fig. 19. Dynamic Test

Effluent gas temperature and Relative Humidity (at 25 C) with 1% CO_2 and 50% Relative Humidity Input.

CO_2 absorption by overall reaction (1) resulting from reactions (2), (3), and (4) requires that the molar ratio H_2O/CO_2 absorbed be unity. If this occurs, the molar ratio of $2LiOH/Li_2CO_3$ found in the product should be unity for samples still containing unreacted Li_2O:

$$2Li_2O + CO_2 + H_2O \rightarrow Li_2CO_3 + 2LiOH \qquad (1)$$

$$Li_2O + H_2O \rightarrow 2LiOH \qquad (2)$$

$$2LiOH + CO_2 \rightarrow Li_2CO_3 + H_2O \text{ (absorbed)} \qquad (3)$$

$$Li_2O + H_2O \text{ (absorbed)} \rightarrow 2LiOH \qquad (4)$$

In testing, a feed gas H_2O/CO_2 molar ratio of about 1.4 was maintained. However, as shown in table XII which lists the $2LiOH/Li_2CO_3$ molar ratio for all samples containing residual Li_2O on test completion, only some of the samples have a ratio near or exceeding unity in accordance with reaction (1) with the excess moisture provided. This indicates that reaction (5)

$$2LiOH + CO_2 \rightarrow Li_2CO_3 + H_2O \text{ (gas evolved)} \qquad (5)$$

as well as reactions (3) and (4) is occurring with Li_2O present. Therefore, the reaction mechanism may vary as it is influenced by sample porosity, bed temperature, and gas flow rate.

The effect of higher moisture input was studied by increasing feed gas H_2O/CO_2 molar ratio to 2.43 with other test conditions remaining the same. The increase, from 50% to 88% R.H., yielded complete Li_2O consumption and increased conversion to Li_2CO_3 as shown by comparing tables XI and XIII. The initial effluent gas temperature almost doubled as shown in figure 20. The higher humidity did not affect CO_2 absorption rate of the LiOH sample (tables XI and XIII, sample 402-11-3). In this case,

CO_2 absorption is evidently controlled by diffusion and is unaffected by the additional $LiOH \cdot H_2O$ resulting from higher humidity.

TABLE XII

REACTION PRODUCT MOLAR RATIOS

Sample No.	Residual Li_2O %	Molar Ratio $2LiOH/Li_2CO_3$
349-18-2	35.2	1.13
-21-2	87.2	1.12
-23-2	91.8	0.72
-9-5	87.2	0.64
-35-3	14.0	0.61
-42-1C	5.2	0.49
-42-4	2.5	0.91
358-2-3	9.1	0.62
-7-3	20.2	0.59
-21-1	10.3	0.80
-24-1	4.4	1.24
-28-1	6.1	0.74
-31-1	14.1	0.96

TABLE XIII

DYNAMIC TEST RESULTS

Exposure of 4- by 10-Mesh Li_2O to equivalent amount of 1% CO_2 in Oxygen at 88% relative humidity with 28.9 liters per minute gas flow rate.

Sample No.	(Note)	Sample Weight Grams	Bulk Density g/cc	Granular Bed dia. cm	depth cm	Average Pressure Drop mm Hg
358-24-1	(a)	12.6	0.13	3.4	11.2	3.0
358-28-1	(a)	12.6	0.15	3.4	9.3	2.6
358-31-1	(a)	12.6	0.19	3.4	6.5	2.2
402-11-3	(b)	18.5	0.47	3.4	4.5	1.12

Note: (a) Li_2O_2 powder compressed, decomposed and granulated

(b) LiOH, 4- by 14-mesh

TABLE XIII (Continued)

Analysis of Product After Dynamic Test					% of Input CO_2 Absorbed	Peak temp. of Effluent Gas C
Li_2O	$LiOH$	$LiOH \cdot H_2O$	Li_2CO_3	H_2O		
0	6.3	11.1	82.6	0	85.6	193
0	12.1	11.0	76.9	0	76.8	192
0	19.6	6.8	73.6	0	69.1	178
0	39.0	28.6	32.4	0	28.93	47

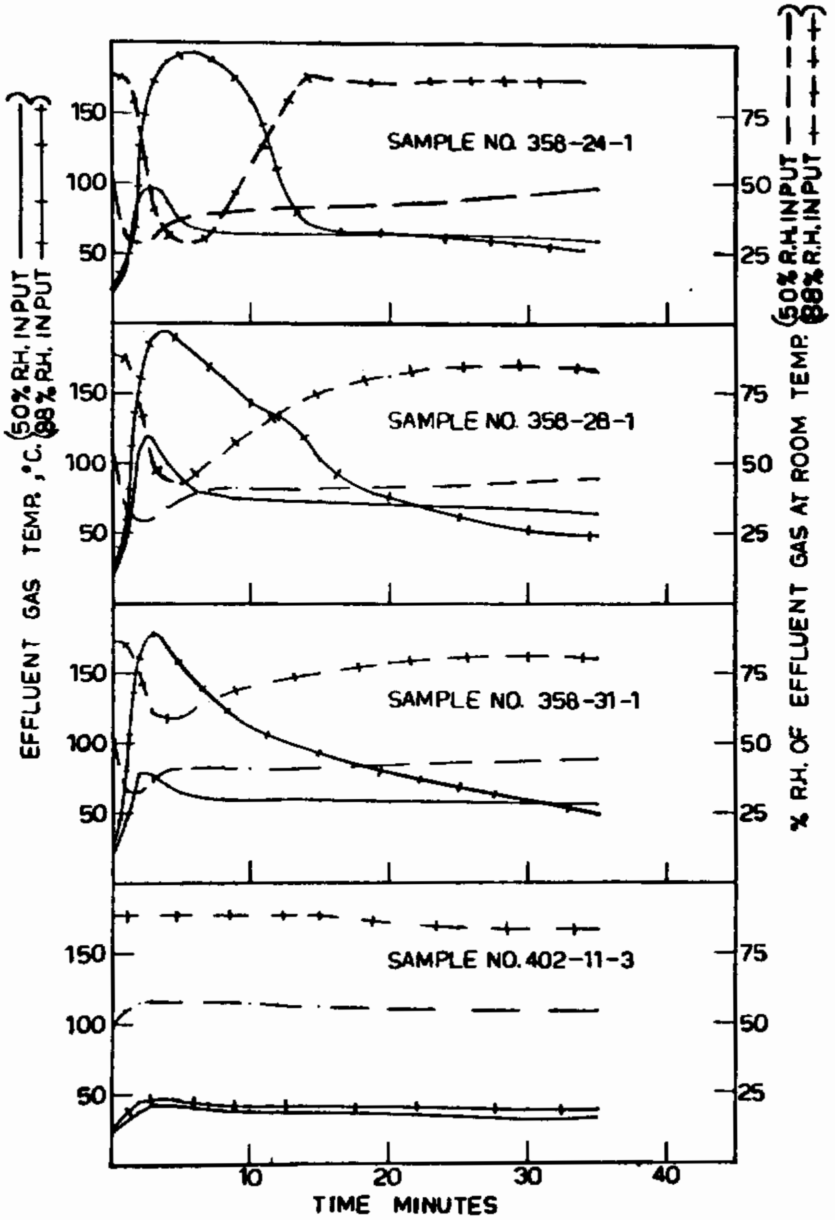

Fig. 20. Dynamic Test.

Effluent Gas Temperature and Relative Humidity at 50 and 88% Relative Humidity Input.

SECTION III

CONFIGURATION TESTS WITH LOW MOISTURE AVAILABILITY

1. APPARATUS AND PROCEDURES

The test apparatus consisted of a bell jar environmental chamber, recirculating gas lines, and appropriate auxiliaries, controls, and instruments as illustrated in figure 21. Apparatus details were as follows --

Bell jar volume	12.7 liters; 2.14 cm ID
Total system volume	17.0 liters
Electric hygrometer:	Cat. No. 15-3000, Hygrodynamics Inc. Silver Springs, Md.
CO_2 analyzer :	Model 405-Cl, Gow-Mack Instrument Co., Madison, N. J.

Air was used as the carrier gas. The thermoconductivity cell was calibrated at 0, 1, and 4% CO_2 before each run with preanalyzed gas mixtures and was rechecked after each run. CO_2 readout was not affected by flow rate but varied slightly with pressure changes. Gas temperature, relative humidity, and CO_2 concentration were logged by a strip chart recorder. CO_2 volume, temperature, and pressure at the gas meter were periodically noted and recorded.

Granular Li_2O was used in all tests. Except as noted, all samples were prepared by pelletizing Li_2O_2 powder, decomposing at various temperatures to yield desired density, crushing the sintered Li_2O pellet, and sieving to 4- by 10-mesh size (i.e., process 2a-(5), section II). Tests were conducted under both passive and dynamic conditions.

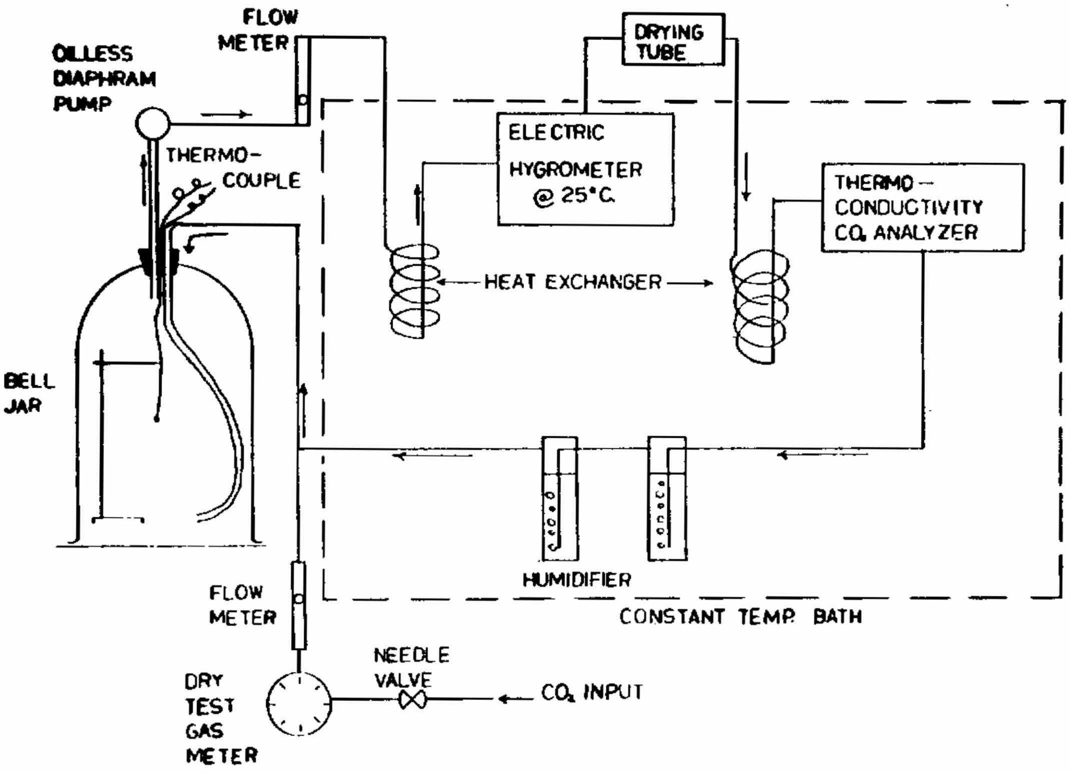

Fig. 21. Apparatus For 1-Atmosphere Tests

2. EXPLORATORY RUNS

Four exploratory runs were made to check the apparatus and evaluate the use of polypropylene for supporting granular beds. In each run granular Li_2O, bulk density 0.1 g/cc, was displayed in a single rectangular bed 12.2 cm wide, 16.5 cm high, and 1.5 cm thick containing about 41 grams Li_2O. The granules were enclosed and supported by 12-mesh, polypropylene netting (0.5 mm strand diameter, about 55% open area). Polypropylene spacer wires were run through the bed and fused to the netting to prevent wall sagging. Gas flow to the chamber was 6.6 liter/min, yielding a nominal velocity of 18 cm/min (based on chamber cross-section) for passive runs. Two runs were made under passive conditions and with 50% and 100% input relative humidity respectively. Two runs were made with the gas stream directed at the bed face. As shown in table XIV, chamber humidity could not be maintained and fell below the hygrometer range. Chamber CO_2 concentration rose rapidly. In one case, directing 100% R.H. gas at the bed face raised temperature sufficiently to sinter the sample and melt the polypropylene (melting point 160 to 177 C).

3. PASSIVE TESTS

Run 368-39

Further data were obtained on the effect of low moisture availability by making a passive run with three rectangular beds (identical to those described above) suspended in the chamber with nominal gas velocity at 18 cm/min. Figure 22 gives CO_2, temperature, and humidity (within the 40% to 60% R.H. range

TABLE XIV

PASSIVE TEST DATA, GRANULE RECTANGULAR BED

Run	Time Min.	Chamber Temp. C	Chamber % R.H. at 25 C	Vol.% CO_2	Accumulative g CO_2 Input	Remarks
(a)	0	23	50	0	0	4.6 g H_2O/hr
	1	26	< 40	trace		
	2	28	< 40	0.15		
	3	31	< 40	0.30		
	4	34	< 40	0.68		
	5	35	< 40	1.40		
	6	37	< 40	2.0		
	7	38	< 40	2.6		
	8	39	< 40	3.1		
	9	39	< 40	3.7		
	10	39	< 40	4.3	4.5	
(b)	0	23	50	0	0	4.6 g H_2O/hr
	1	23	< 40	trace		
	2	24	< 40	trace		
	3	25	< 40	0.1		
	4	26	< 40	0.3		
	5	26	< 40	0.95		
	6	26	< 40	2.0		
	7	26	< 40	3.2		
	8	26	< 40	4.8		
	10	26	< 40	off scale	4.5	

(c) Same results as (a) and (b)

(d) 100% R.H. input 0.5 cm from the bed caused excessive localized heating sintering the sample and melting the polypropylene netting

Notes:

Run (a) Single rectangular bed mounted vertically in the center of the chamber; 50% relative humidity input

(b) Single rectangular bed mounted horizontally on the bottom of the chamber with input gas recirculating lines 0.5 cm above the face of the bed; 50% relative humidity input

(c) As with (a) but at 100% relative humidity input

(d) As with (b) but at 100% relative humidity input

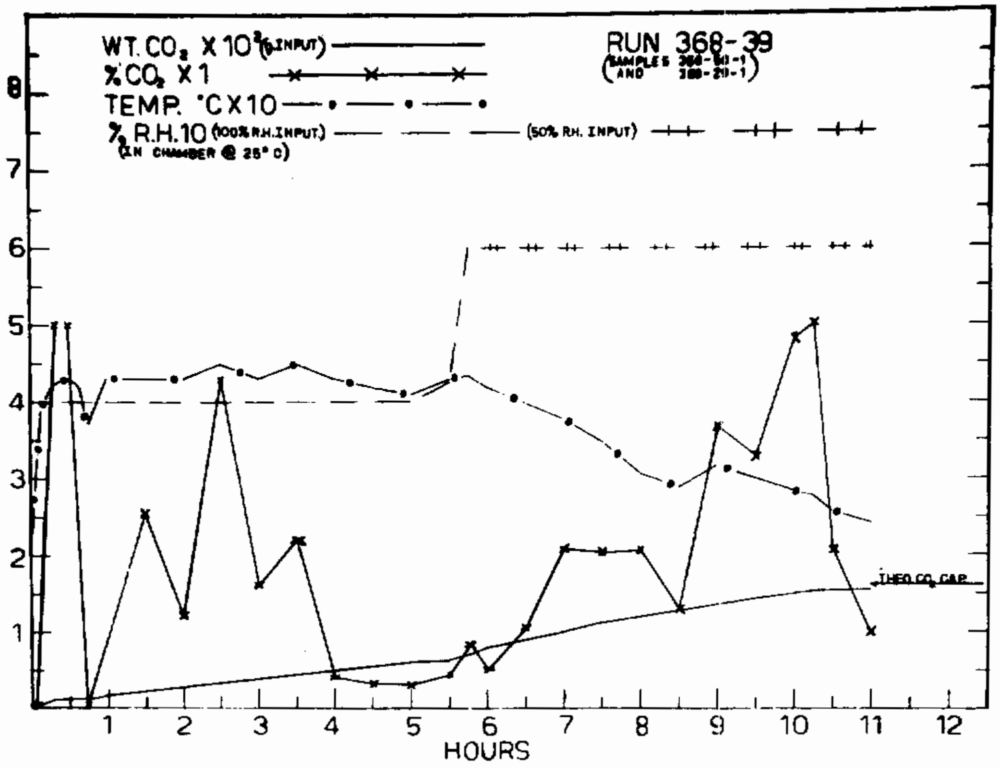

Fig. 22. Passive Test Profiles, Granule Rectangular Bed.
Run 368-39

of the available hygrometer) profiles. Test data are given in table XV. On starting, gas feed to the chamber was held at 100% R.H. introducing 9.22 g H_2O/hr. Relative humidity in the chamber was beyond instrument range but was less than 40%. When chamber CO_2 concentration rose to 5%, the CO_2 feed was

TABLE XV

TEST DATA AT ONE ATMOSPHERE

Run No.	Configuration	Lithium Oxide Wt. g	Lithium Oxide Bulk Dens. g/cc	Lithium Oxide Hardness No.	Run Time hr	Chamber Gas Average Velocity cm/min	Chamber Gas Avg. CO_2 %	Avg. CO_2 Absorp. Rate(b) g/hr
368-39	Rect. Beds	109.9	0.10	52.0	11.0	18.0	1.94	13.9
368-45	Cyl. Bed	103.3	0.10	52.0	7.5	18.0	2.59	17.3
376-11	Cyl. Bed	92.2	0.10	52.0	5.5	38.7	1.88	24.5
376-13	Cyl. Bed	306.7	0.34	79.2	12.8	38.7	2.18	18.4
376-15	Cyl. Bed	242.3	0.24	66.9	10.5	38.7	2.79	27.3
376-16	Belt	134.5	0.11	---	6.0	38.7	2.02	28.7
376-17	Belt	263.0	0.18	---	10.5	38.7	2.36	30.0
376-19	Dynamic Bed	139.8	0.10	53.0	5.0	---	0.93	35.3
376-38	Dynamic Bed	272.0	0.31	66.6	8.8	---	1.61	33.9

Notes: (a) 10- by 30-mesh granular Li_2O in Run No. 376-17; all other runs 4- by 10-mesh granules

(b) Based on cumulative g CO_2 feed up to run termination at 1% CO_2 in chamber gas

TABLE XV (Continued)

Run No.	Li_2O Used %(c)	Li_2O	LiOH	Li_2CO_3	Li_2O_2	Analysis of Reaction Product				
						Li_2O	LiOH	$LiOH \cdot H_2O$	Li_2CO_3	H_2O
		%	%	%	%	%	%	%	%	%
368-39	95.2	89.5	8.9	1.5	0.1	0	0	0.7	96.9	2.4
368-45	85.2	92.4	4.5	3.0	0.1	0	0.3	5.9	93.8	0
376-11	96.3	94.5	0.0	5.8	0.1	0	0	2.1	94.8	3.1
376-13	52.1	90.4	4.6	5.0	0.1	6.3	24.4	0	69.3	0
376-15	80.4	85.0	12.3	2.7	0.01	1.3	7.8	0	91.0	0
376-16	86.9	91.2	6.8	2.0	0.14	0	2.7	5.7	91.6	0
376-17	81.2	90.5	7.5	1.9	0.05	0	9.5	4.3	86.3	0
376-19	98.6	90.7	8.5	0.7	0.08	0	0	0	97.0	3.0
376-38	74.1	92.7	5.4	2.0	0.0	0	8.6	11.3	80.0	0

Note: (c) Based on treating absorbent charge as 100% Li_2O

cutoff and water feed was continued. Up to CO_2 cutoff the cumulative input H_2O/CO_2 molar ratio was 0.7 (note: all cumulative H_2O/CO_2 molar ratios are calculated from time zero and represent input to the chamber, not molar ratio actually absorbed by the sample). With continued moisture addition and no CO_2 feed, chamber CO_2 concentration declined and the cumulative molar ratio had increased to 1.84 when CO_2 concentration reached zero. CO_2 feed was then resumed on a demand, rather than fixed rate, basis.

The feed adjustments are not obvious from the input CO_2 profile but are magnified in the CO_2 concentration profile because of the small chamber volume. A fairly steady and low concentration of 0.4% CO_2 was maintained during the 4th and 5th hours. The cumulative molar ratio had attained 1.9 at the end of this period. The correspondence between CO_2 removal and the H_2O/CO_2 molar ratio agrees with earlier research (references 2, 3) indicating poor absorption rate when the gas H_2O/CO_2 molar ratio is below unity.

Figure 22 also illustrates the rapid humidity increase occurring after the Li_2O has been converted to Li_2CO_3 and LiOH and absorption proceeds via reactions (5) and (7). Chamber humidity reached 100% at 6 hours as evidenced by condensation.

$$2LiOH + CO_2 \rightarrow Li_2CO_3 + H_2O \text{ (gas)} \qquad (5)$$

$$2LiOH \cdot H_2O + CO_2 \rightarrow Li_2CO_3 + 3H_2O \text{ (gas)} \qquad (7)$$

<u>Run 368-45</u>

A thin-walled, cylindrical configuration (see figure 23) was tested. The unit, fashioned from polypropylene netting cutoff and water feed was continued. Up to CO_2 cutoff the cumulative input H_2O/CO_2 molar ratio was 0.7 (note: all cumulative H_2O/CO_2 molar ratios are calculated from time zero and represent input to the chamber, not molar ratio actually absorbed by the sample). With continued moisture addition and no CO_2 feed, chamber CO_2 concentration declined and the cumulative molar ratio had increased to 1.84 when CO_2 concentration reached zero. CO_2 feed was then resumed on a demand, rather than fixed rate, basis.

The feed adjustments are not obvious from the input CO_2 profile but are magnified in the CO_2 concentration profile because of the small chamber volume. A fairly steady and low concentration of 0.4% CO_2 was maintained during the 4th and 5th hours. The cumulative molar ratio had attained 1.9 at the end of this period. The correspondence between CO_2 removal and the H_2O/CO_2 molar ratio agrees with earlier research (references 2, 3) indicating poor absorption rate when the gas H_2O/CO_2 molar ratio is below unity.

Figure 22 also illustrates the rapid humidity increase occurring after the Li_2O has been converted to Li_2CO_3 and LiOH and absorption proceeds via reactions (5) and (7). Chamber humidity reached 100% at 6 hours as evidenced by condensation.

$$2LiOH + CO_2 \rightarrow Li_2CO_3 + H_2O \text{ (gas)} \qquad (5)$$

$$2LiOH \cdot H_2O + CO_2 \rightarrow Li_2CO_3 + 3H_2O \text{ (gas)} \qquad (7)$$

Run 368-45

A thin-walled, cylindrical configuration (see figure 23) was tested. The unit, fashioned from polypropylene netting

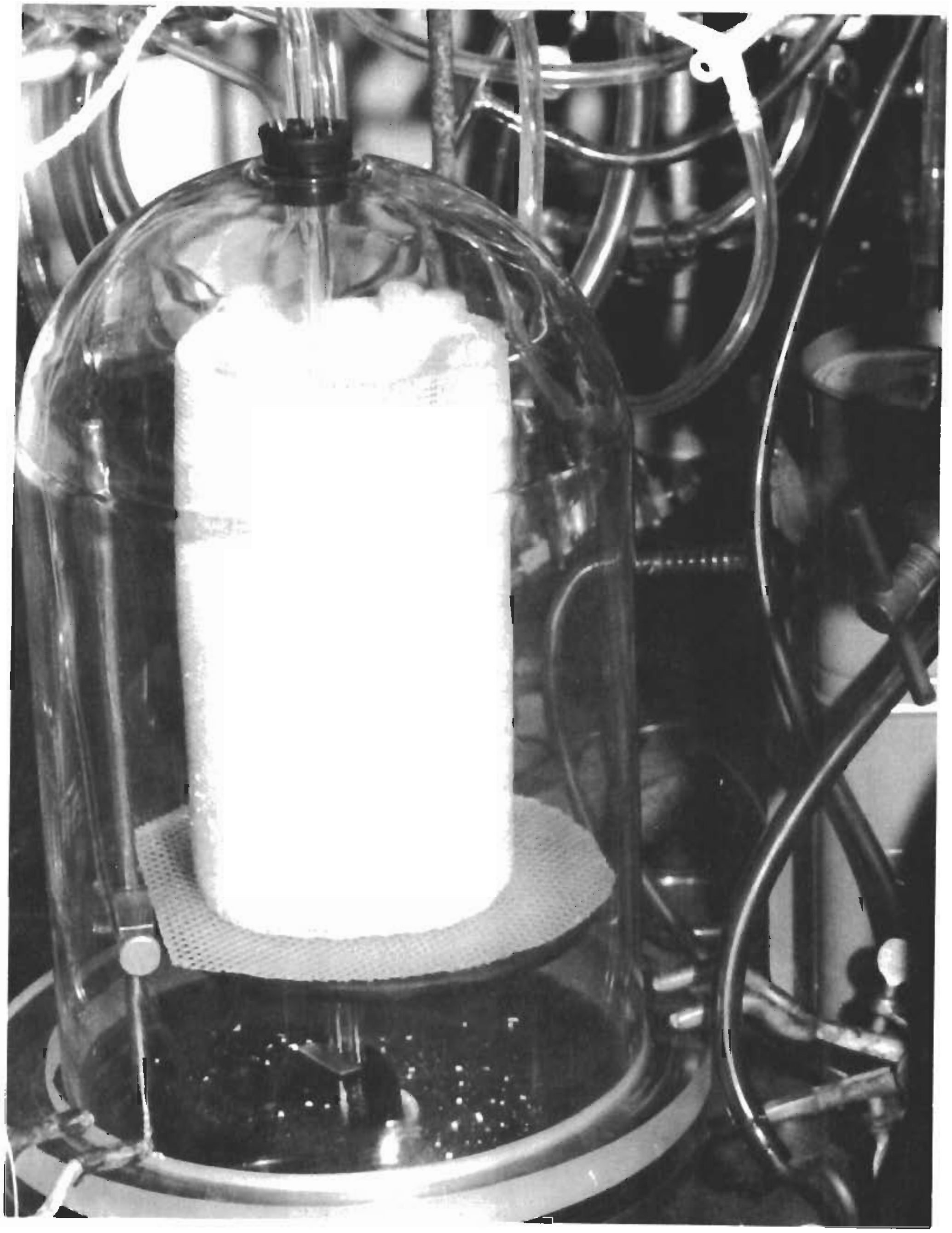

Fig. 23. Passive Cylindrical Bed Configuration

as previously described, had an 11.6-cm outer diameter, 1.3-cm thick bed walls, and was 20 cm in height. Li_2O charge weight and test conditions were similar to the previous run, but a higher CO_2 concentration was maintained throughout the run, with input CO_2 controlled on a demand basis. Profiles (humidity again limited by hygrometer range) are given in figure 24, data in table XV. Cumulative H_2O/CO_2 molar ratio was 1.7 at the 4-hour point.

Run 376-11

The previous results suggested that performance of the passive displays might be improved by increased gas recirculation rate. Higher flow would increase moisture input rate to the chamber and, hence, raise ambient humidity. Chamber superficial gas velocity was increased to 38.7 cm/min versus 18 cm/min previously used, thus increasing moisture input to 19.5 g/hr. A wider range (5% to 95% R.H.) electric hygrometer was installed to allow calculation of the H_2O (absorbed)/CO_2 (absorbed) molar ratio as well as the H_2O (input)/CO_2 (input) ratio. A cylindrical configuration and granular Li_2O were used, both identical to the previous run. CO_2 feed was controlled on a demand basis. In the first 45 minutes of test, the input ratio was 1.33, whereas the molar ratio H_2O (absorbed)/CO_2 (input) was only 0.86 which explains the steady CO_2 concentration rise shown in the profiles of figure 25. The rate of initial CO_2 absorption via reaction (3) was limited by the rate of reaction (2).

$$Li_2O + H_2O \rightarrow 2LiOH \qquad (2)$$

$$2LiOH + CO_2 \rightarrow Li_2CO_3 + H_2O \text{ (absorbed)} \qquad (3)$$

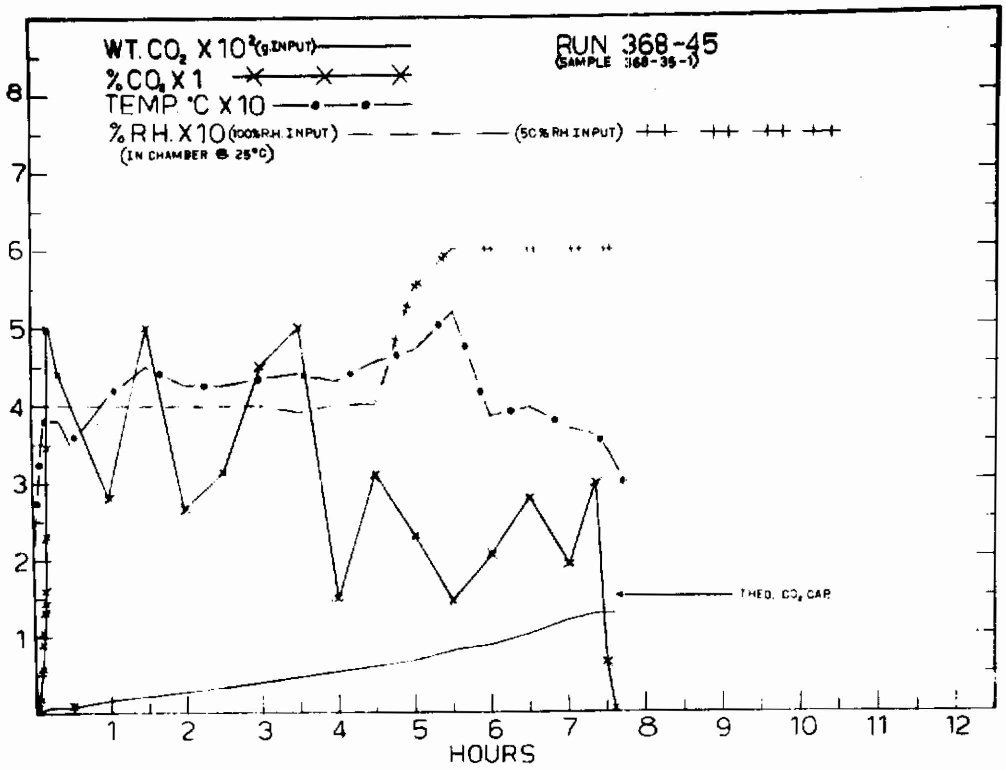

Fig. 24. Passive Test Profiles, Granule Cylindrical Bed

Run 368-45

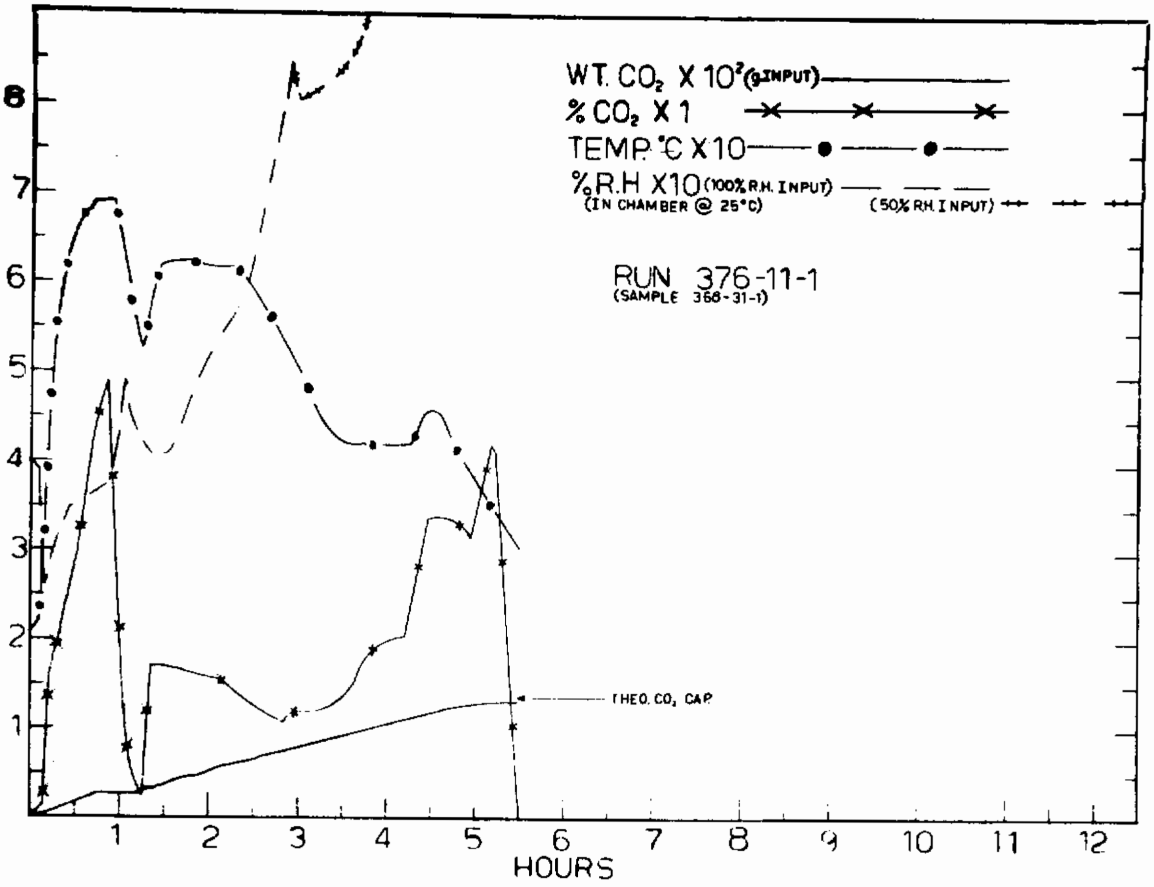

Fig. 25. Passive Test Profiles, Granule Cylindrical Bed

Run 376-11

CO_2 input was cutoff and moisture feed continued until chamber concentration had dropped to 0.45% CO_2. At this point, cumulative H_2O (input)/CO_2 (input) ratio was 2.04 and the cumulative H_2O (absorbed)/CO_2 (input) ratio was 1.3. These results indicated the passive array could maintain a low ambient CO_2 concentration, provided H_2O (input)/CO_2 (input) ratio was near 2. Test data are given in table XV.

Runs 376-13 and 376-15

Cylindrical configurations, demand basis CO_2 feed, and test conditions were similar to the previous run. However bulk density of the granular Li_2O was increased to 0.34 g/cc in Run 376-13 and 0.24 g/cc in Run 376-15. Figures 26 and 27 and table XV give results.

Runs 376-16 and 376-17

The need for a high percentage of open area in granular bed supports was studied by testing beds enclosed in tightly woven monofilament polypropylene fabric. Belt-type configurations, shown in figure 28 and 29, were fabricated by folding 42-cm-wide fabric in half and sewing or stapling seams to form a series of pouches for the granular Li_2O charge. The fabric (6-mil yarn, 148 by 74 filaments per inch, weight 116 g/m^2) had only about 6.2% open area. Test profiles for Run 376-16, made with 4- by 10-mesh granules at 0.11 g/cc bulk density, are given in figure 30. Profiles for Run 376-17, 10- by 30-mesh granules at 0.18 g/cc bulk density, are shown in figure 31. Table XV gives test data. Results indicated the low open area fabric did not significantly hinder CO_2 and moisture access to the bed.

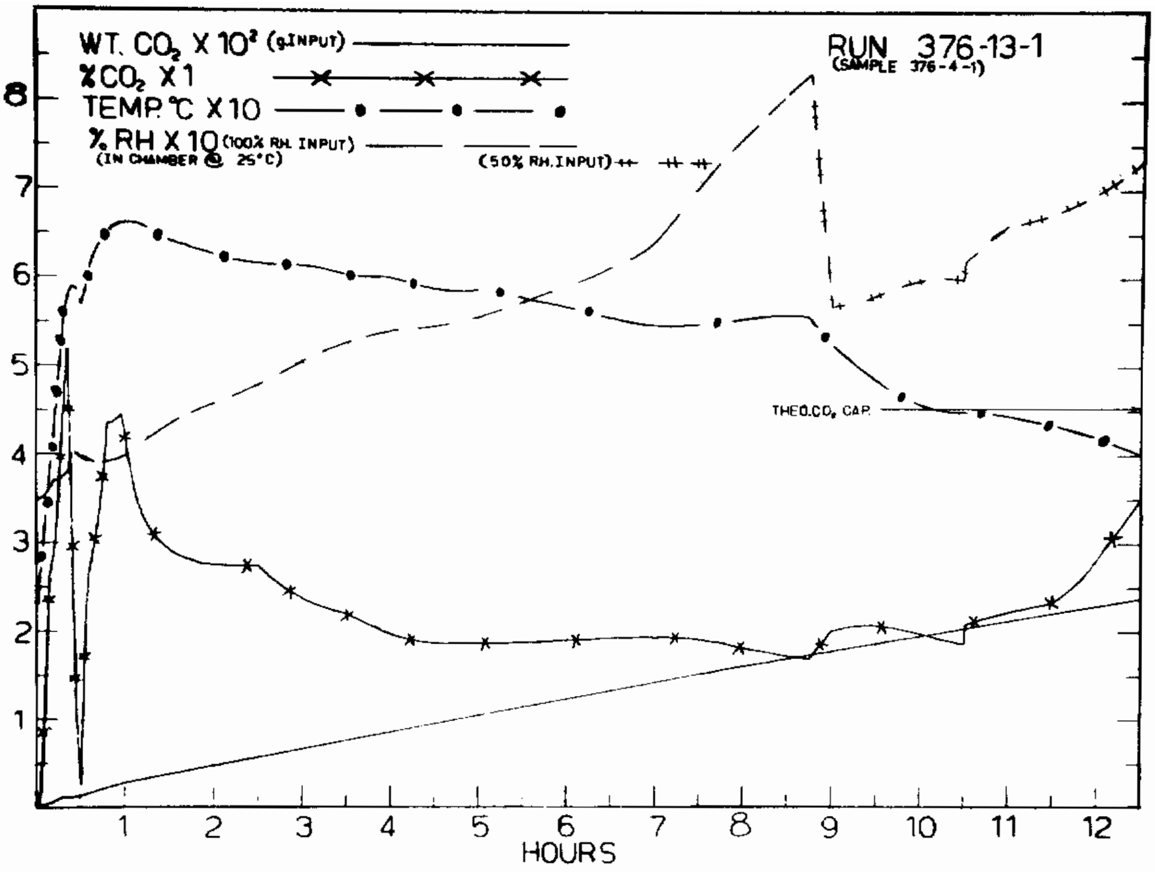

Fig. 26. Passive Test Profiles, Granule Cylindrical Bed

Run 376-13

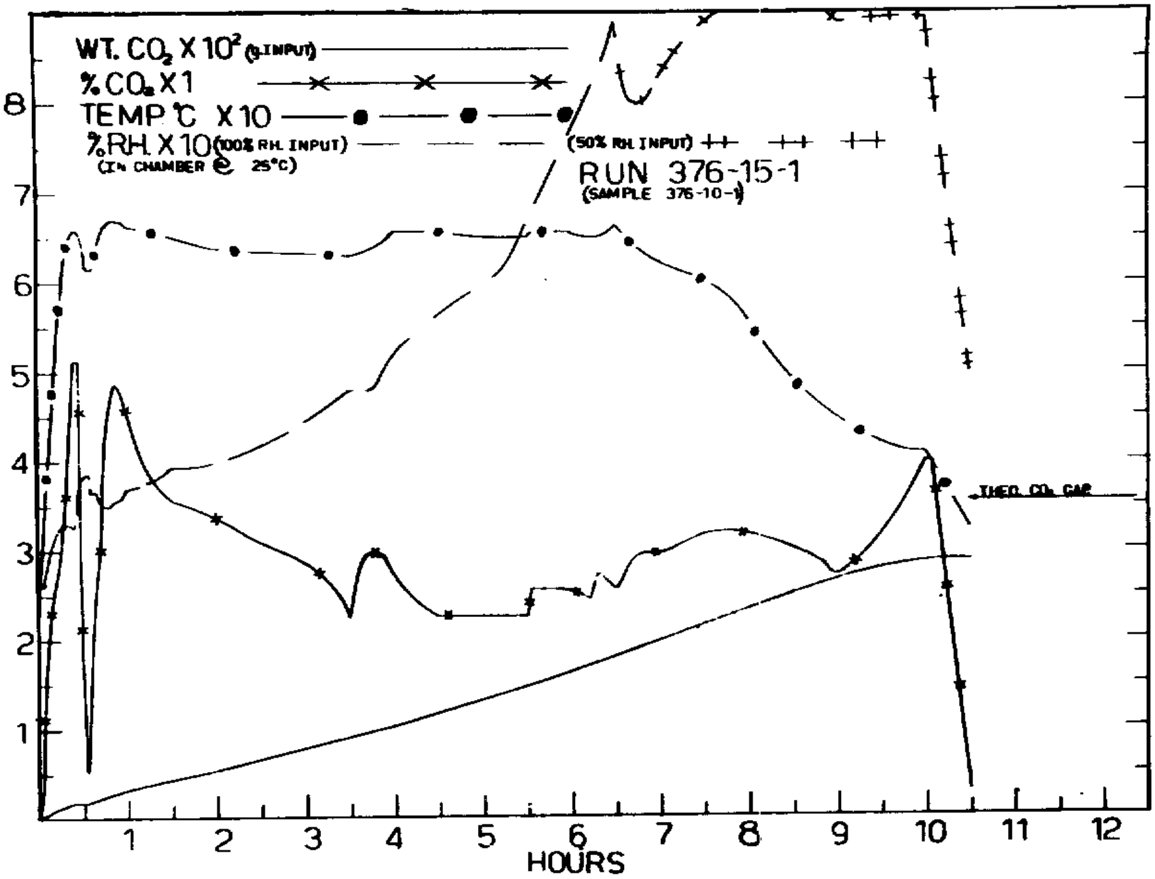

Fig. 27. Passive Test Profiles, Granule Cylindrical Bed

Run 376-15

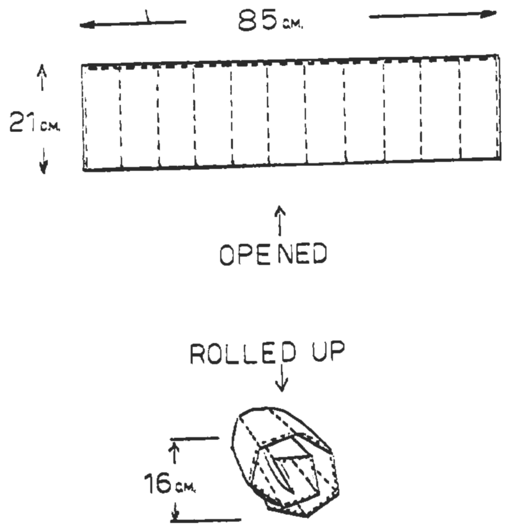

POUCHES MADE FROM POLYPROPYLENE CLOTH

Fig. 28. Granule Belt Configuration

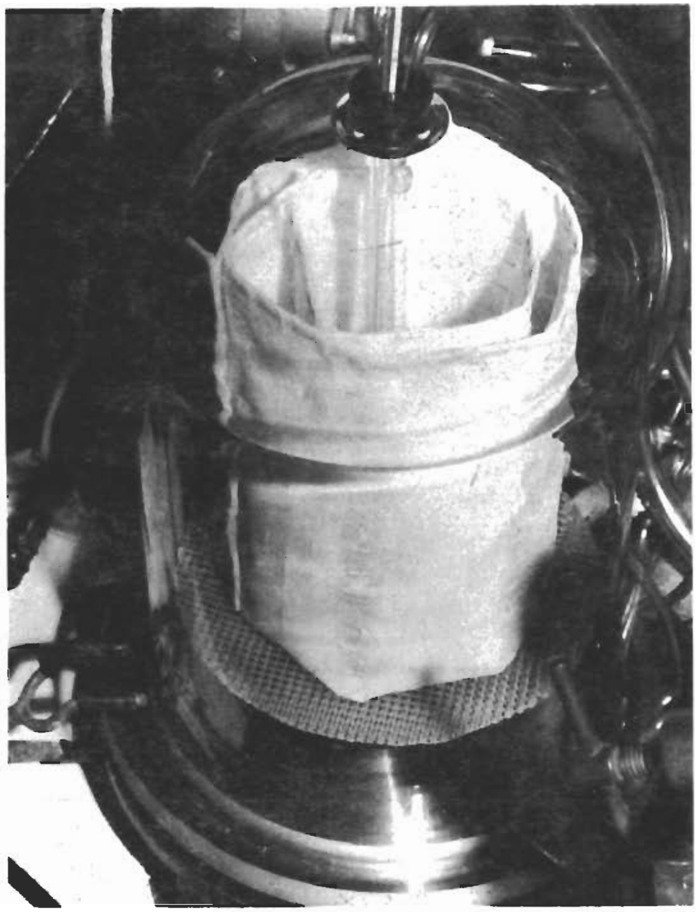

Fig. 29. Granule Belt Configuration
In Test Apparatus

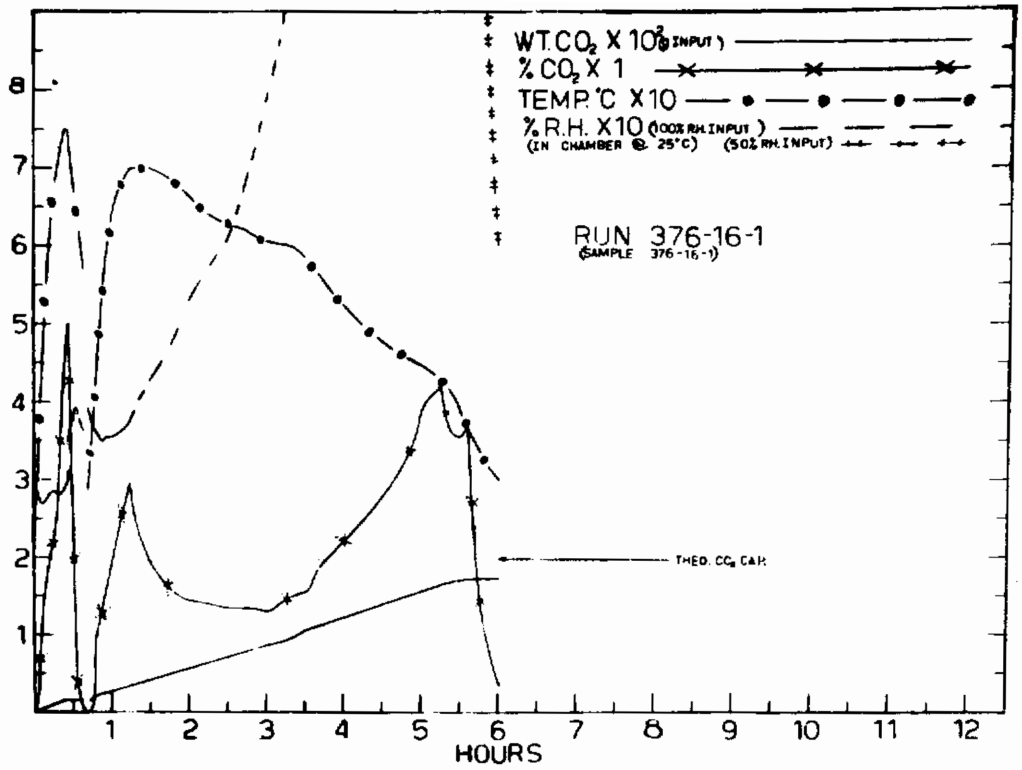

Fig. 30. Passive Test Profiles, Granule Belt

Run 376-16-1

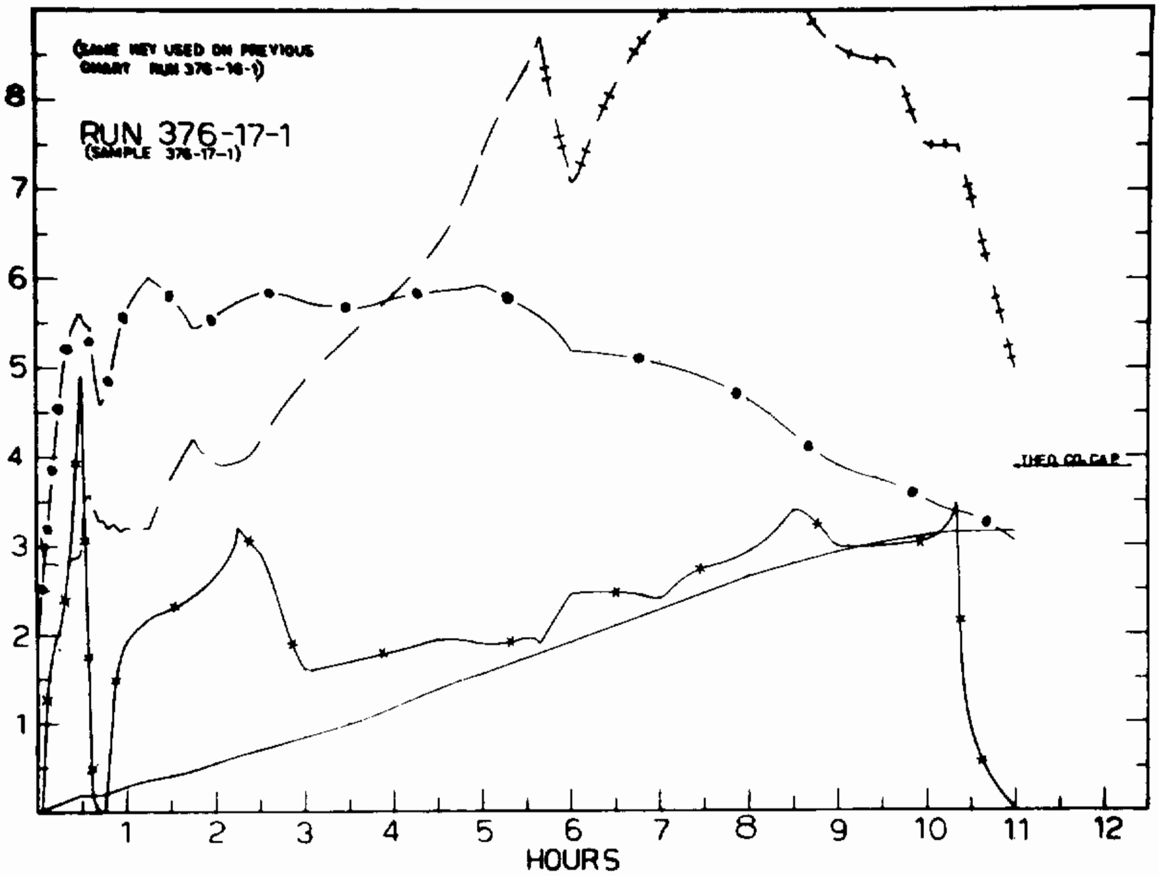

Fig. 31. Passive Test Profiles, Granule Belt

Run 376-17-1

4. DYNAMIC TESTS

a. Dynamic Test Unit

A supported bed, forced circulation, type CO_2 absorber was fabricated and mounted within the test chamber as shown in figures 32 and 33. Operating characteristics with the motor-blower at 24 to 27 volts and a 4- by 10-mesh granular Li_2O bed in place were as follows--

Gas rate through bed	214 liters/min
Average velocity across bed face plate	15 m/min
Blower exhaust velocity	780 m/min
Pressure loss across granule bed	0.16 mm Hg
Bed - diameter	13.5 cm
depth	9.0 cm
volume	1.29 liters
Weights - blower	79 g
- unit, less Li_2O	623 g

b. Tests

Run 376-19

Bulk density of the granular charge was 0.10 g/cc. The test profile given in figure 34 was similar to the passive test experience in demonstrating that hydrolysis must proceed carbonation. As before, the CO_2 feed was cutoff to increase the H_2O (input)/CO_2 (input) molar ratio, and subsequent CO_2 feed was on a demand basis. At 2 hours, a sharp increase in absorption occurred, followed by falling chamber CO_2 concentration and rising relative humidity. At the 2-hour point, 69.3 g CO_2 and 39 g H_2O had been fed to the chamber. The corresponding

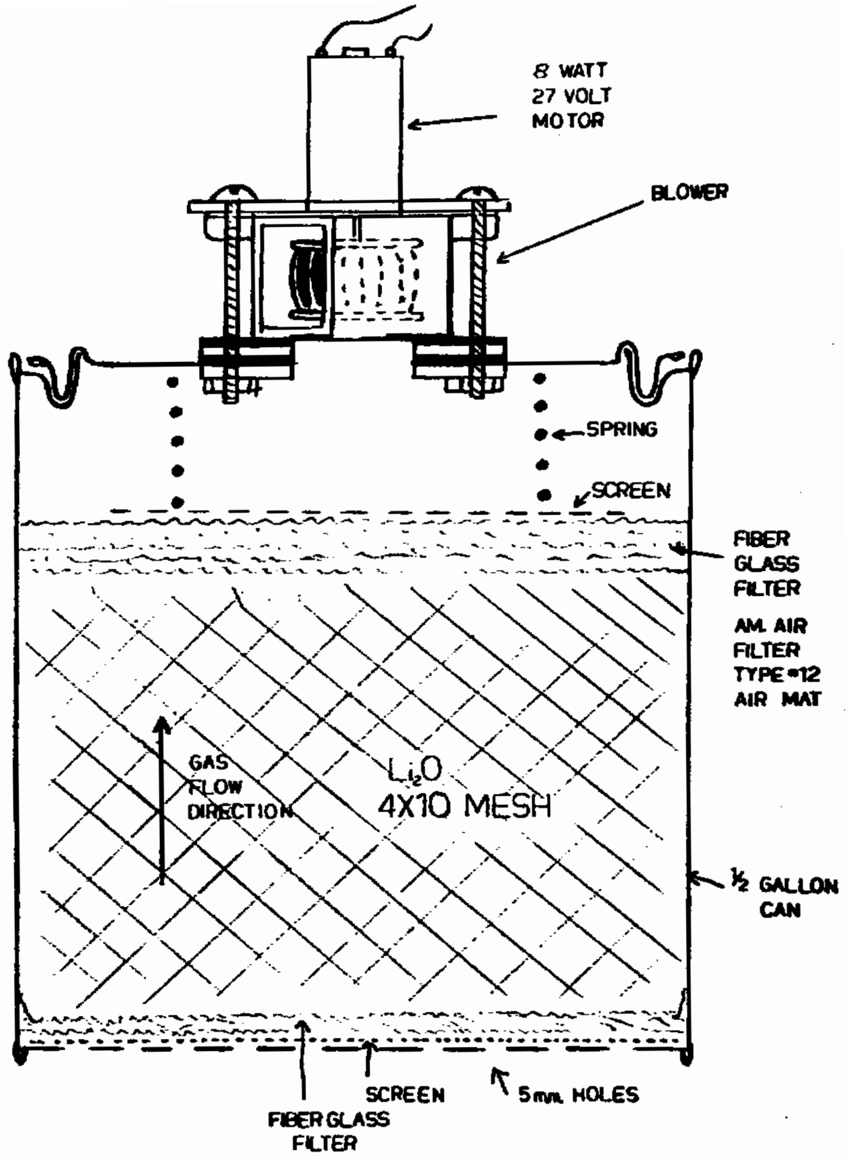

Fig. 32. Dynamic Absorber

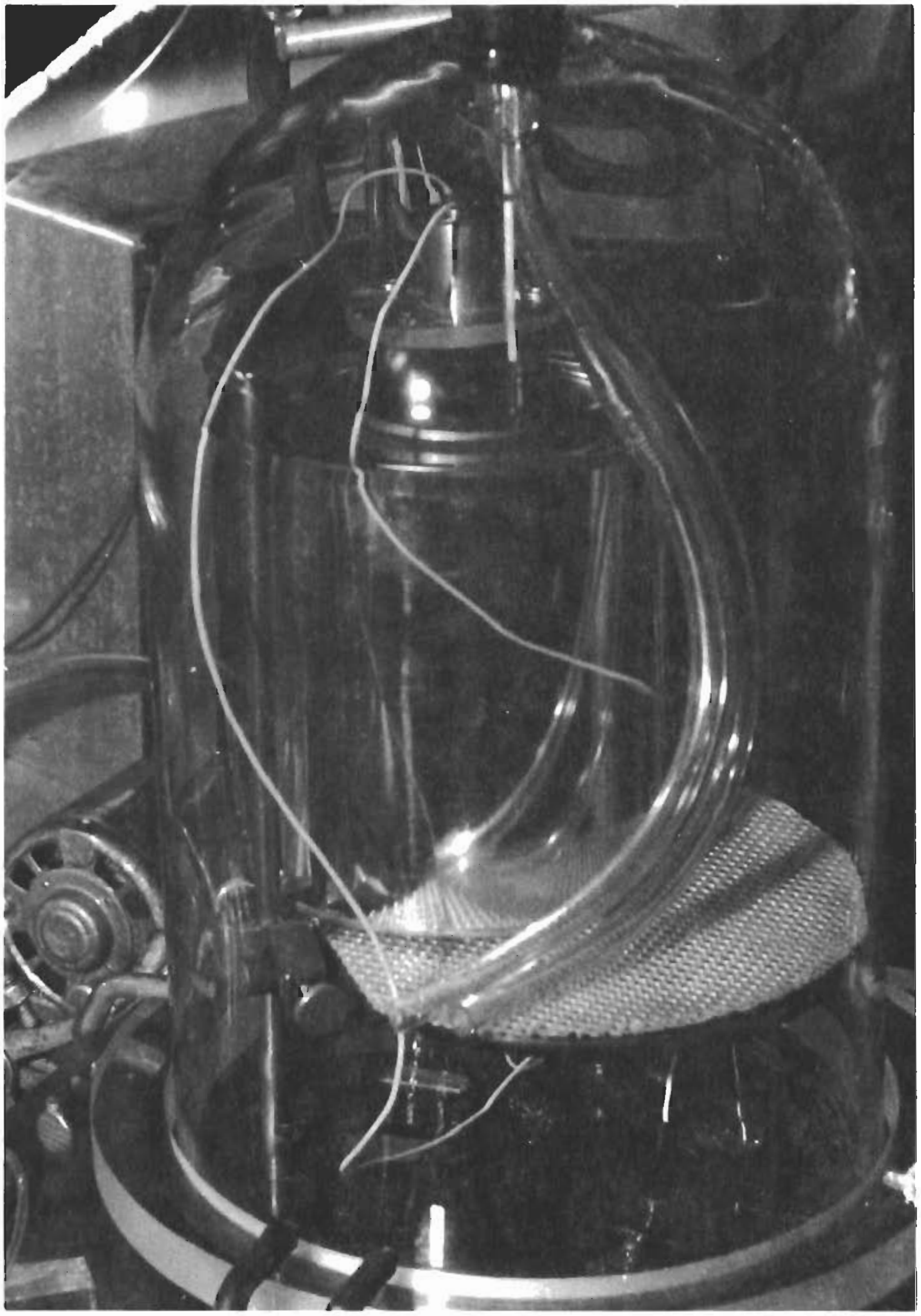

Fig. 33. Dynamic Absorber In Test Apparatus

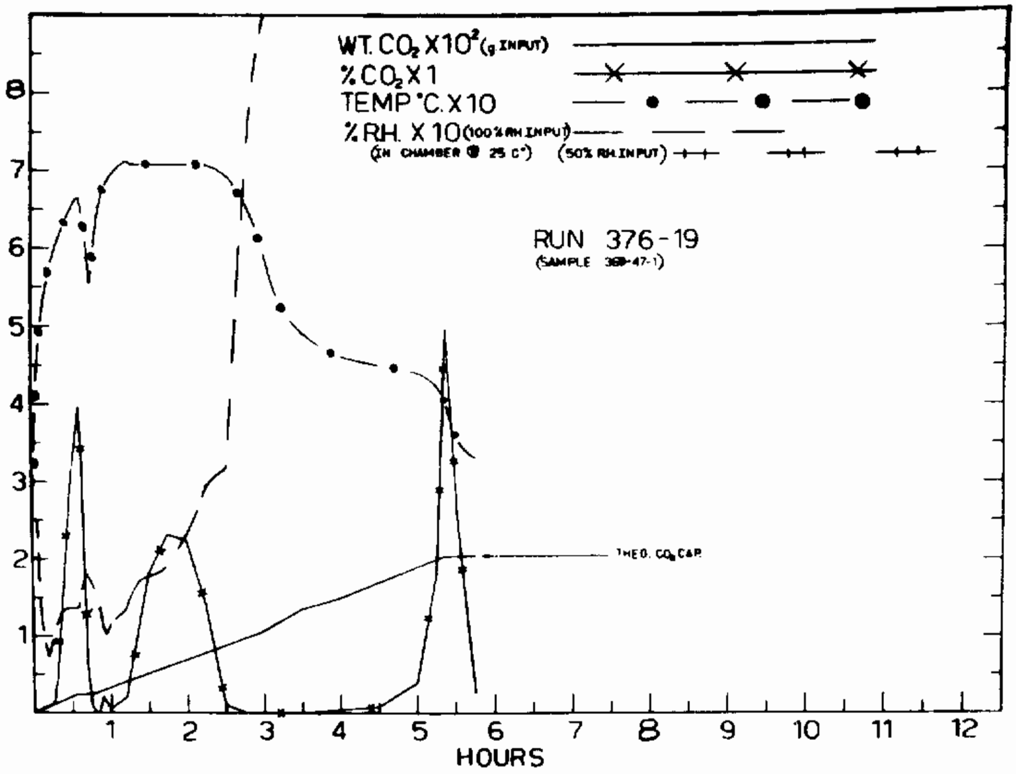

Fig. 34. Dynamic Test Profiles

Run 376-19

cumulative molar ratios were 1.3 H_2O (input)/CO_2 (input) and 1.1 H_2O (absorbed)/CO_2 (input). At the 2.5-hour point, calculations indicate 112 g Li_2O had been carbonated and hydrated via reaction (1).

$$2Li_2O + CO_2 + H_2O \rightarrow Li_2CO_3 + 2LiOH \qquad (1)$$

Since the initial sample charge was 126.4 g Li_2O, little oxide remained at this time and a sharp rise in humidity signaled the occurrence of reaction (5):

$$2LiOH + CO_2 \rightarrow Li_2CO_3 + H_2O\ (gas) \qquad (5)$$

Absorption after 2.5 hours proceeded at a high and steady rate, maintaining low chamber CO_2 concentration. Test data are given in table XV.

Run 376-38

Test conditions were identical with the previous run, except that the bulk density of the charge was 0.31 g/cc and charge weight was correspondingly greater. Profiles are given in figure 35 (notation "a" indicates interruption of the run with the absorbent removed from the chamber, stored overnight, and restarted the next day). Table XV gives test data.

c. Analysis of Results

Results with granular Li_2O arrays, whether under passive or dynamic conditions, indicate the cumulative H_2O (input)/CO_2 (input) must be well above unity to initiate absorption and maintain low chamber CO_2 concentration during initial operation. Experience suggests this ratio should be no less than 2 for passive displays (at 38 cm/min gas velocity) and no less than 1.44 for granular dynamic beds. Product analyses

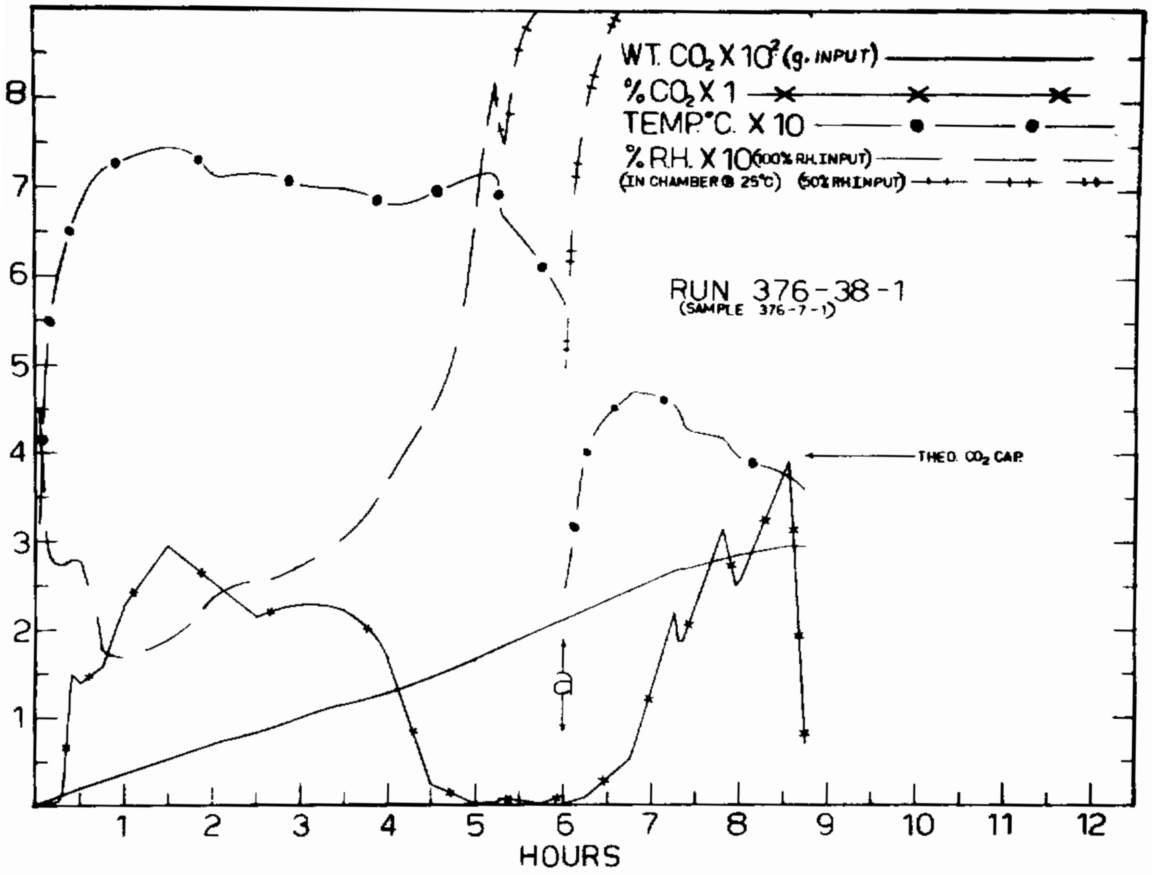

Fig. 35. Dynamic Test Profiles

Run 376-38-1

indicate that reactions (1) and (5)

$$2Li_2O + CO_2 + H_2O \rightarrow Li_2CO_3 + 2LiOH \qquad (1)$$

$$2LiOH + CO_2 \rightarrow Li_2CO_3 + H_2O \text{ (gas)} \qquad (5)$$

can proceed concurrently in passive operation even while a relatively large amount of unreacted Li_2O is available. Under dynamic operation, the consumption of Li_2O via reaction (1) is more complete before reaction (5) proceeds. Therefore, reaction mechanism in the absorption process is influenced by the design of the system.

SECTION IV

ABSORBER DEVELOPMENT AND TESTING AT ONE ATMOSPHERE

1. APPARATUS

Tests were conducted in a large (118.3 cm long, 60.6 cm wide, 58.7 cm high) environmental chamber fabricated of "Plexiglass" and fitted with glove ports, gas expansion bag, and electrical power, gas, and instation connections. Samples were introduced through an airlock chamber extending (35 cm diameter, 44 cm long) from one end of the main chamber. In operation the main and airlock chambers were connected making total chamber volume about 463 liters (16.3 ft^3). A blower mounted within the chamber circulated the chamber gas through a humidity control circuit at the rate of 168 liters/min. A 2-liter flask in this circuit, filled with crumpled absorbent paper to provide high surface area, was heated or cooled to evaporate or condense water as required. The evaporation or condensation rate was manually controlled to maintain 50% R.H. in the main chamber.

With the chamber atmosphere at design conditions for absorption, i.e. 25 C, 50% R.H. (11.8 mm Hg partial pressure H_2O), and 1% CO_2 (7.6 mm Hg partial pressure CO_2) the ambient H_2O/CO_2 molar ratio would exceed unity, a condition suitable for CO_2 absorption as established in section III. Gas returning to the main chamber from the humidity control circuit was introduced through a porous dispersing tube. Measurements indicated the return gas did not impart a detectable velocity to the gas volume within the main chamber. Gas velocities within the chamber itself were produced by a 40-watt fan mounted in the chamber and controlled by a "Powerstat". The chamber gas velocities were measured by an anemometer located within the chamber and manipulated through the glove ports. With the fan operating, gas circulation within the chamber, viewed from above, was counterclockwise. Table XVI gives gas velocity, parallel and perpendicular to this general circulatory movement, for various locations within the chamber. Chamber gas temperature, humidity, and CO_2 concentration were continuously recorded. To insure collection of representative mixed samples of chamber gas, samples were simultaneously pumped from each corner of the chamber via sampling tubes of identical length. Temperature measurements were taken at the downstream gas end of dynamic and semi-dynamic configurations. For passive configurations, temperature was measured on the center surface of the absorbent. A diagram of the apparatus showing gas sampling points, humidity control circuit , CO_2 feed, and location of the blower and fan, is given in figure 36.

TABLE XVI

CHAMBER GAS VELOCITIES WITH FAN OPERATING

Direction--	Parallel To Main Gas Flow		Perpendicular To Main Gas Flow
Fan Voltage--	55v	110v	55v
Gas Velocity--	m/min	m/min	m/min
Probe Location:			
Above, Behind Fan	6.1	13.7	---
Corner No. 1	8.5	18.3	3.1
Corner No. 2	7.0	13.7	6.1
Position A	10.6	---	3.1
Corner No. 3	8.5	12.8	6.7

The chamber, without absorbent chemical in place but with blower and fan operating, was fed with 46.7 g CO_2/hr. Average

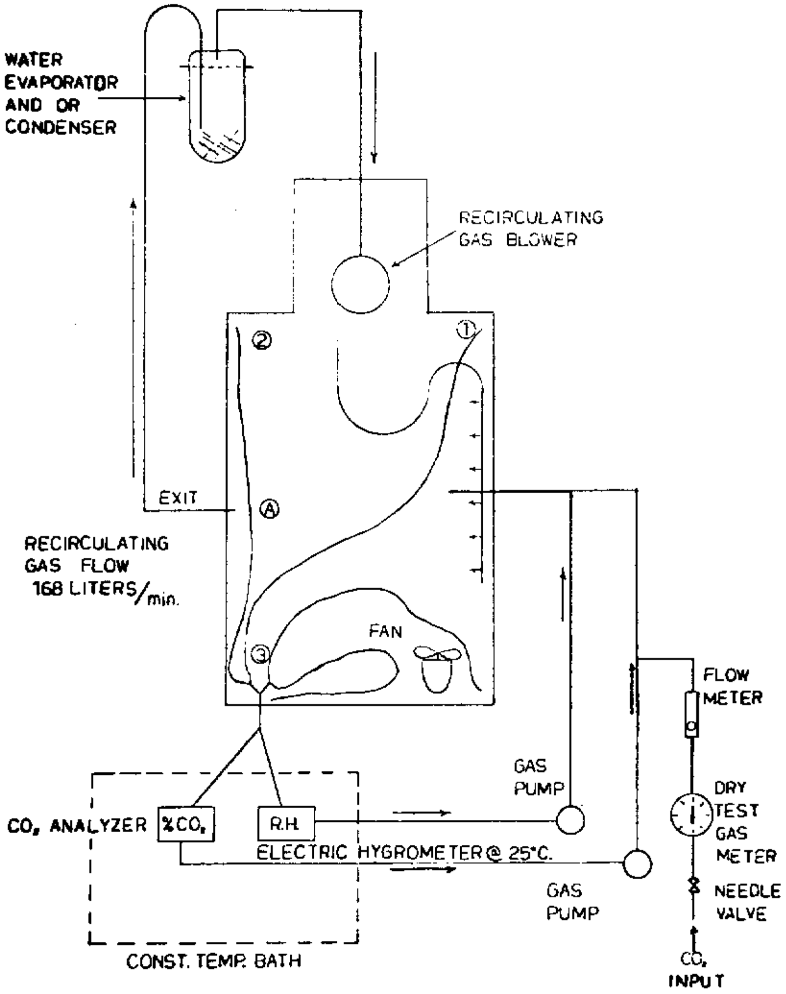

Fig. 36. Apparatus For 1-Atmospnere Tests

human CO_2 production during intense activity is 41.3 g/manhour (reference 10). Table XVII gives the resulting CO_2 concentration buildup with time.

TABLE XVII

CHAMBER CO_2 CONCENTRATION WITH ZERO ABSORPTION

Time Min	Cumulative CO_2 Feed g	Chamber CO_2 Concentration % (Vol)
15	11.2	1.12
30	22.9	2.45
45	35.1	3.60

2. GRANULAR Li_2O DEVELOPMENT

Previous experience had suggested the best process for reactive Li_2O granules was pelletizing high surface area Li_2O_2 powder, decomposing at temperatures consistent with desired bulk density, and crushing and sieving the resulting Li_2O pellets to the appropriate, granule size. Therefore, efforts at improving the dusting characteristics of granular Li_2O were concentrated on this product. Three methods--granule coating, dedusting, and fabric encasement, were investigated as outlined below.

a. Granule Coating

The general technique visualized was that of spraying a light porous film of nonreactive material on the granules, which coated their surface and bounded any dust particles to the surface. Polyethylene and polypropylene, although unreactive with strong bases, proved unsuitable since they are insoluble in suitable solvents. A hydroscopic poly vinylpryrrolidone-vinylacetate copolymer solution (PVP/VA, 70/30 ratio, 50% ethanol solution) appeared suitable and was diluted further with ethanol for spraying. Copolymer to the extent of 5% of the Li_2O weight was applied, and the sprayed granules were heated at 100 C under vacuum until they appeared dry. The treatment did not improve dusting, and the granules had a strong sweet odor.

b. Dedusting

Observations during hardness testing (basically a measure of attrition during sieving) suggested that granule hardness and dusting might be improved by controlled attrition. The principle was confirmed when a mixture of three granular samples (Nos. 376-10, 376-7, 376-4) with hardness values of 67, 66, and 79 yielded a value of 99.8 on retesting. The technique was studied further by devising a deduster consisting of an inclined rotating (60 rpm) container fitted with a 20-mesh, metal screen at the bottom and a gas inlet at the top. Dry gas at 5 to 15 liters/min was passed through the rotating Li_2O charge, and it exited with entrained dust particles through the screen bottom. The apparatus is shown in figure 37.

As shown in table XVIII, the dedusting procedure improved both the hardness and bulk density of granular oxide prepared from pelletized Li_2O_2 (i.e., process 2a-5 of table II). Granules prepared by decomposing Li_2O_2 powder (process 2a-1) were merely reduced to smaller size during dedusting, with no improvement in hardness. Microphotographs of a Li_2O granule before and after dedusting, figures 38 and 39, show a distinct change in

Fig. 37. Dedusting Apparatus

TABLE XVIII

DEDUSTING OF 4- by 10-MESH GRANULAR Li_2O

Sample No.	Tumbling Time hr	Bulk Density Before g/cc	Bulk Density After g/cc	Wt Loss -20 Mesh %	Hardness No.
361-20-1(a)	24.0	0.21	0.25	7.9	97
361-40-1(b)	2.5	0.12	0.14	14.3	61

Notes: (a) Prepared from compressed Li_2O_2

(b) Prepared from Li_2O_2 powder

the surface and periphery of the granule indicating fine particles and fragile projections have been removed.

c. Fabric Encasement

The dust-retention capability of various support fabrics for granular beds was studied. A dusting test was devised similar to the KO_2 dusting test of McGoff (reference 11). Fabric envelopes were filled with 10 g charges of Li_2O, the open ends were folded over twice and stapled, and each envelope was enclosed in a polyethylene bag. The samples were vibrated in a Rotap machine at 150 cycles/min for 30 minutes. Following vibration, dust collected in the plastic bag was washed out with water and the solution was titrated with standard acid to the methyl orange end point. Table XIX gives results. The data confirm the benefit of rotary dedusting by showing that 4- by 10-mesh granule is less dusty than the 10- by 30-mesh size. The data also indicate that closely woven fabric supports retard dusting. In future work, substituting multifilament fiber glass

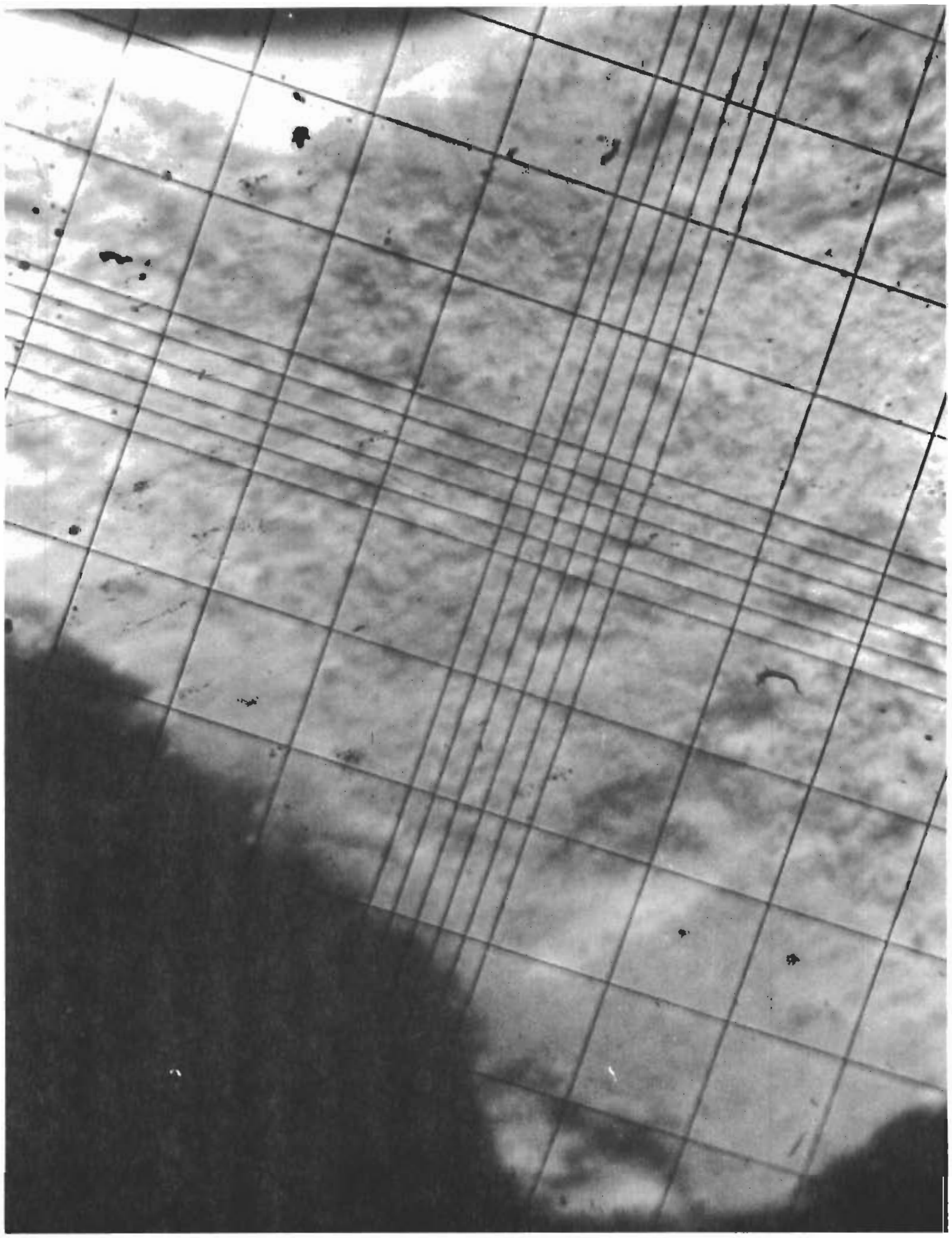

Fig. 38. Microphotograph, Li_2O Granule Before Dedusting

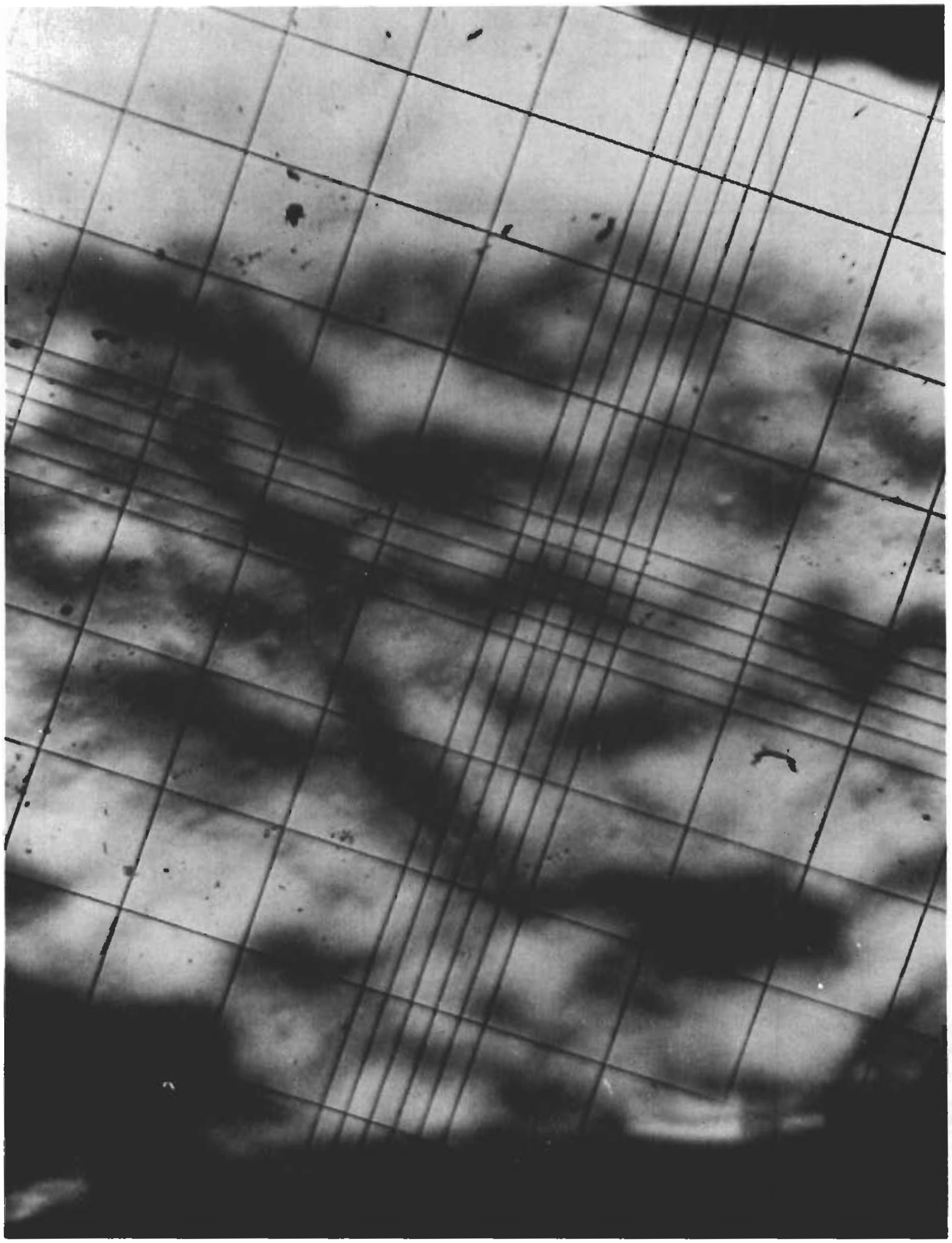

Fig. 39. Microphotograph, Li_2O Granule After Dedusting

TABLE XIX

DUSTING TESTS WITH FABRIC ENCASEMENT

Fabric Type	Granular Li_2O Sample		Li_2O Dust mg/g granules
a	Non-Dedusted	10- by 30-mesh	1.09
a	Dedusted	10- by 30-mesh	0.12
a	Dedusted	4- by 10-mesh	0.09
b	Non-Dedusted	10- by 30-mesh	0.19
b	Dedusted	10- by 30-mesh	0.13
b	Dedusted	4- by 10-mesh	0.08
c	Dedusted	4- by 10-mesh	0.21

Notes:
a. Monofilament polypropylene cloth, 6% open area, No. 6722200, Chicopee Mfg. Co., Cornelia, Ga.

b. Multifilament polypropylene cloth, no visible open area, 60 x 36 count, 2/2 twill weave, 630 mil yarn size, 8.7 oz./sq. yd., No. 6720600, supplier as above.

c. Monofilament polypropylene netting, 25% open area, 52 mesh, No. 6951500, supplier as above.

fabric of equivalent porosity appears desirable since this material can withstand higher temperatures than the polypropylene fabric.

3. SOLID Li_2O CONFIGURATION DEVELOPMENT

The swelling and sintering properties of Li_2O_2 on decomposing, as described in section I, were used to form solid and potentially self-supporting Li_2O configurations. Two variations of the technique were evaluated, one used Li_2O_2 powder and one used Li_2O_2 granules. In the first case, a Li_2O cylinder containing 15 axial holes (further described in section 4 "Configuration Tests" under Run No. 361-26) was prepared by decomposing Li_2O_2 powder. The mold was an aluminum cylinder with perforated plates at each end. Glass rods inserted through the perforations and extending through the cylinder formed the axial holes. Figure 40 shows this shape after decomposition and removal of the plates and rods. The oxide had low strength, tended to crack into loose pieces, and was left in its casing to expedite handling. A second and larger shape (further described under Run No. 361-21) was made in similar fashion except that granular Li_2O_2, produced by pelletizing the powder to 0.8 g/cc pellet density and crushing and sieving, was used. Decomposition at 288 C for 24 hours yielded a hard, sound shape as shown in figure 41. The oxide was tightly bound in the aluminum cylinder and the possibility of breakage precluded removing it from the case.

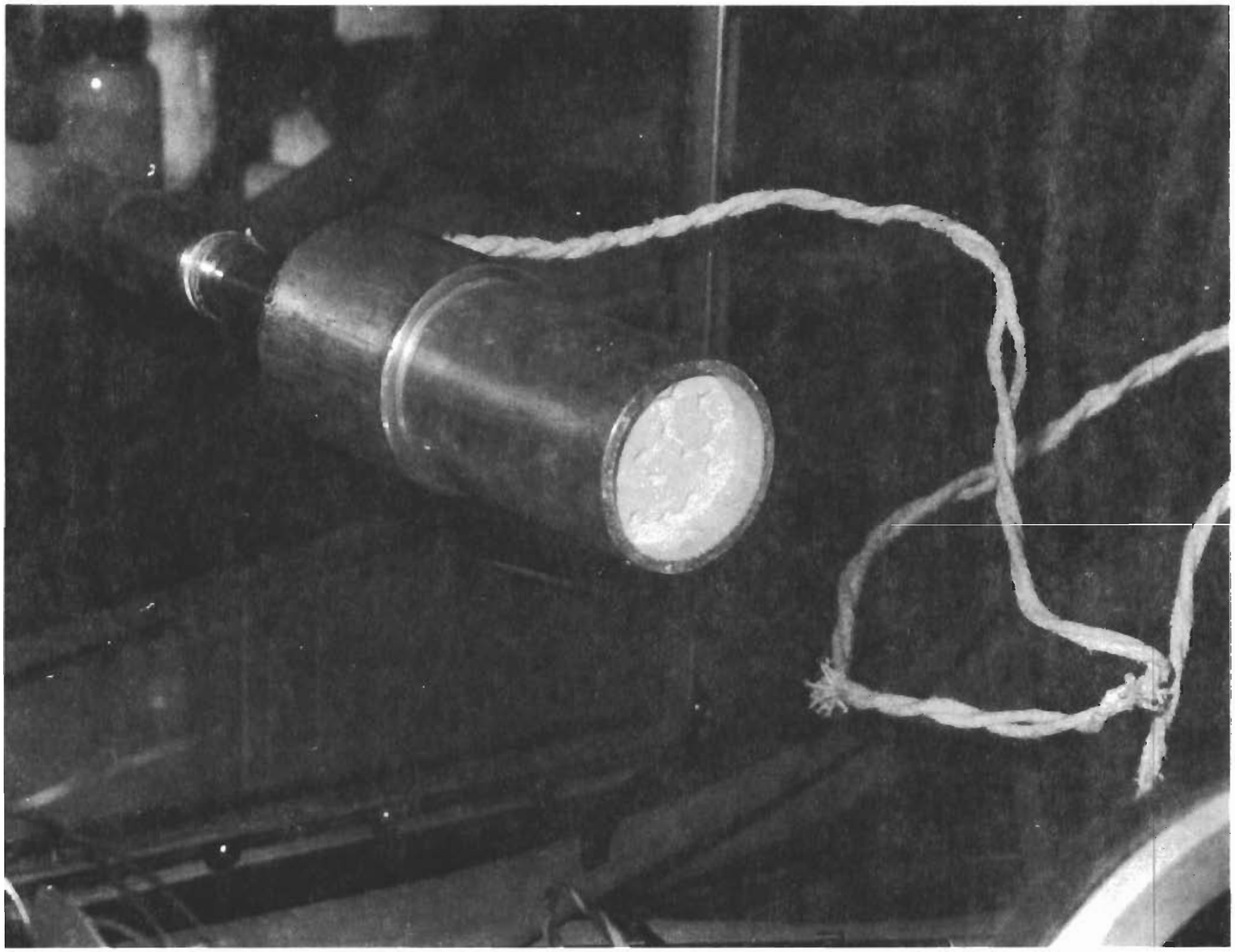

Fig. 40. Pierced Cylinder Configuration, Decomposed Li_2O_2 Powder

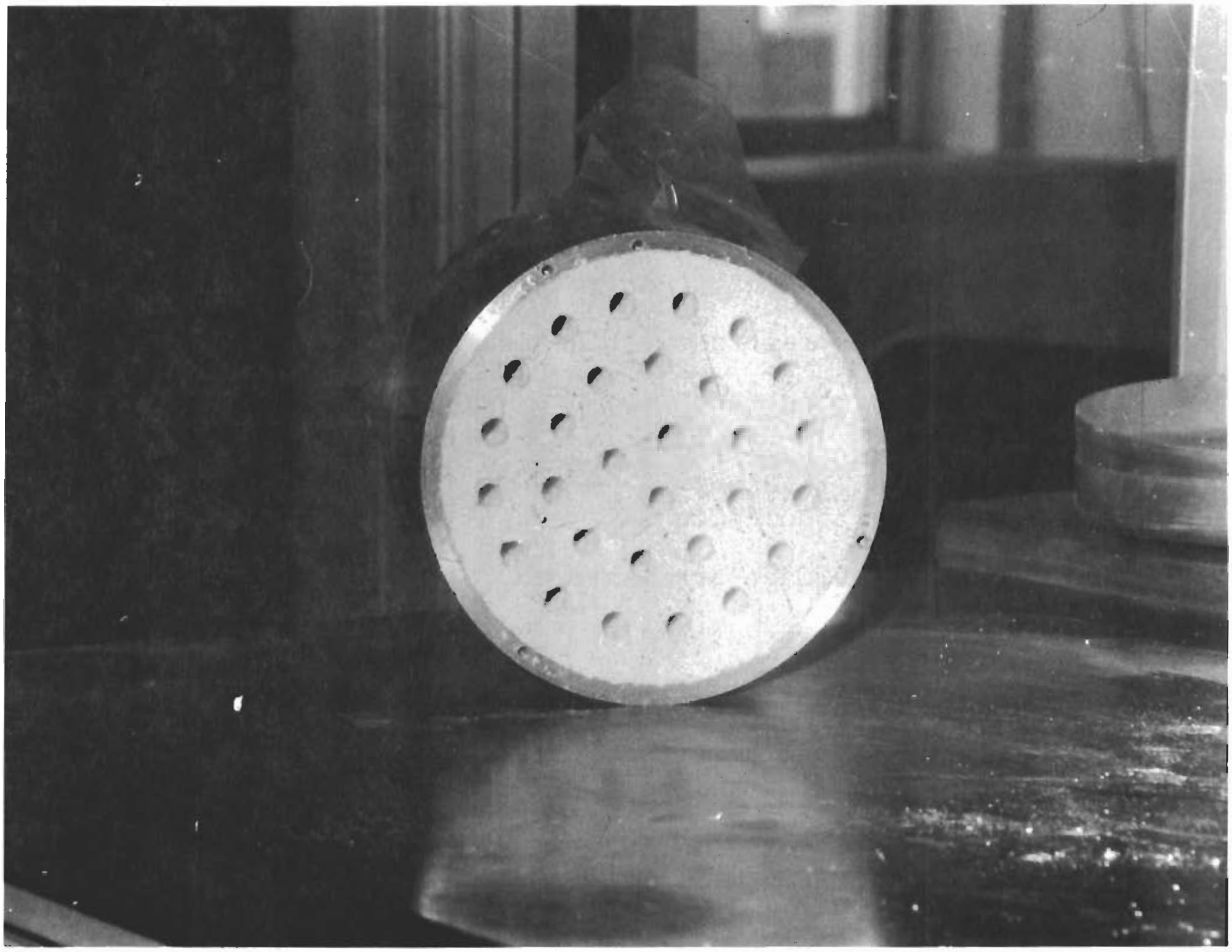

Fig. 41. Pierced Cylinder Configuration, Decomposed Li_2O_2 Granules

4. CONFIGURATION TESTS

Dynamic Test: Runs 361-26 and 361-30

The granular and pierced cylinder forms of the oxide were compared under dynamic conditions with the configurations housed in identical aluminum cylinders. Gas was drawn through each sample at 126 liters/min by connecting the cylinders to the suction side of the humidity control circuit (position A, figure 36). Table XX gives test data. The profiles of figure 42 can best be compared during the first hour where CO_2 feed rates were roughly the same (40 g/hr for run 361-26 and 49 g/hr for run 361-30). The superior absorption rate of the granular form, by virtue of greater surface area exposed to the gas, is evident. A constant CO_2 feed rate was maintained on the granular sample. CO_2 feed to the cylindrical sample was reduced (point A, figure 42) to demonstrate that almost complete utilization of the solid form was feasible.

Passive and Semipassive Test: Run 361-21

A large, pierced-cylinder configuration prepared via Li_2O_2 granule was tested under passive and semipassive conditions. With the configuration initially positioned for passive operation (location A, figure 36), CO_2 absorption was poor. Relocating the unit directly in front of the chamber gas circulating fan as shown in figure 43 yielded a moderate absorption rate. Later in the run, chamber relative humidity was deliberately increased to 90%. No significant change in absorption rate resulted. This indicated maximum H_2O diffusion rate into the sample had already been attained at 50% R.H. and was limited

TABLE XX

TEST DATA OF RUNS 361-26 AND 361-30

Run No. Configuration Type		361-26 Pierced Cylinder(a)	361-30 4- by 10-Mesh Granular
Li_2O charge	- g	88.1	99.0
Configuration size: diam.	- cm	6.3	6.3
length	- cm	13.0	13.0
Configuration density	- g Li_2O/cc	0.22	0.26
Theo. CO_2 capacity	- g	130	145
Sample weight gain	- g	108.3	126.7
Total CO_2 feed	- g	105.0	143.0
Average CO_2 feed	- g/hr	33.3	47.7
2% breakthrough:			
Time	- hr	3.0	2.0
g CO_2 feed/g Li_2O charge		0.91	0.97
Final CO_2 concentration	- %	2.55	3.92
Total run time	- hr	4.5	3.0
Product Analysis:			
	% Li_2O	2.9	0
	% Li_2CO_3	93.3	89.9
	% LiOH	3.8	5.3
	% $LiOH \cdot H_2O$	0	4.8

Notes: (a) 15 axial holes, each 0.6 cm diameter

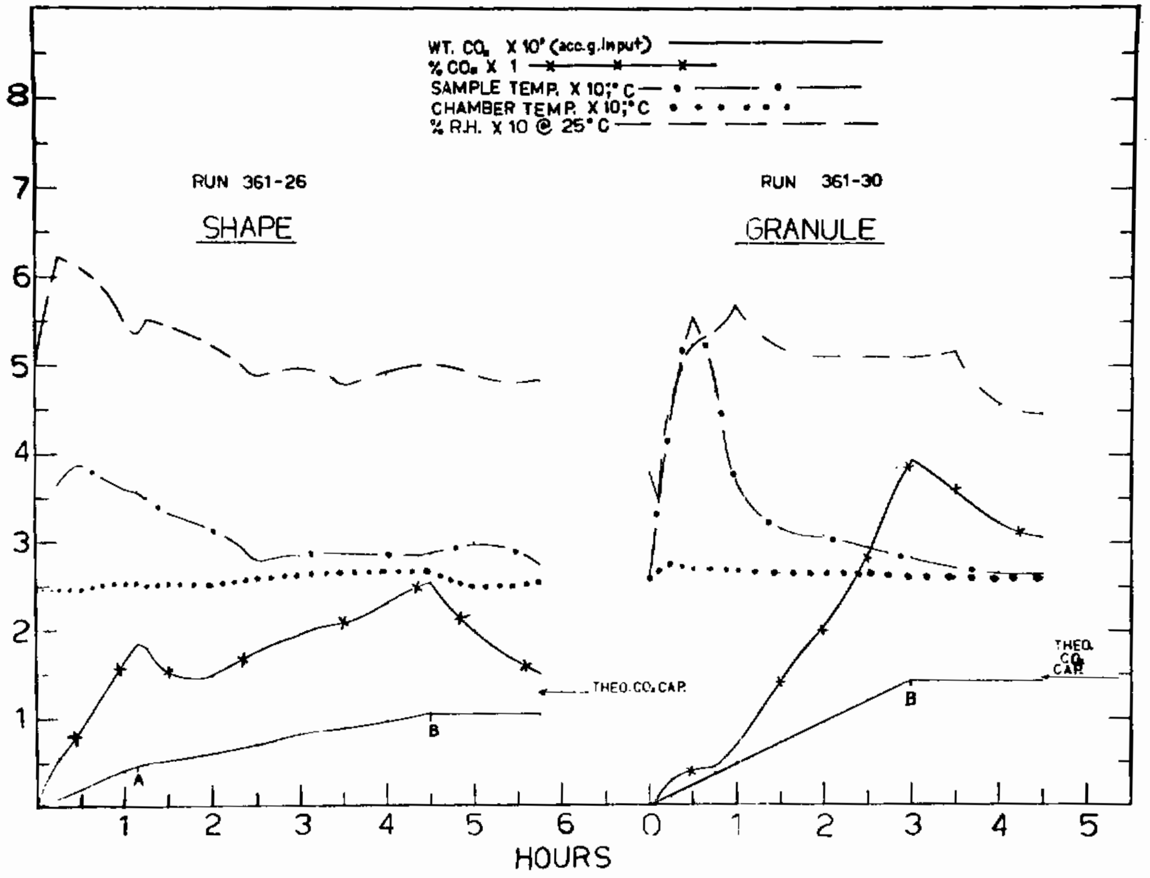

Fig. 42. Test Profiles (Runs 361-26 and 361-30)

Notes: A - CO_2 feed decreased

B - CO_2 feed terminated

Fig. 43. Apparatus Arrangement, Pierced Cylinder Configuration

by configuration design and Li_2O density rather than ambient humidity. The experimentation outline and the resulting effects are illustrated in the profiles of figure 44. Table XXI gives test data. Reaction product analyses indicate the configuration was porous enough, relative to moisture, for complete conversion of the Li_2O to hydroxide.

Passive Tests: Runs 361-29 and 361-34

Two belt-type configurations consisting of granular Li_2O contained in a series of fabric pouches were tested to study the effect of granule size and bed thickness. The pouches were made of identical fabric but in one case contained 4- by 10-mesh granule, and in the second, contained 10- by 30-mesh granule with pouch width reduced to decrease average Li_2O bed thickness. The support fabric was monofilament polypropylene (fabric type a, Table XX) with an average air permeability of 1.02 m^3/min as measured under ASTM Standard Specification D737-46 (i.e., - cfm air through 1 sq. ft. of fabric at 0.5 inches H_2O pressure). The belts were suspended in a passive arrangement (location A, figure 36) as illustrated in figure 45 so that chamber gas flow induced by the circulating fan was mainly parallel to the belt length. The test profiles of figure 46 and the fan voltage adjustments noted thereon suggest that gas velocity changes make little effect on CO_2 absorption rate. Test data given in table XXII indicate the 10- by 30-mesh granule small pouch design was the better of the two-belt configurations.

Passive Tests: Runs 361-43 and 361-46

The above configuration was further studied by

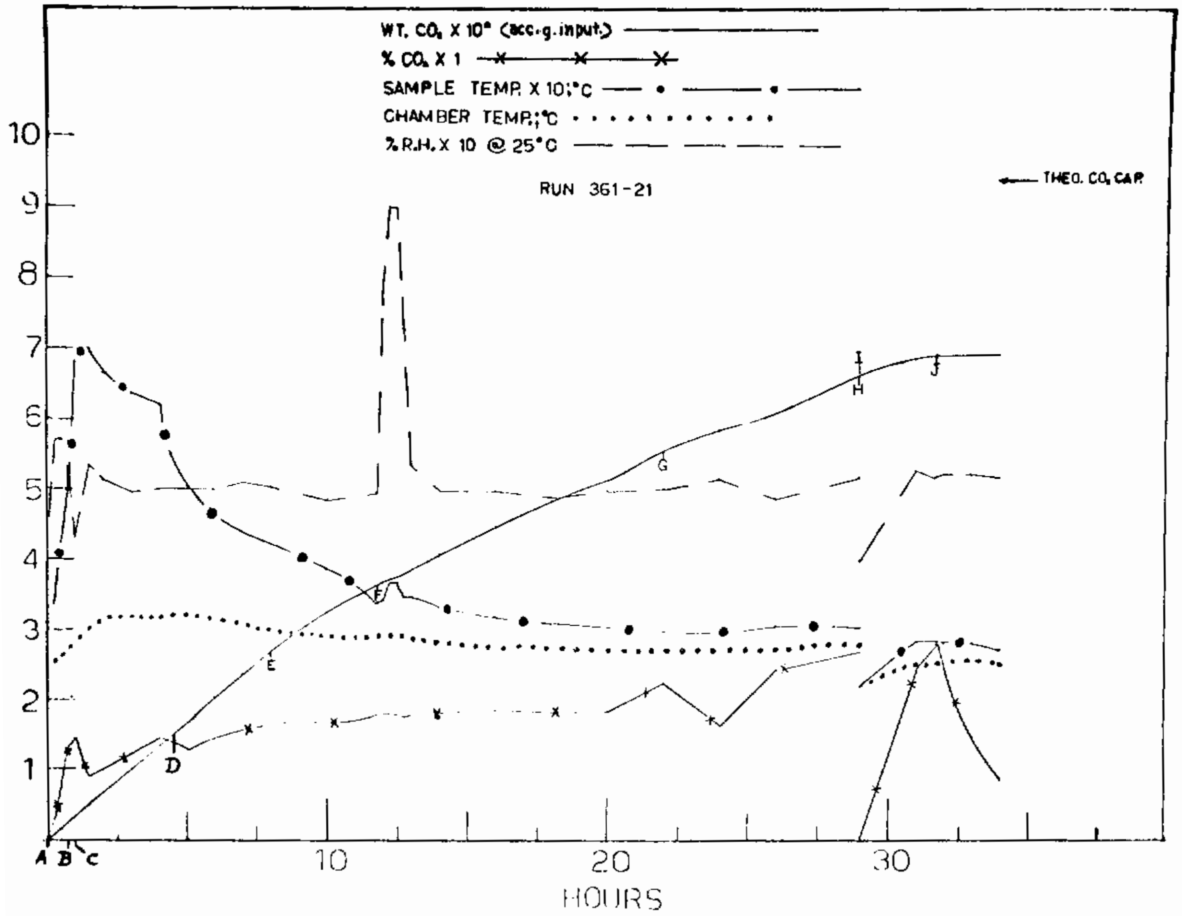

Fig. 44. Test Profiles (Run 361-21)

Notes:

A. & B.	Fan on at 55 Volts Sample positioned at (A) passively.
C.	Sample positioned directly in front of Fan
D.	Increase Fan to 110 Volts
E.	Decrease CO_2 input rate
F.	Determined the affect of increasing relative humidity
G.	New CO_2 cylinder
H.	CO_2 Input off - all power off for 16 hrs
I.	CO_2 Input on - all power on
J.	CO_2 Input off

TABLE XXI

TEST DATA, RUN 361-21

PIERCED CYLINDER, SEMIPASSIVE EXPOSURE

			Pierced Cylinder(a)
Configuration Type			
Li_2O charge		- g	639
Li_2O config. size:	diam.	- cm	16.3
	length	- cm	14.7
	volume(b)	- liter	3.07
Configuration density		- g Li_2O/cc	0.21
Li_2O density		- g/cc	0.25
Theo CO_2 capacity		- g	942
Sample weight gain		- g	809.8
Total CO_2 feed		- g	698
Average CO_2 feed		- g/hr	22.1
2% breakthrough:			
	Time	- hr	14.0
	g CO_2 feed/g Li_2O charge		0.644
	cumulative avg. CO_2 feed	- g/hr	29.4
Final CO_2 concentration		- %	2.8
Total run time		- hr	31.5
Product analysis:			
		% Li_2O	0
		% Li_2CO_3	74.2
		% LiOH	19.7
		% $LiOH \cdot H_2O$	6.1

Notes: (a) 29 axial holes, each 1.0 cm diameter

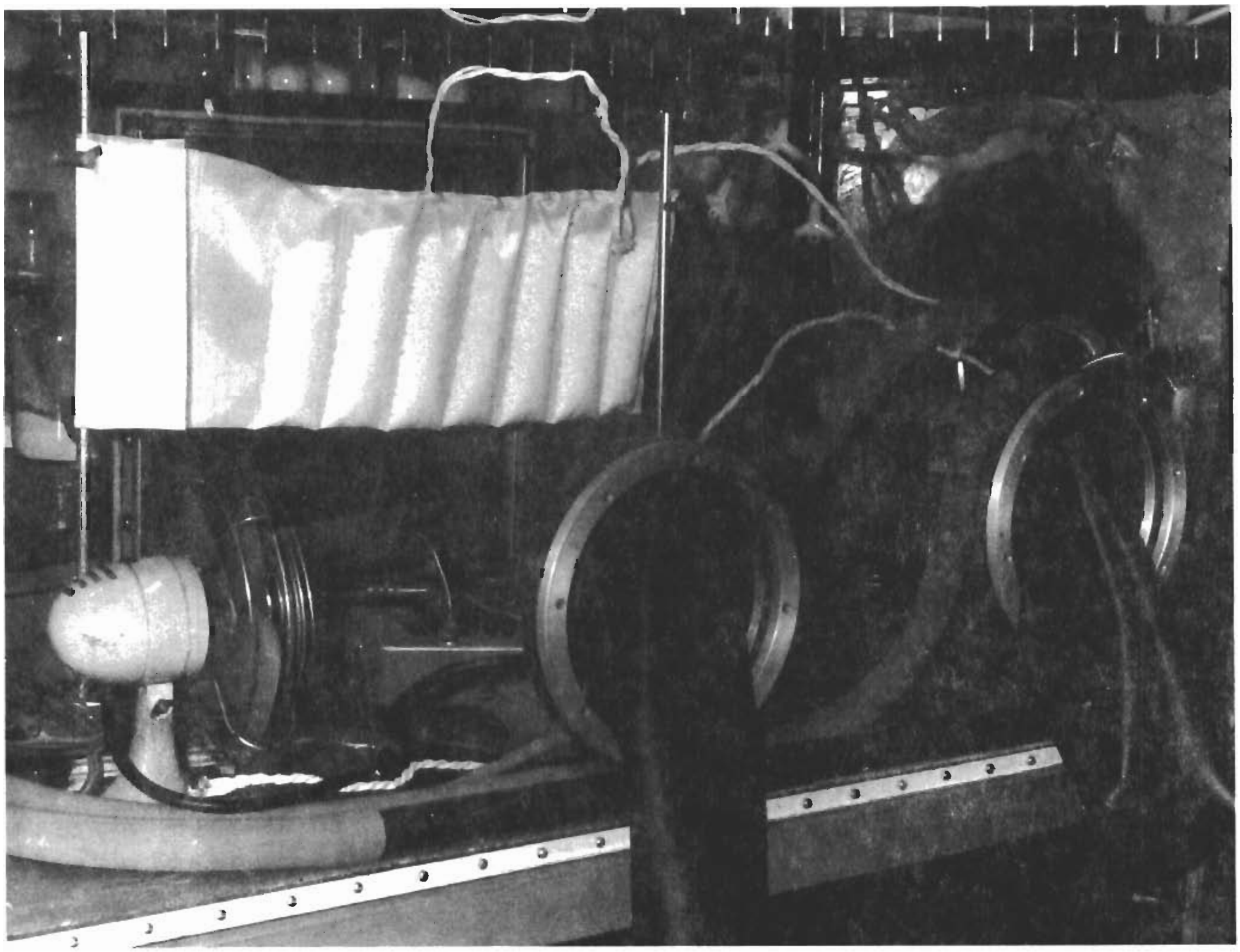

Fig. 45. Apparatus Arrangement, Passive Belt Configuration

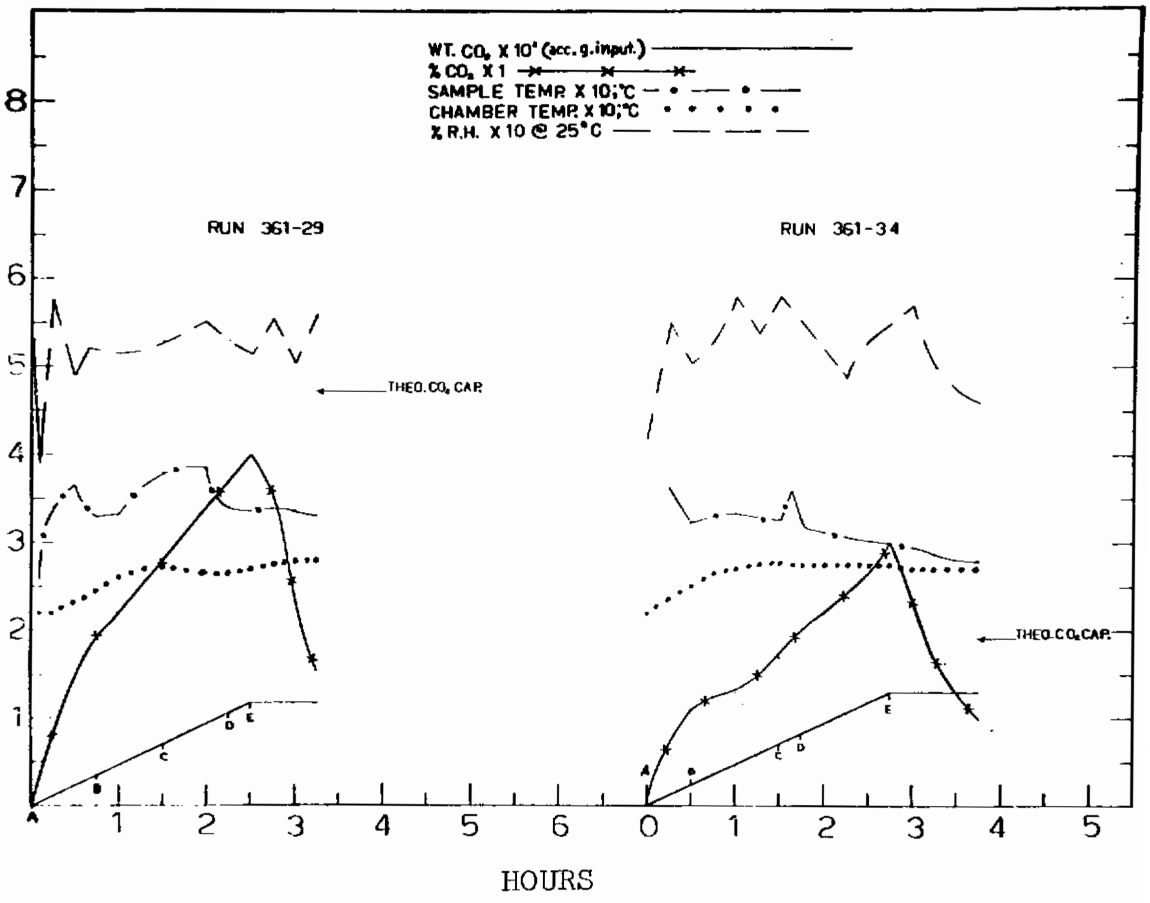

Fig. 46. Test Profiles (Runs 361-29 and 361-34)

Notes:
- A Fan at 55 V
- B Fan at 110 V
- C Fan at 55 V
- D Fan at 110 V
- E CO_2 Input off

TABLE XXII

TEST DATA, RUNS 361-29 AND 361-34

GRANULE BELT, PASSIVE EXPOSURE

Configuration type		Granule Belt	
Run No.		361-29	361-34
Granule mesh size		4 by 10	10 by 30
Li_2O charge	- g	321	129
Configurations:			
Total belt length	- cm	76	76
number of pouches		11	22
width empty pouch	- cm	6.2	3.0
pouch bed height	- cm	20	20
Li_2O bulk density	- g/cc	0.26	0.29
Gas velocity	- m/min	(a)	(a)
Theo. CO_2 capacity	- g	473	191.5
Sample weight gain	- g	46.5	167.4
Total CO_2 feed	- g	117.8	128.2
Average CO_2 feed	- g/hr	47.1	46.9
2% breakthrough:			
Time	- hr	0.83	1.75
g CO_2 feed/g Li_2O charge		0.124	0.638
Final CO_2 concentration	- %	4	3
Total run time	- hr	2.5	2.75
Product analysis:			
	% Li_2O	33.6	0
	% Li_2CO_3	43.1	76.4
	% LiOH	23.4	20.7
	% $LiOH \cdot H_2O$	0	2.9

Notes: (a) Gas velocities with fan at 55 volts, 7.6 m/min parallel and 3.0 m/min perpendicular to belt. At 110 volts, 30.4 m/min parallel and 14.6 m/min perpendicular.

similarly testing two narrow pouch type belts containing low (0.14 g/cc) and high (0.24 g/cc) bulk density 10- by 30-mesh granules. The belts were made of multifilament polypropylene fabric because of superior dust retention (table XIX, fabric b versus fabric a) although ASTM air permeability at 0.59 m^3/min was only half that of the previous fabric. Pouch side seams were sewn with Nylon thread and the tops were sealed by folding over and stapling. To compensate for the reactivity difference caused by bulk density difference, a greater charge of high density granule was used. Also, pouches of the high-density belt (run 361-46) were only partially filled to increase granule and cloth exposure area. The resulting test profiles, figures 47 and 48 were almost identical. The test data of table XXIII indicate performance of the low density configuration was best.

Passive Eight Hour Mission: Run 397-1

A belt design was selected compromising the advantages and penalties established by previous tests. The resulting configuration was passively exposed to a constant rate of CO_2 input of 49.1 g/hr through the entire run. The run profile is shown in figure 49. Table XXIV gives configuration design details and test data.

Dynamic Test: Runs 361-48 and 390-6

The performance of granular beds at two bulk densities, 0.26 and 0.35 g/cc, was tested using the induced draft canister illustrated in figure 32 and described in section III. Figure 50 shows the apparatus arrangement with the canister located in position A (figure 35). The canister blower discharge was

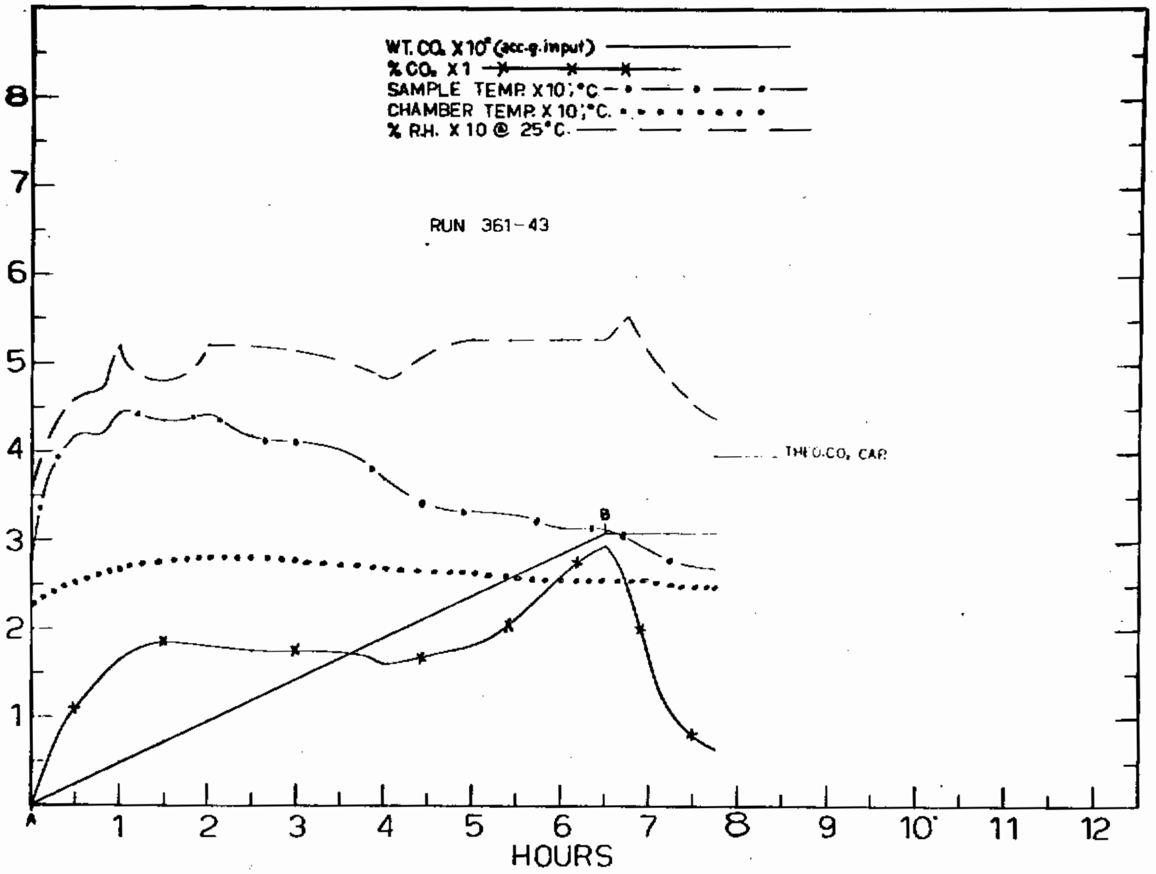

Fig. 47. Test Profiles (Run 361-43)

Notes: A. Start CO₂ Input - Fan at 50 Volts

B. End CO₂ Input

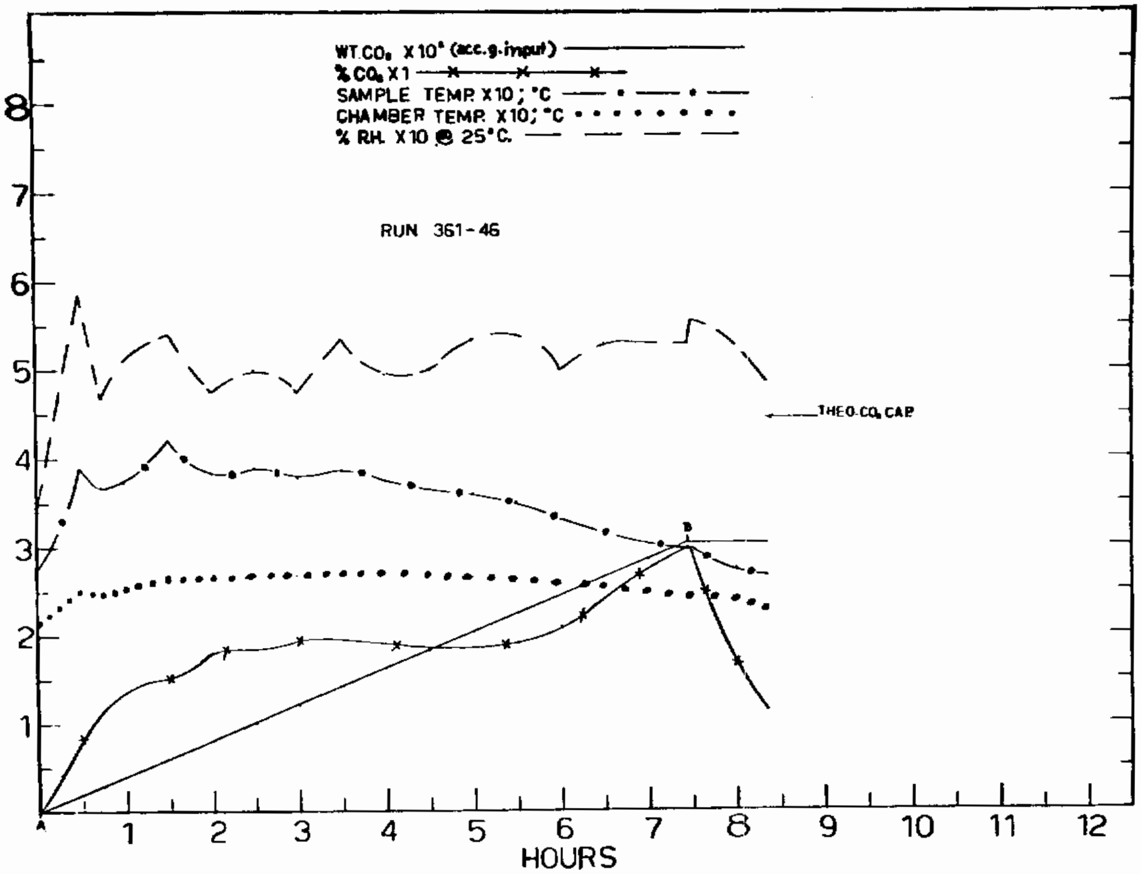

Fig. 48. Test Profiles (Run 361-46)

Notes: A. Start CO_2 Input - Fan at 50 Volts

B. End CO_2 Input

TABLE XXIII

TEST DATA, RUNS 361-43 AND 361-46

GRANULE BELT, PASSIVE EXPOSURE

Configuration type		Granule Belt	
Run No.		361-43	361-46
Granule mesh size		10 by 30	10 by 30
Li_2O charge	- g	270.4	301.7
Configuration:			
Total belt length	- cm	114	140
number of pouches		30	38
width empty pouch	- cm	3.8	3.8
pouch bed height	- cm	20	13
Li_2O bulk density	- g/cc	0.14	0.24
Theo. CO_2 capacity	- g	398	445
Sample weight gain	- g	342.4	346.9
Total CO_2 feed	- g	309.5	303.0
Average CO_2 feed	- g/hr	47.6	41.0
2% breakthrough:			
Time	- hr	5.25	5.75
g CO_2 feed/g Li_2O charge		0.913	0.778
Final CO_2 concentration	- %	2.9	2.9
Total run time	- hr	6.5	7.4
Product analysis:			
	% Li_2O	0	0
	% Li_2CO_3	84.0	77.5
	% LiOH	7.0	22.0
	% $LiOH \cdot H_2O$	8.9	0.5

Note: Gas velocities with fan at 55 volts, 6.1 m/min parallel and 3.0 m/min perpendicular to belt.

TABLE XXIV

TEST DATA RUN 397-1

GRANULE BELT, PASSIVE 8-HOUR MISSION

Configuration type		Granule Belt
Granule mesh size		10 by 30
Li_2O charge	- g	540.8
Configuration:		
Total belt length(a)	- cm	140
number of pouches		38
width empty pouch	- cm	3.8
pouch bed height	- cm	20
pouch bed thickness	- cm	1.5
Li_2O bulk density	- g/cc	0.19
Theo. CO_2 capacity	- g	796
Sample weight gain	- g	634.8
Total CO_2 feed	- g	555
Average CO_2 feed rate	- g/hr	49.1
2% breakthrough:		
Time	- hr	9.0
g CO_2 feed/g Li_2O charge		0.808
Final CO_2 concentration	- %	2.85
Total run time		11.5
Product Analysis:		
	% Li_2O	0
	% Li_2CO_3	78.3
	% $LiOH$	10.9
	% $LiOH \cdot H_2O$	10.8

Notes: (a) Belt fabric multifilament polypropylene, 0.59 m^3/min ASTM air permeability.

Gas velocities 6.1 m/min parallel and 3.0 m/min perpendicular to belt.

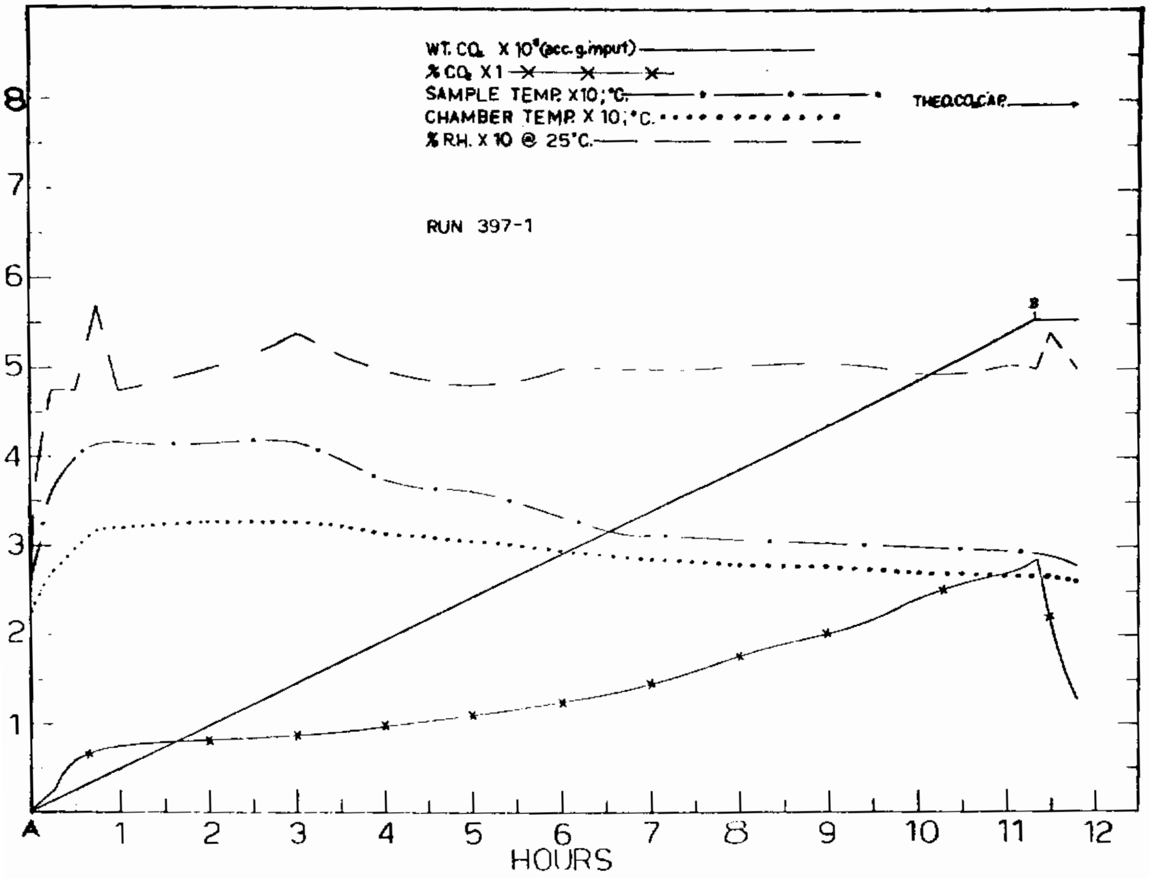

Fig. 49. Test Profiles, Passive 8-Hour Mission (Run 397-1)

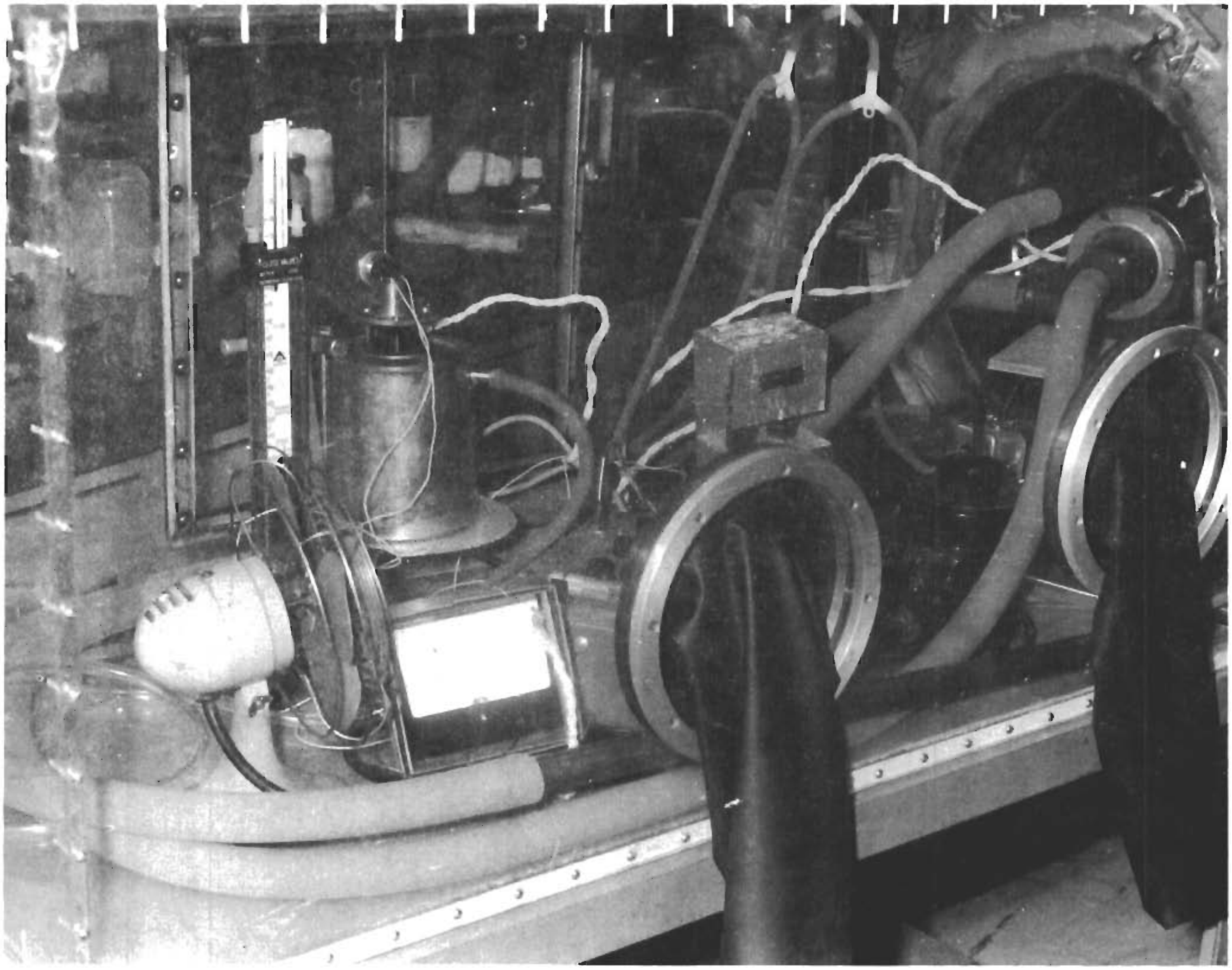

Fig. 50. Apparatus Arrangement, Dynamic Granular Bed

directed toward the suction side of the humidity control circuit so that most of the reaction heat was promptly removed. The chamber circulating fan was left on during tests. Maximum gas velocity measured in the chamber, excluding the canister blower discharge region, was 3 m/min. As shown in the low density bed profiles (Run 361-48) of figure 51, high initial canister exhaust temperature reflected ample moisture availability and rapid CO_2 absorption. Bulk density of the second bed (0.35 g/cc, Run 390-6) was clearly too high for reactivity. Bed characteristics and test data are given in table XXV. Dismantling and inspection on test completion (Run 361-48) revealed no evidence of granule sintering anywhere in the bed. The test results coupled with the findings of section III suggest that granular bulk densities up to about 0.3 g/cc are feasible at appropriate gas flow rates through the bed. The estimated conditions for maintaining 1% CO_2 concentration with 46 g/hr CO_2 feed over an 8-hour mission are 350 g of 4- by 10-mesh Li_2O at 0.25 to 0.28 g/cc bulk density. Gas volume recirculated through the bed should be at least 200 liters/min. With CO_2 partial pressure at 7.6 mm Hg, moisture partial pressure in the chamber should be 11 mm Hg minimum based on the finding that 1.44 H_2O/CO_2 molar ratio is required for efficient absorption.

Semipassive Test: Run 397-3

A granular oxide supported bed configuration consisting of concentric cylindrical beds was fabricated from 12 mesh polypropylene netting. Axial gas flow channels were provided between the beds and between the outermost bed and its aluminum

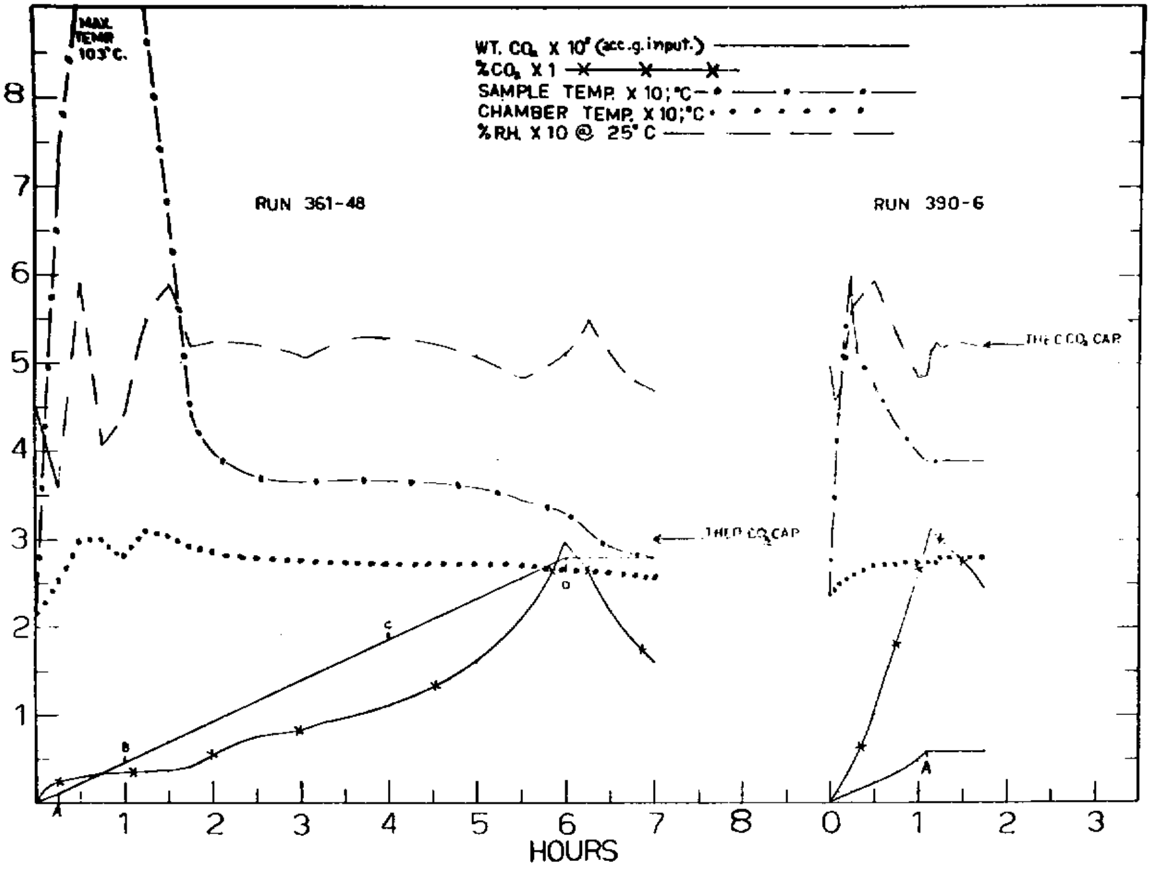

Fig. 51. Test Profiles (Runs 361-48 and 390-6)

TABLE XXV

TEST DATA, RUNS 361-48 AND 390-6

GRANULAR BED, DYNAMIC EXPOSURE

Configuration type		Granular Bed	
Run No.		361-48	390-6
Granule mesh size		4 by 10	4 by 14
Li_2O charge	- g	205	354.4
Configuration:			
bed diameter	- cm	13.4	13.4
bed depth	- cm	5.7	7.2
initial gas flow	- liters/min	190 (c)	
pressure loss(a)	- cm H_2O	0.63 (b)	1.01
Li_2O bulk density	- g/cc	0.256	0.348
Theo. CO_2 capacity	- g	302	522
Sample weight gain	- g	289.2	44.6
Total CO_2 feed	- g	280.5	50.9
Average CO_2 feed	- g/hr	46.7	46.2
2% breakthrough			
Time	- hr	5.4	0.6
g CO_2 feed/g Li_2O charge		1.227	0.115
Final CO_2 concentration	- %	2.95	2.98
Total run time	- hr	6.0	1.1
Product analysis:			
	% Li_2O	0	83.0
	% Li_2CO_3	89.6	12.4
	% LiOH	2.1	4.6
	% $LiOH \cdot H_2O$	8.3	0

Notes: (a) Initial pressure loss through Li_2O bed only, filters removed.

(b) Initial pressure loss with filters and hardware in was 1.65 cm H_2O, increasing to 2.54 cm H_2O after 4 hours.

(c) Declined to 170 liters/min as pressure loss increased.

Absorber hardware (case, blower, filters, etc.) weight 623 g case. Figures 52 and 53 show the assembly. Of necessity, the beds were filled with relatively low assay oxide (84.6% Li_2O, 10.4% LiOH, 5.0% Li_2CO_3), but this apparently was not detrimental to overall performance. Filling holes in the netting were plugged with glass wool. A few oxide granules came through the netting during handling but, as previously demonstrated, a much finer mesh is feasible. Table XXVI gives dimensions of the unit and the gas velocities imparted by a propellor fan connected by duct to one end of the case. The test setup is shown in figure 54. Gas temperature was measured at the exhaust end between the No. 2 and 3 beds. The unit contained no filters, and pressure loss through it was low, about 0.3 cm H_2O at 0.9 to 1.5 m^3/min gas flow (30 to 50 cfm) and 21.2 watts power to the fan. Table XXVII gives test data and figure 55 shows profiles. The unit, exposed to constant rate CO_2 input of 48.9 g/hr maintained 1% or less CO_2 concentration over eight hours.

5. ANALYSIS OF RESULTS

For granular Li_2O, test experience indicates a good bulk density compromise between reactivity and volume efficiency is 0.20 g/cc for passive exposure and 0.26 g/cc for semipassive or dynamic exposure. Depending on gas velocity, the density under dynamic exposure can be somewhat higher but the maximum appears to be about 0.28 g/cc. These values are initial reference points, since the optimum bulk density as related to an overall system will vary with mission length, power availability, and the relative importance of weight versus volume constraints.

A rough appraisal of passive versus dynamic configuration

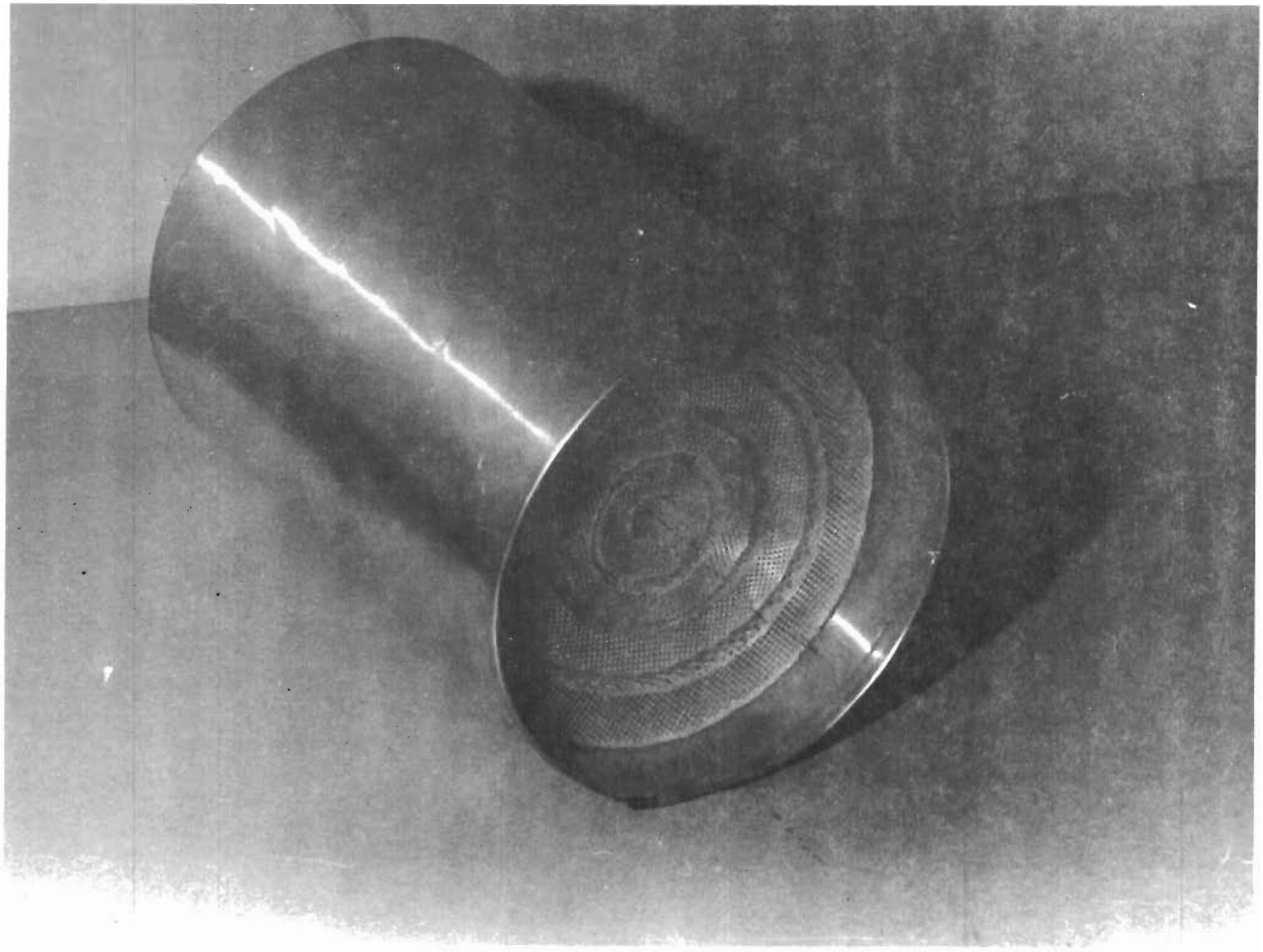

Fig. 52. Semipassive Granular Configuration

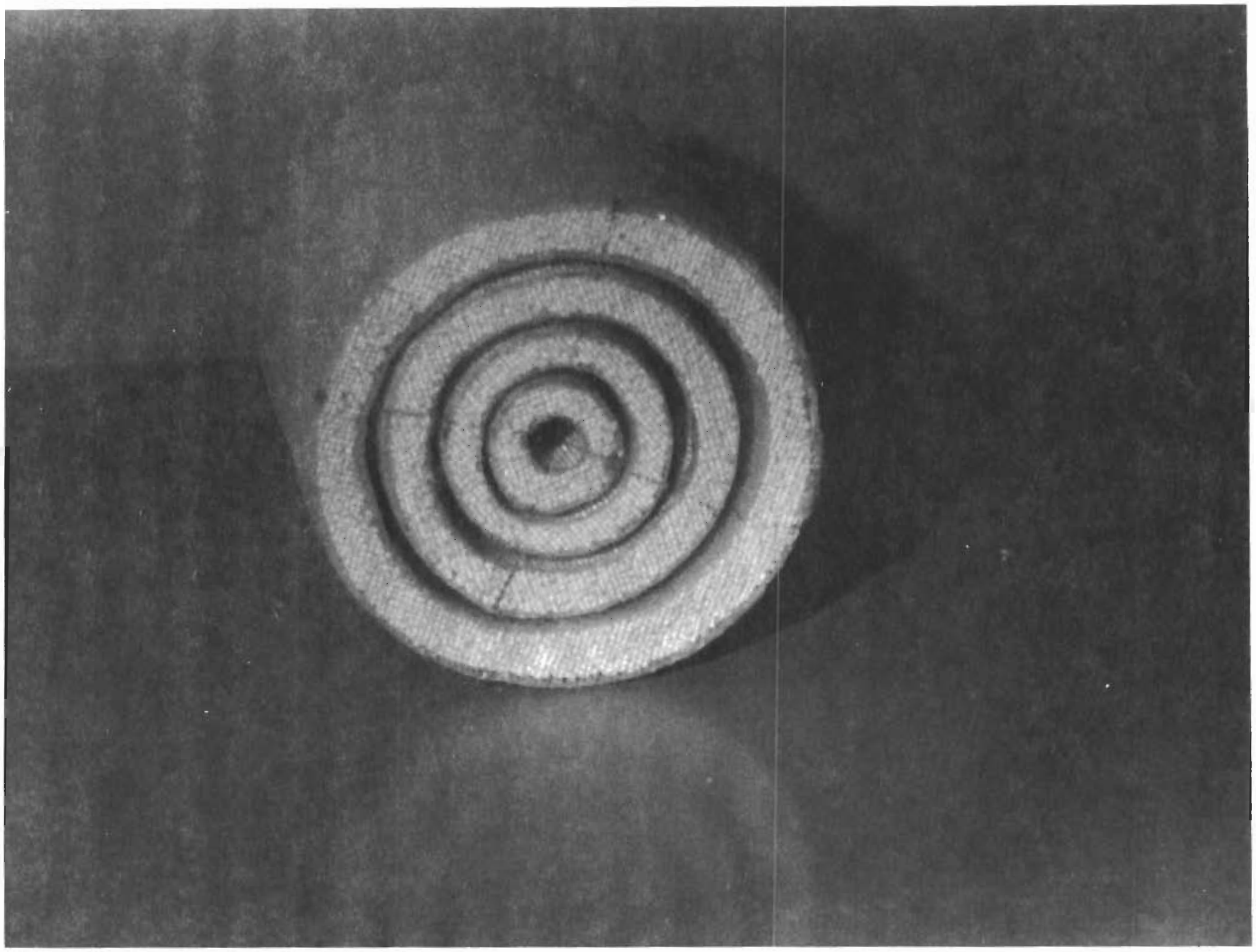

Fig. 53. Granular Li_2O Bed For Semipassive Configuration

TABLE XXVI

CONFIGURATION DIMENSIONS AND GAS VELOCITIES, RUN 397-3

Li_2O Cylinder No.	Bed Dimensions			Bed Volume cc
	Outside Diam. cm	Inside Diam. cm	Length cm	
1	4.2	2.0	20	200
2	7.4	5.4	20	400
3	11.6	9.0	20	840
4	16.6	13.5	20	1460
Case	---	17.5	30	---

		Chamber Gas Velocity Parallel To Main Flow	
Fan Power	- watts	8.3	21.2
Location (a):			
Behind Fan	- m/min	3.0	5.5
Corner No. 1	- m/min	6.1	8.8
Corner No. 2	- m/min	3.6	7.0
Position A	- m/min	10.0	13.4
Corner No. 3	- m/min	3.4	8.2
Center of Chamber	- m/min	1.5	6.1

		Gas Velocity At Li_2O Bed Exit	
Fan Power	- watts	8.3	21.2
Location (b)			
Bed centerline	- m/min	13.7	61.0
2.5 cm from center	- m/min	6.1	15.2
5.1 cm from center	- m/min	3.0	15.2
7.6 cm from center	- m/min	21.3	47.0

Notes: (a) Chamber locations as defined in figure 21.
(b) Velocity traverse across bed exit face, location measured from axial centerline of bed.

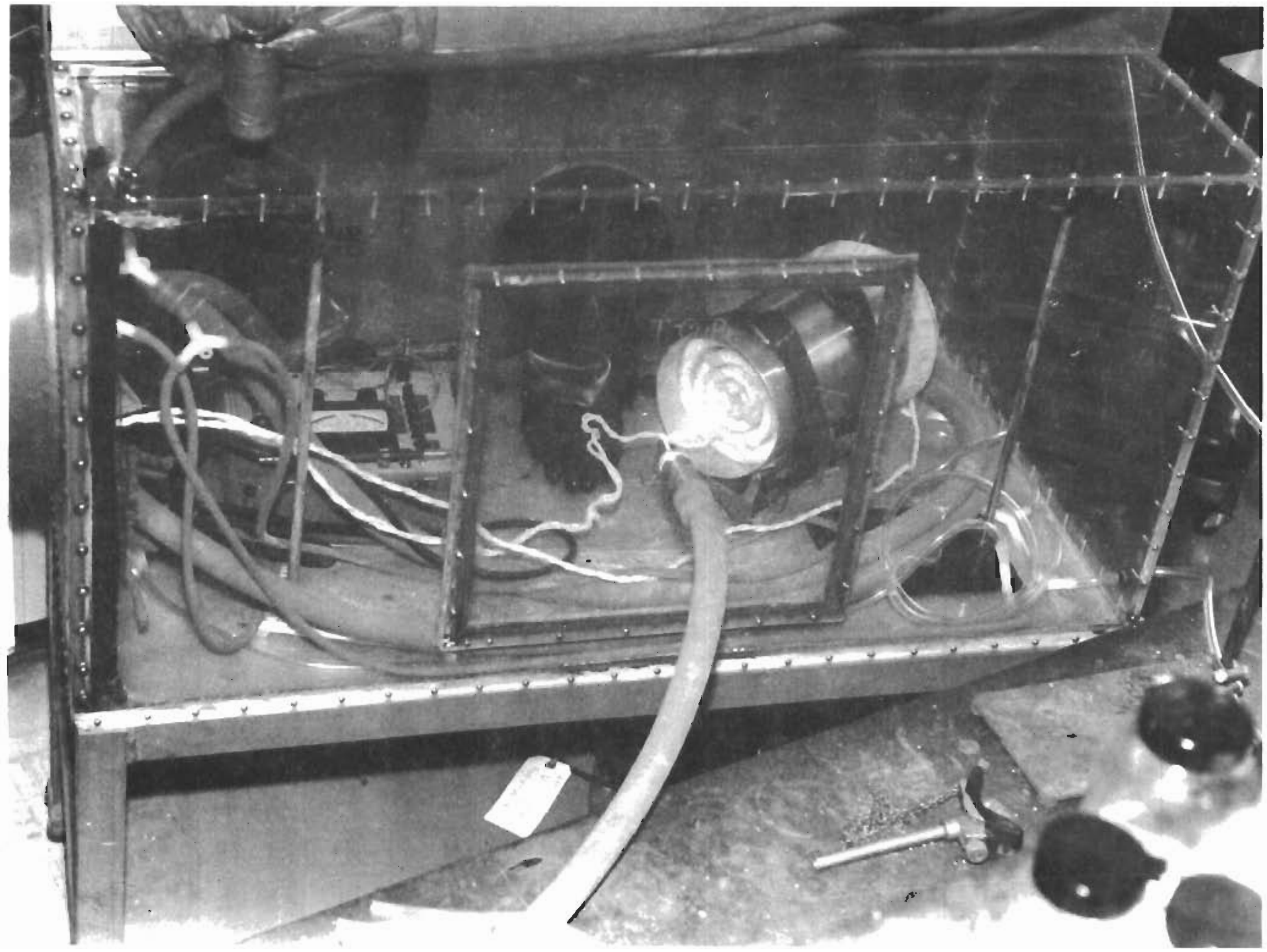

Fig. 54. Apparatus Arrangement, Semipassive Test

TABLE XXVII

TEST DATA, SEMIPASSIVE 8-HOUR MISSION,

RUN 397-3

Configuration type		Concentric Cylinders
Granule mesh size		4 by 10
Li_2O charge	- g	768.5
Li_2O bulk density	- g/cc	0.26
Configuration density	- g Li_2O/cc	0.152 (a)
Theo. CO_2 capacity	- g	1030 (b)
Sample weight gain	- g	949.4
Total CO_2 feed	- g	930
Average CO_2 feed	- g	48.9
2% breakthrough:		
Time	- hr	18.0
g CO_2 feed/g Li_2O charge		1.144 (c)
Final CO_2 concentration	- %	2.83
Total run time	- hr	19.0
Product analysis:		
	% Li_2O	0
	% Li_2CO_3	91.3
	% LiOH	4.5
	% $LiOH \cdot H_2O$	4.2

Notes: (a) Based on volume of external case
(b) Based on sample analysis 84.6% Li_2O and 10.4% LiOH
(c) Based on sample weight

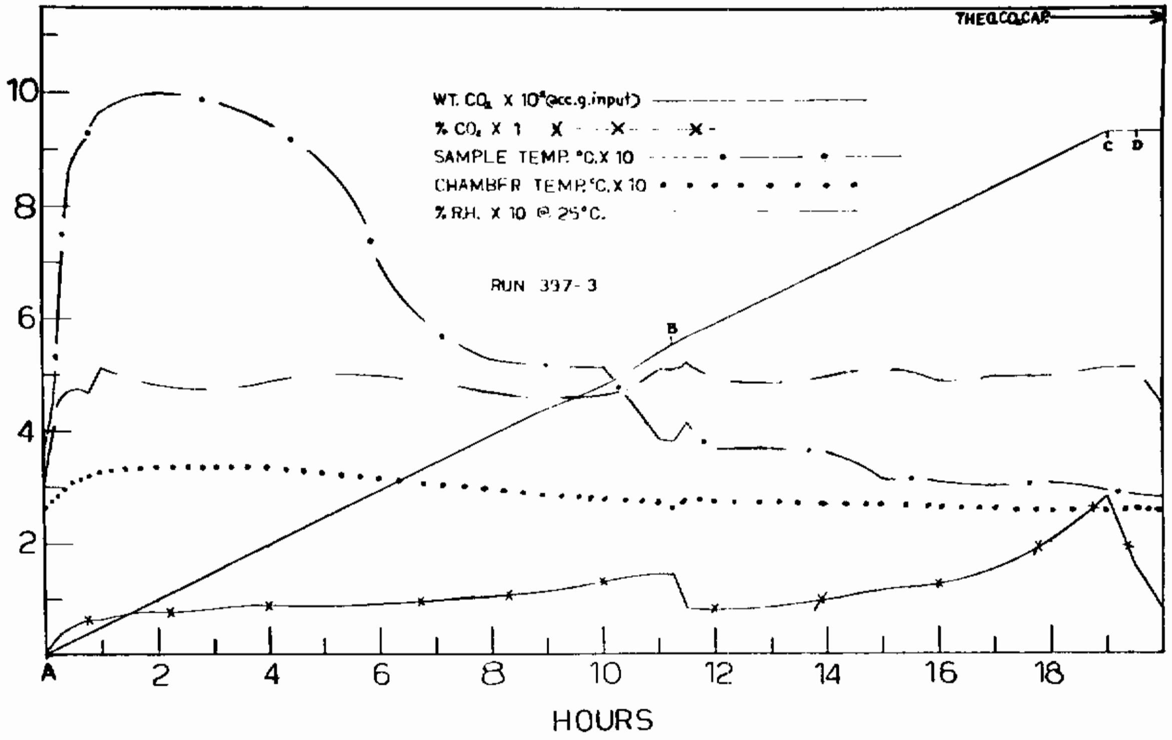

Fig. 55. Test Profiles, Semipassive 8-Hour Mission (Run 397-3)

Notes:
- A. Fan power, 8.3 watts
- B. Fan power, 21.2 watts
- C. CO_2 input off
- D. Power off

can be derived by extrapolating test results to a 9-hour run terminating at 2% CO_2 breakthrough as shown in table XXVIII. Under these conditions the estimates indicate the passive belt system is advantageous from a weight standpoint but inferior on a volume basis.

Dynamic system weight performance would improve in missions requiring larger Li_2O charges. For example the dynamic CO_2 absorption unit reported under Contract No. AF 33(615)-1588, if filled with 4- by 10-mesh Li_2O at 0.25 g/cc, would contain about 2100 g of absorbent and have a total weight of 3150 g. With about 80% utilization as indicated by Run 361-48, this Li_2O charge would remove 2500 g CO_2 yielding a weight performance of 0.79 g CO_2/g system weight. The weight performance of passive belt systems would probably improve slightly in longer missions. Although the fabric to Li_2O weight ratio would remain essentially constant for larger belts, it seems likely that oxide utilization would improve as additional area was exposed to the atmosphere.

Absorbent-grade LiOH meeting specification MIL-L-20213D has a minimum capacity of 0.75 g CO_2/g LiOH but commonly absorbs 0.8 g/g before 2% breakthrough. In comparison, the oxide forms reported herein performed as follows to 2% breakthrough--

a. 0.8 g CO_2/g Li_2O for a granular belt configuration under passive exposure (Run 397-1).

b. 1.14 g CO_2/g Li_2O for a granular bed, concentric cylinder configuration under semipassive exposure (Run 397-3), representing 42% weight improvement.

TABLE XXVIII

COMPARISON OF PASSIVE BELT AND DYNAMIC BED

Configuration type		Passive belt-pouch	Dynamic flow-through packed bed
Run No.		397-1	361-48
Granule mesh size		10 by 30	4 by 10
Li_2O bulk density	- g/cc	0.190	0.256
CO_2 feed rate	- g/hr	49.1	46.7
At 2% breakthrough:			
cumulative CO_2 feed	- g	442	252
time	- hr	9.0	5.4
Li_2O charge	- g	541	205
Comparison basis:		test data only	extrapolated test data
At 2% breakthrough, 9 hr:			
cumulative CO_2 feed	- g	442	419
Li_2O charge	- g	541	341
hardware weight	- g	226 (a)	623 (a)
system weight	- g	767	964
Li_2O bulk volume	- cc	2850	1335
System performance			
g CO_2 feed/g system weight		0.58	0.43
g CO_2 feed/cc Li_2O bulk volume		0.16	0.31

Notes: (a) Includes fabric weight for passive system; case, blower, filters and screens for dynamic system.

c. 1.23 g CO_2/g Li_2O for a granular-packed bed configuration under dynamic exposure (Run 361-48), representing 52% weight improvement.

SECTION V

TESTS AT ONE-THIRD ATMOSPHERE

1. GENERAL CONSIDERATIONS

The performance of Li_2O configurations under one-third normal pressure and in an oxygen atmosphere is of interest since these conditions are frequently selected for space capsule environments. The three basic modes of operation--passive, semipassive, and dynamic, were investigated using configurations and oxide forms judged best from tests at normal pressure. Partial pressures of the constituent gases in the test atmosphere selected were 160 mm Hg O_2, 11 mm Hg H_2O, and 7.6 mm Hg CO_2.

2. APPARATUS

A low-pressure test chamber was assembled from two bell jars and fitted with instrumentation and a 100 liters/min gas recirculation circuit as shown in figure 56. Chamber CO_2 concentration was determined by measuring per cent transmission through a gas cell with sodium chloride windows at 4.2 microns wave length. Transmission was calibrated with 0, 0.5, 1.0, and 4.0% CO_2 in oxygen (corrected to 760 mm Hg pressure) using a spectrophotometer (Perkin-Elmer Infracard Model 137B, Perkin-Elmer Corp., Norwalk, Conn.). Traps were located just upstream of the vacuum pump to absorb CO_2 and H_2O lost during any pressure adjustments. The chamber and piping were evacuated and purged with dry oxygen for 15 minutes before starting each test.

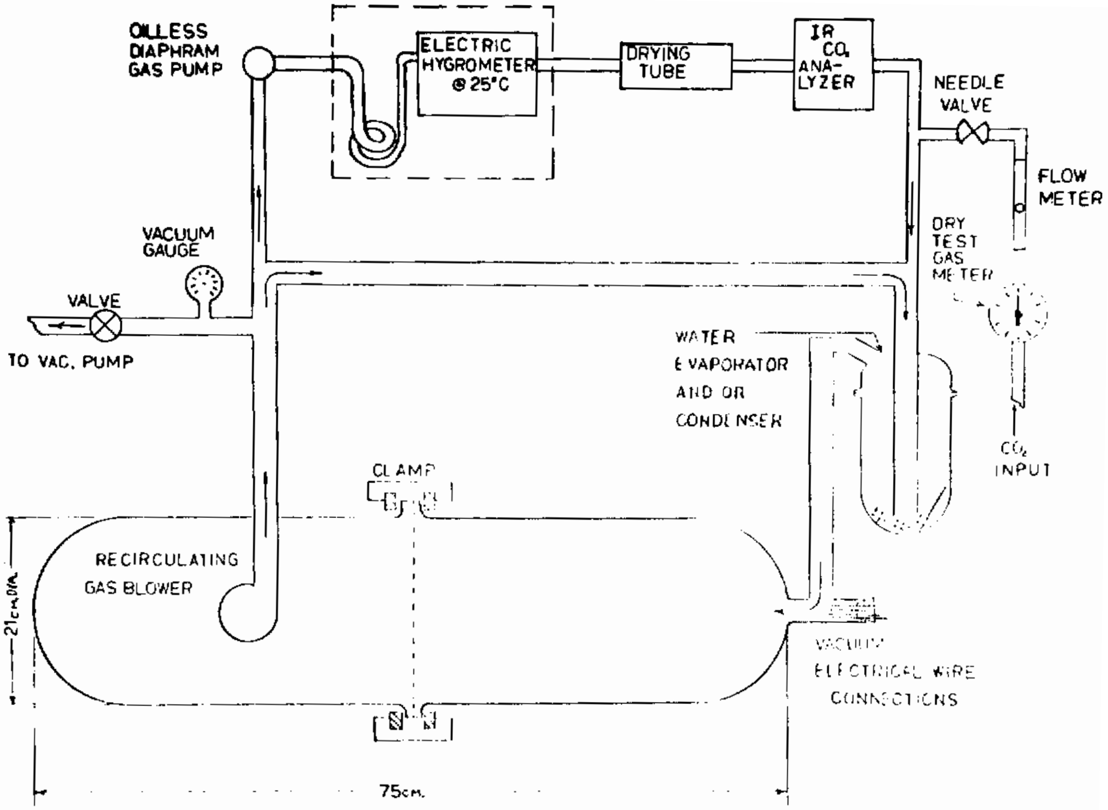

Fig. 56. Apparatus Arrangement, One-third Atmosphere Tests

3. CONFIGURATION TESTS

a. Dynamic Exposure, Packed Granular Bed
Run 397-16

The dynamic test canister (described in section III and figure 32), charged with 376 g of 4- by 10-mesh granules at 0.23 g/cc bulk density, was tested with chamber gas circulating at 190 liters/min. The run was terminated when the canister inlet screen failed because of excessive localized temperature (225 C or higher). Up to this point, feed rates indicated 76.0 g CO_2 and 39.4 g H_2O had been absorbed, corresponding to 1.26 H_2O/CO_2 molar ratio. Test data were as follows:

Time hrs:min	Effluent gas temp C	% R.H. at 25 C	Cumulative CO_2 Input g	Chamber Pressure mm Hg	Chamber CO_2 %
0:30	56	10	23.5	159	0.12
0:45	60	26	36.2	174	0.30
1:00	67	4	48.0	174	0.03
1:15	89	50	60.6	189	0.45
1:30	130	43	76.0	191	0.55

Inspection of the bed indicated the CO_2 concentration increase logged at 1.25 hr resulted from sintering and gas channeling. Samples drawn from sintered regions of the bed had the following analysis:

Sample Appearance	% Li_2CO_3	% Li_2O	% LiOH
Fused solid	46.7	41.6	11.7
sintered granules	31.7	29.8	38.9
unsintered granules	17.9	63.7	18.4

The apparatus arrangement, in which the canister inlet directly faced the test chamber gas inlet, apparently caused the difficulty. Feed gas containing CO_2 and moisture (100% R.H., in an attempt to increase low humidity in the chamber) had little chance to mix with the chamber gas. The resulting high CO_2 concentration stream directed at the bed face caused localized overheating. Time limitations precluded a test re-run.

b. Passive Exposure, Granular Belt
Run 390-46

A tight-weave fabric belt configuration was tested. Because of test chamber space limitations the belt was simply laid along the jar wall length and being flexible, conformed to its curvature. Although only half its area was thus directly exposed to the gas stream, performance was apparently unaffected. Test data are given in table XXIX and profiles in figure 57. One notable difference from the passive belt exposure at one atmosphere (as reported in section IV, figure 49) was higher fabric temperature. Reaction zone movement along the belt, starting from the chamber gas inlet end, could be observed by a progressive yellowing of the belt. Generally, chamber CO_2 concentration ran lower than in the one atmosphere test. Lower resistance to CO_2 diffusion within the granule pores because of fewer inert molecules in the carrier gas may have been a significant factor. Absorption was initially poor as atmosphere humidity could not be maintained in the relatively small chamber because of moisture removal by the oxide. CO_2 feed was

TABLE XXIX

TEST DATA, RUNS 390-46 AND 397-19

GRANULE BELT, PASSIVE EXPOSURE
PIERCED CYLINDER, SEMIPASSIVE EXPOSURE

Configuration type		Granule Belt(a)	Pierced Cylinder(b)
Run No.		390-46	397-19
Granule mesh size		10 by 30	---
Li_2O charge	- g	414.6	594.6
Configuration:			
total belt length	- cm	78	---
number of pouches		26	---
width empty pouch	- cm	3.3	---
pouch bed height	- cm	20	---
diameter	- cm	---	13.4
length	- cm	---	14.0
fabric or canister weight	- g	226	246
Li_2O bulk density	- g/cc	0.19	0.30
Theo. CO_2 capacity	- g	611	875
Sample weight gain	- g	531.3	475
Total CO_2 feed	- g	511	439
Average CO_2 feed rate	- g/hr	44	48
2% breakthrough:			
time	- hr	---	8.2
g CO_2 feed/g Li_2O charge		1.22	0.664
Final CO_2 concentration	- %	1.45	2.42
Product analysis:			
	% Li_2O	0	18.4
	% Li_2CO_3	88.8	67.4
	% LiOH	8.4	14.1
	% $LiOH \cdot H_2O$	2.7	0

Notes: (a) Fabric, multifilament polypropylene No. 6720600
(b) 44 axial holes, each 0.6 cm diameter, 1.2 cm minimum center to center.

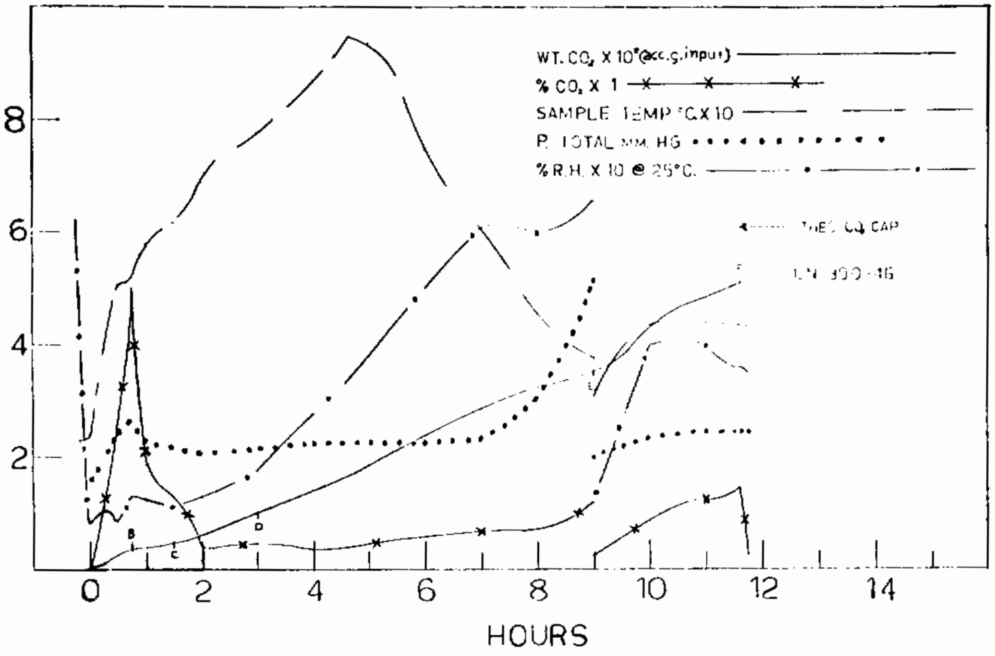

Fig. 57. Test Profiles, Passive 8-Hour Mission At One-third Atmosphere (Run 390-46)

Notes: A. Start CO_2 input
B. CO_2 input rate reduced
C&D. CO_2 input rate increased - 100% R.H. input
E. Leak corrected, no CO_2 lost from system
F. CO_2 input off.

increased as humidity recovered and, as shown in the profile, good absorption was realized during the balance of the run.

c. Semipassive Exposure, Pierced Cylinder Run 397-19

Two pierced-cylinder configurations were prepared using techniques previously described, and the one appearing structurally superior was tested. To avoid the risk of breaking the piece while stripping it from the mold, the outer cylindrical case was left in place. The axial holes were smooth and without visible cracks or dust. Chamber gas was passed through the unit at 311.5 liters/min, entering at the face marked "1" in the cross-section diagram of figure 58. The exhaust end faced the test chamber gas inlet port. Pressure drop across the shape was 0.25 cm H_2O. Test data and profiles are given in table XXIX and figure 59. Inspection revealed no evidence of sintering in any portion of the bed. Chemical analyses of samples drawn from various regions of the bed as located in figure 58 are given below. These indicate excellent conversion of the oxide at the surface of the axial holes and in between them.

Composite Sample Location	Li_2CO_3 %	Li_2O %	LiOH %	$LiOH \cdot H_2O$ %
(1) bed inlet face	95.8	0	1.6	2.6
(2) between axial holes	89.9	0.7	9.4	0
(3) walls of axial holes	96.6	0	1.4	1.9
(4) near case wall	19.4	53.5	27.1	0
(5) bed exhaust face	92.2	1.4	6.4	0

Because of the axial hole placement and the metal case almost half of the oxide was inaccessible to the gas. About 22

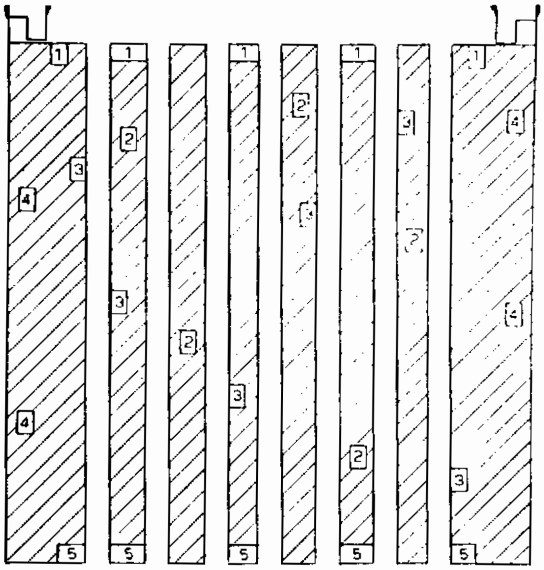

Fig. 58. Cross-section of Pierced Cylinder Configuration

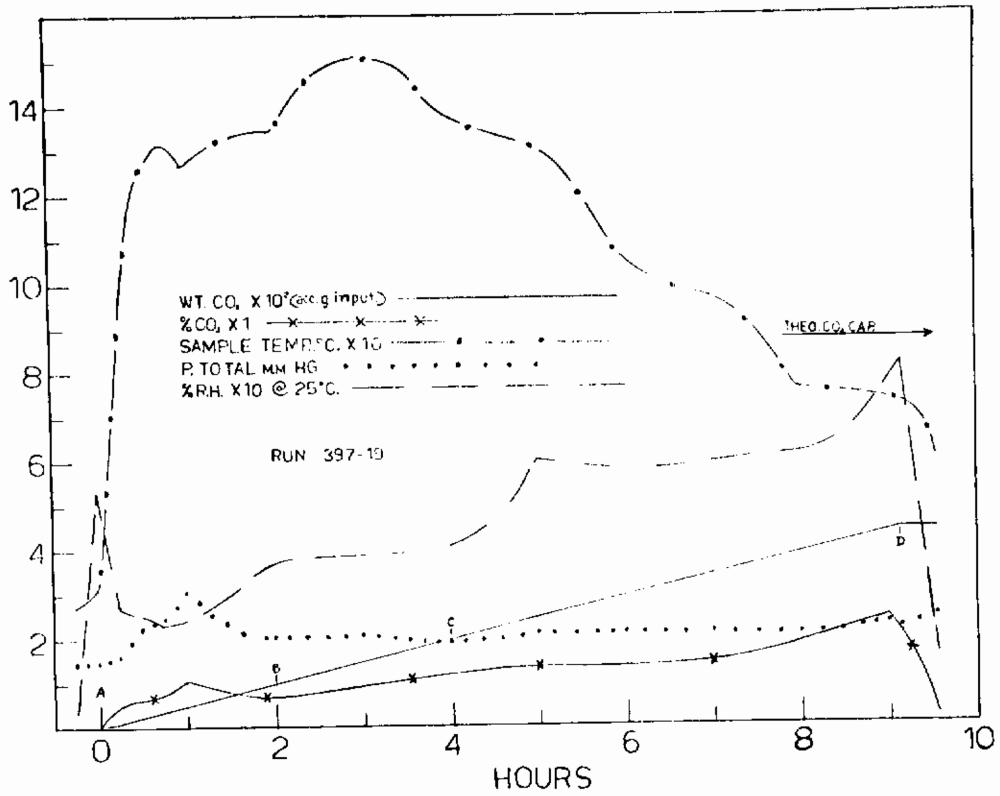

Fig. 59. Test Profiles, Semipassive 8-Hour Mission At One-third Atmosphere (Run 397-19)

Notes:
- A. Start CO_2 input
- B. Input recirculating gas at 100% R.H.
- C. Input recirculating gas below 100% R.H.
- D. End CO_2 input

more holes, which could easily be located in the outer ring of oxide, would reduce the configuration density (g Li_2O/cc total cylinder volume) to 0.28 but would also increase utilization to above 90%.

4. ANALYSIS OF RESULTS

The tests indicate lithium oxide based absorption systems are applicable under one-third atmosphere conditions. The passive belt configuration absorbed CO_2 at an average rate of 44 g/hr, and following an initial humidity problem, maintained chamber CO_2 concentration below 1% (7.6 mm Hg) for about 6 hours. Oxide conversion to carbonate was almost 90%. The semipassive, pierced-cylinder configuration averaged 48 g/hr CO_2 absorption, and its conversion can be readily increased by providing additional flow channels. This porous, solid configuration appears to have excellent potential. In future work, structural strength might be further improved by providing a matrix of inert fiberous material in the Li_2O_2 before decomposing. Testing of the dynamic-packed bed configuration was prematurely terminated, but the initial data indicate high CO_2 absorption rate. The sintering resulting from a high concentration CO_2-H_2O stream indicates design of the gas intake and its location relative to the CO_2 source are important. Bed intake area should be large so the reaction and corresponding heat are not localized. In general, operating at one-third atmosphere versus normal pressure resulted in lower chamber CO_2 concentration and higher temperatures.

SECTION VI

EFFECT OF ATMOSPHERE COMPOSITION

1. GENERAL CONSIDERATIONS

Excluding CO_2 and moisture, closed environmental systems may be based on three types of atmospheres: O_2, O_2-N_2, and O_2-He. An oxygen partial pressure close to 160 mm Hg is a requirement of any system (reference 10). The effect of these atmosphere variations on CO_2 absorption is of interest. This was investigated by the gravimetric analysis technique, using small samples of granular Li_2O passively exposed to the various gas compositions at 50% relative humidity. The effect of humidity variations in the O_2 and O_2-N_2 systems was also studied. Since moisture is a prime factor during initial absorption, the merit of partially hydrating the oxide before exposure was explored.

2. APPARATUS

Three-gram samples of 10- by 30-mesh Li_2O, contained in a 1.2 cm diameter by 16 cm high basket of 100-mesh (43.5% open area), stainless steel screen, were suspended in the gravimetric apparatus (described in section I and figure 2). The sample depth was about 9.8 cm and gas flow was 2.8 liter/min equivalent to 520 cm/min velocity based on the chamber cross-section. Premixed gas cylinders: 1% CO_2 - 99% O_2; 1% CO_2 - 21% O_2-78% He; and 1% CO_2 - 21% O_2-78% N_2 were purchased from the Mathieson Company. Humidity was controlled by a series of sulfuric acid (H_2SO_4) solutions with their densities checked before and after the runs.

3. EXPERIMENTAL DATA

Table XXX gives data and reaction product analyses for three series of tests:

(1) Li_2O exposed to O_2, O_2-N_2, and O_2-He atmospheres at 50% relative humidity. The corresponding gravimetric curves are shown in figure 60.

(2) Li_2O exposed to O_2 and O_2-N_2 atmospheres at 25, 50, and 75% R.H. Figure 61 shows gravimetric curves.

(3) Partially hydrated Li_2O exposed to O_2, O_2-N_2, and O_2-He atmospheres. Gravimetric curves are shown in figure 62.

4. ANALYSIS OF RESULTS

With 1% CO_2 concentration (1% = 7.6 mm Hg) the effect of atmospheric moisture on CO_2 absorption rate is greatest in the range 0 to 50% R.H. Since LiOH formation must preceed CO_2 removal, the H_2O/CO_2 molar ratio must exceed unity for reasonable CO_2 absorption rate during initial absorption. This ratio at 22 C, 25% R.H. is only 0.65, too low for efficient absorption. Runs 2a and 2b (table XXX) reflect this water deficiency, showing poor utilization and residual Li_2O after 8 hours exposure. With higher humidity and a molar ratio exceeding unity (22 C, 50% R.H., 1.32 moles H_2O/mole CO_2), the CO_2 absorption rate nearly doubles as in Runs 2c and 2d. At 75% R.H. the additional moisture merely increases $LiOH{\cdot}H_2O$ content as illustrated by Runs 2e and 2f.

Results on the effect of gas composition, O_2 versus O_2-N_2 atmospheres, show some inconsistencies. However, the bulk of

TABLE XXX

ABSORPTION TESTS IN VARIOUS ATMOSPHERES

Run No. (a)	Gas Comp.	Rel. Hum. %	Run Time Hr	Absorbed Gases Millimoles		Mole Ratio H_2O/CO_2	Li_2O Used %	Reaction Product Analysis			
				H_2O	CO_2			Li_2O %	Li_2CO_3 %	LiOH %	$LiOH \cdot H_2O$ %
1-	---	---	---	---	---	---	---	91.0	2.1	6.8	0
1a	O_2	50	3.7	46	33	1.39	34.2	6.6	47.7	45.7	0
1b	O_2+N_2	50	3.7	60	16	3.75	16.6	9.8	26.2	64.0	0
1c	O_2	50	8	41	65	0.63	67.4	0	73.1	18.2	8.7
1d	O_2+He	50	8	79	48	1.65	49.8	0	55.1	22.4	22.1
1e	O_2+N_2	50	8	82	30	2.73	31.2	0	39.5	46.5	14.1
2-	---	---	---	---	---	---	---	94.7	3.3	2.0	0
2a	O_2	25	8	42.6	33.0	1.29	33.9	11.9	48.2	39.9	0
2b	O_2+N_2	25	8	43.0	41.6	1.034	42.7	6.37	56.14	37.49	0
2c	O_2	50	8	46.6	65.0	0.72	66.8	0	72.4	18.8	8.8
2d	O_2+N_2	50	8	45.6	64.6	0.70	66.4	0	72.8	18.1	9.0
2e	O_2	75	8	57.8	69.4	0.83	71.3	0	73.66	7.32	19.02
2f	O_2+N_2	75	8	71.3	63.4	1.12	65.1	0	67.58	9.08	23.33
3-	---	---	---	---	---	---	---	58.0	3.6	38.4	0
3a	O_2	25	8	15.5	42.2	0.36	51.2	0.6	62.6	36.8	0
3b	O_2	25	22.7	13.6	60.7	0.22	73.6	0	77.5	11.5	11.1
3c	O_2+N_2	25	8	15.5	40.6	0.38	49.2	1.6	61.1	37.3	0
3d	O_2+He	25	8	2.5	60.8	0.04	73.7	0	80.2	16.4	3.4
3e	O_2+N_2	75	8	43.1	50.6	0.85	61.4	0	64.0	11.6	24.5
3f	O_2+He	75	8	5.6	77.5	0.07	93.9	0	89.6	0	6.1

Notes: (a) 0.22 g/cc Li_2O bulk density for Run Nos. 1
0.21 g/cc Li_2O bulk density for Run Nos. 2
0.25 g/cc Li_2O bulk density for Run Nos. 3

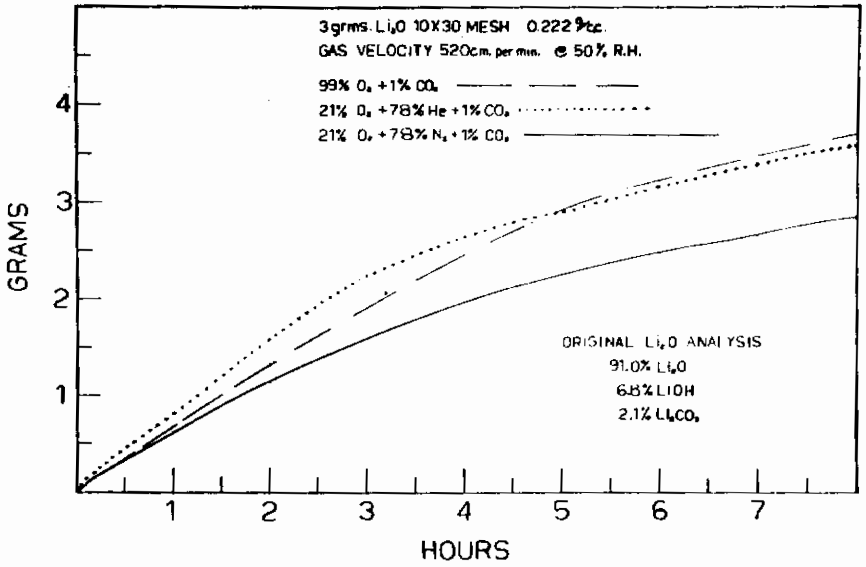

Fig. 60. Gravimetric Curves For O_2, O_2-N_2, and O_2-He Atmospheres At 50% Relative Humidity.

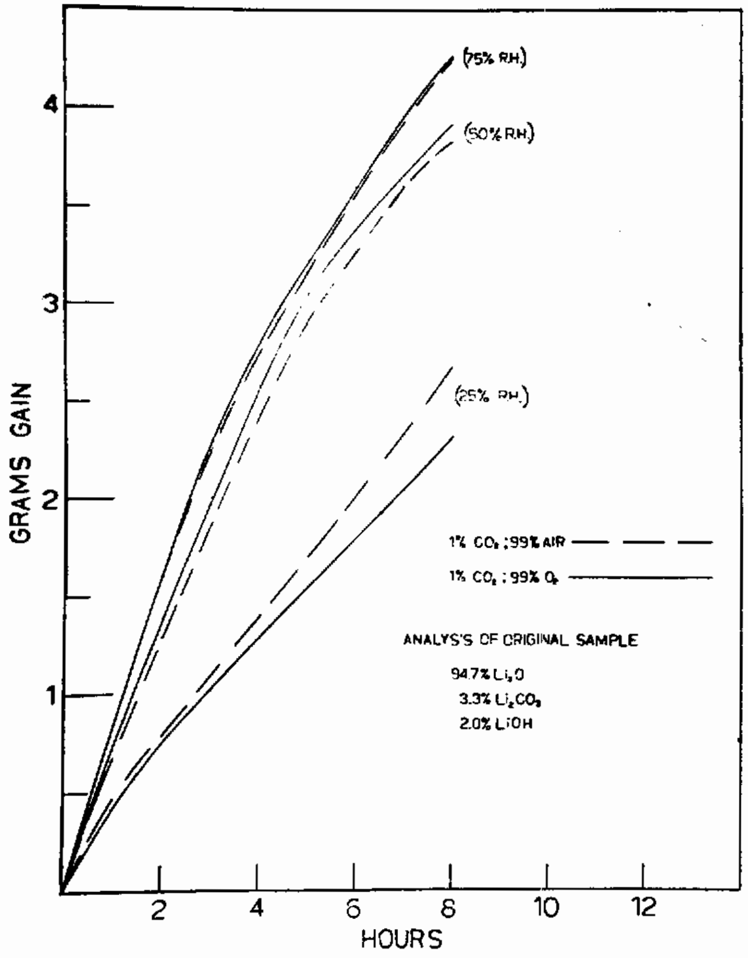

Fig. 61. Gravimetric Curves For O_2 and O_2-N_2 Atmospheres At 25, 50, and 75% Relative Humidity

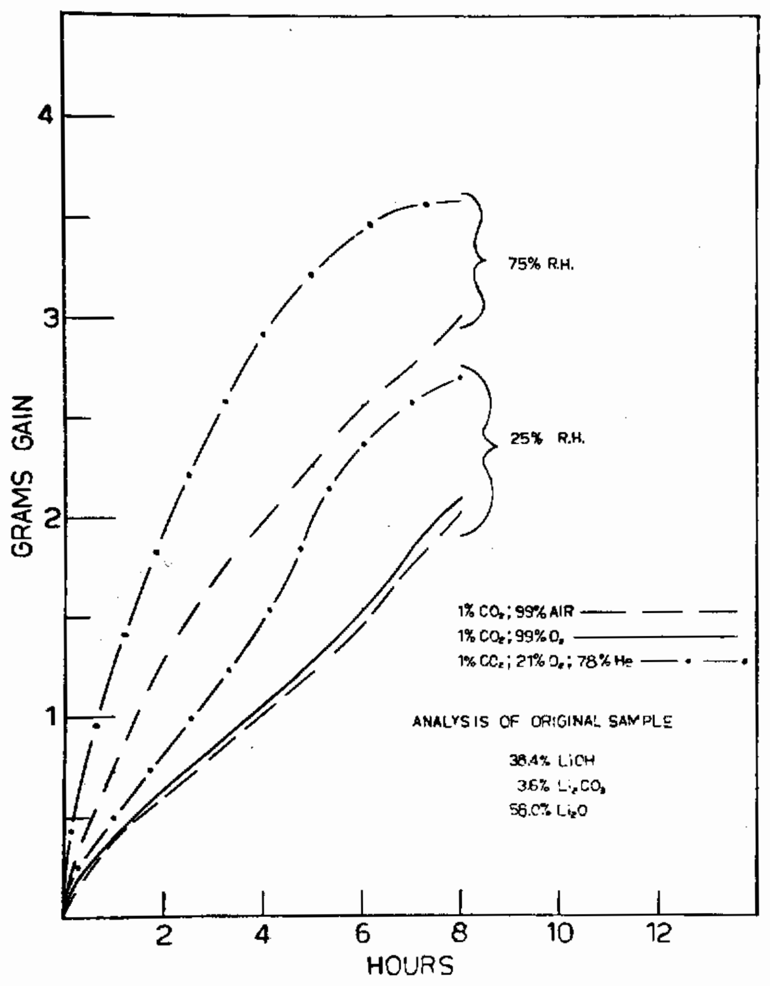

Fig. 62. Gravimetric Curves For Partially Hydrated Li_2O

the data, the Run 2 series, wherein these atmospheres were studied over a wide humidity range, indicate absorbent performance is above the same in either atmosphere. The gravimetric curves at various humidities are shown in figure 61. Helium had a significant effect on the absorption process. The higher diffusion rates occurring in O_2-He versus O_2 and O_2-N_2 atmospheres are best illustrated in figure 62. The small size and high velocity of the He molecule improves diffusion of the CO_2 and moisture.

Exploratory results indicate that partial hydration of Li_2O has merit. This step pre-supplies moisture in the form of LiOH, thereby improving CO_2 absorption under low humidity conditions. Comparison of Runs 2a and 3a (O_2 atmospheres) and Runs 2b and 3c (O_2-N_2 atmospheres) illustrates improved oxide utilization under 25% relative humidity. With partially hydrated absorbent, the H_2O/CO_2 molar ratio of the gas does not have to exceed unity.

SECTION VII

CONCLUSIONS

1. LITHIUM OXIDE PREPARATION AND PERFORMANCE

The bulk density of various forms of Li_2O has been substantially increased while retaining good reactivity. Absorbent Li_2O shapes and granular forms can be prepared with bulk densities ranging between 0.18 and 0.28 g/cc. At the present state of knowledge, reactivity declines sharply at bulk densities exceeding about 0.30 g/cc. The granular oxide can meet standard hardness specifications for granular LiOH, currently a widely used absorbent. Key factors in preparing the improved density oxide are high-surface lithium peroxide (about 18 m^2/g Li_2O_2), decomposition temperature, and techniques in processing the Li_2O_2 to Li_2O.

Granular LiOH, currently the best chemical absorbent available, will typically remove 0.8 g CO_2/g LiOH before the 2% breakthrough point. In the reported work the corresponding performance attained with various forms of Li_2O was as follows:

a. 0.8 g CO_2/g Li_2O for a granule belt configuration passively exposed (Run 397-1).

b. 1.14 g CO_2/g Li_2O for a granule bed concentric cylinder absorber under semipassive exposure (Run 397-3).

c. 1.23 g CO_2/g Li_2O for a granular-packed bed under dynamic exposure (Run 361-48).

A variety of processes were studied for producing the oxide in supported and self-supported forms. For supported beds, the best process involved pelletizing high surface area Li_2O_2 powder, thermally decomposing, and crushing and sieving the resulting Li_2O cake. This technique yielded granular Li_2O with improved bulk density while maintaining good reactivity. The swelling and sintering properties of Li_2O_2 on decomposition can be used for preparing self-supported shapes. Testing indicates that good absorption can be realized with such shapes but higher strength would be desirable. The conflicting requirements of high density for strength and low density for reactivity suggest that pursuit of mechanical compaction techniques will not be fruitful. Further development should probably be aimed at using some reinforcing technique such as a matrix of inert fibrous material.

Two techniques were developed for reducing the potential dusting of granular Li_2O. Controlled abrasion in a rotary gas flushed dedusting apparatus largely removed adherent dust and dust producing granule edges. This treatment also improved bulk density. The fabric encasement of granular Li_2O displays also appears promising. Contrary to expectation, a high percentage of open area in the fabric proved unnecessary. Good diffusion and absorption was obtained with a relatively tight fabric which can also serve as a dust filter. Development efforts on directly coating the Li_2O granules were unsuccessful.

2. EFFECT OF ATMOSPHERE VARIATIONS

Tests at one-third normal atmospheric pressure revealed that absorption rates were improved at reduced pressure. A study of atmosphere composition indicated no significant difference in absorption rate in O_2 and O_2-N_2 atmospheres. A marked improvement in CO_2 and H_2O diffusion rates was found in O_2-He atmospheres.

Atmospheric moisture, in terms of adequate H_2O/CO_2 molar ratio, is required during initial CO_2 absorption. With 7.6 mm Hg CO_2 partial pressure, the 0 to 50% relative humidity range is the most critical. The corresponding minimum water vapor pressures required for efficient absorption are about 11 mm Hg for a dynamic granular bed and 15 mm Hg for a passive granular display. In general, the H_2O/CO_2 molar ratio of the environmental chamber input to granular Li_2O configurations should be about 1.44 for dynamic systems and 2.0 for passive systems. The ratio for human exhalation is about 2.4. Exploratory work indicates that partial hydration of the Li_2O has merit. This step pre-supplies moisture in the form of LiOH thereby improving CO_2 absorption under low humidity conditions.

3. CONFIGURATION DESIGN

Gravimetric analysis work has confirmed the importance of the molar volume relations between reaction product and substrate. Density limitations can be estimated from these relations thereby providing guidelines for absorbent design and further experimentation. For granular Li_2O, experience indicates that a good bulk density compromise between reactivity and volume efficiency is about 0.20 g/cc under passive exposure and 0.26 to 0.28 g/cc under semipassive or dynamic exposure.

Various Li_2O forms were developed, capable of absorbing 46 g CO_2/hr under passive, semipassive, or dynamic conditions. For reporting purposes, the following definitions have been adopted for these exposure modes--

Passive - Gas velocity past or through the absorbent configuration is essentially the same as the gas velocity within the chamber itself and is relatively low. There is no pressure loss across the configuration. Any power required for this nominal gas circulation is chargeable to other systems, such as humidity or temperature control.

Semipassive - The configuration requires a positive gas flow, causes a measurable pressure loss, and does impose a power penalty. The major gas flow is through channel voids in the configuration and its direction is essentially parallel to the exposed absorbent surfaces.

Dynamic - The configuration requires a positive gas flow, causes a pressure loss, and imposes a power penalty. The major gas flow is through bulk voids with gas flow through multiple circuitous paths.

Factors to be considered in selecting the best exposure mode for a given mission length include-- ambient atmosphere (composition and humidity), weight and volume penalties assessed for power consumption, and the relative importance of weight versus volume. These factors are not yet firmly defined. However, the reported results suggest that passive exposure could be employed in missions up to about 12 hours duration. Beyond this point semipassive or dynamic exposure would appear preferable because of higher volume efficiency. General guidelines for designing Li_2O based systems for the various exposure modes can be summarized as follows:

a. Passive Exposure

The absorbent requirement is estimated to be 50 to 60 g of 10- by 30-mesh granular Li_2O per manhour. However, this value is greatly dependent on chamber pressure. For example only 38 g Li_2O/hr was required to absorb 44 g CO_2/hr in a one-third atmosphere test. A tight-weave, multifilament fiberglass fabric envelope should provide adequate CO_2 and moisture diffusion while retaining even fine particles (10 microns) Li_2O dust.

b. Semipassive Exposure

Tests with pierced cylinders indicate that a configuration density (i.e., - g Li_2O/cc total volume including channel voids) of about 0.28 g/cc is suitable. The oxide shape should preferably be formed by decomposing granular Li_2O_2 as described in section IV-3. A pressure loss of 0.3 cm H_2O, or less, at 1.5 m^3/min is feasible.

c. Dynamic Exposure

The best choice is considered 4- by 10-mesh granular Li_2O at about 0.28 g/cc bulk density. The absorbent requirement is estimated to be 38 g Li_2O per manhour. A pressure loss of 0.6 cm H_2O, or less, at 0.2 m^3/min gas flow is feasible.

In configuration design, the increased heat evolution of Li_2O based systems, as noted below, should be recognized. The bed should not be directly exposed to the CO_2 and H_2O concentrations of human exhalation, since excessive temperature and absorbent sintering can result. The problem can be eliminated by diluting the gas to 1% CO_2 and 50% R.H. before processing.

$$2\ Li_2O + CO_2(g) + H_2O(g) \rightarrow Li_2CO_3 + 2\ LiOH$$

H^{25}; - 86.8 Kcal/mole CO_2 absorbed

$$2\ LiOH + CO_2(g) \rightarrow Li_2CO_3 + H_2O(g)$$

H^{25}; - 20.4 Kcal/mole CO_2 absorbed

REFERENCES

1. Markowitz, M. M., Dezmelyk, E. W., A Study of the Application of Lithium Chemicals to Air Regeneration Techniques in Manned Sealed Environments, Technical Documentary Report AMRL-TDR-64-1, Aerospace Medical Research Laboratories, Wright-Patterson Air Force Base, Ohio, February 1964.

2. Bach, R. O., Boardman, W. W., Jr., Robinson, J. W., Jr., Application of Lithium Chemicals for Air Regeneration of Manned Spacecraft, Technical Documentary Report TR-65-106, Aerospace Medical Research Laboratories, Wright-Patterson Air Force Base, Ohio, June 1965.

3. Boryta, D. A. and Markowitz, M. M., Lithium Oxide as a Carbon Dioxide Absorbent, Unpublished Research Report, Foote Mineral Company, Exton, Pa., August 1964.

4. Pilling, N. B. and Bedworth, R. E., "The Oxidation of Metals at High Temperatures," J. Inst. Metals 29, 577(1923).

5. Cohen, A. J., "Lithium Hydroperoxide 1 Hydrate, Lithium Peroxide, and Lithium Oxide," Inorganic Synthesis, Vol. V, T. Moeller, editor, McGraw-Hill Book Company, New York, pp. 1-6, 1957.

6. Markowitz, M. M., Boryta, D. A., "A Convenient System of Thermogravimetric Analysis and of Differential Thermal Analysis," Anal. Chem., 32, 1588(1960).

7. Gregory, N. W., Mohr, R. H., "The Equilibrium 2LiOH(g) = Li_2O(g) + H_2O (g)," J.A.C.S. 77, 2142-4(1955).

8. Yuji Ueda, "Thermodynamic Studies of Lithium Hydroxide and Lithium Chloride," Sci. reports, Tohoku Univ. A22: 448-74 (1933).

9. Keating, D. A., Weiswurm, K., Potassium Superoxide Passive Air Regeneration Studies for Manned Sealed Environments, WADD Technical Report 60-707, Life Support Systems Laboratory Aerospace Medical Division, Wright-Patterson Air Force Base, Ohio, December 1960.

10. Keating, D. A., Design Parameters for the Engineering of Closed Respiratory Systems, WADC Technical Report 59-766, Aerospace Medical Laboratory, Wright-Patterson Air Force Base, Ohio, December 1959.

11. McGoff, M. J., Potassium Superoxide Atmosphere Control Unit, Technical Report AMRL-TR-65-44, Aerospace Medical Research Laboratories, Air Force Medical Division, Wright-Patterson Air Force Base, Ohio, September 1965.

12. Markowitz, M. M., The Absorbing Story of Lithium Hydroxide, Foote Prints 34, 9(1965).

13. Standard Methods of Chemical Analysis, N, Howell Furman, Ph.D., editor, D. Van Nostrand Company, Inc., Princeton, New Jersey, p. 298.

Security Classification

DOCUMENT CONTROL DATA - R & D

(Security classification of title, body of abstract and indexing annotation must be entered when the overall report is classified)

1. ORIGINATING ACTIVITY *(Corporate author)*

Foote Mineral Company
Research and Engineering Center
Exton, Pennsylvania 19341

2a. REPORT SECURITY CLASSIFICATION
UNCLASSIFIED

2b. GROUP
N/A

3. REPORT TITLE

CONFIGURATION INVESTIGATION FOR LITHIUM OXIDE
CARBON DIOXIDE CONTROL SYSTEMS

4. DESCRIPTIVE NOTES *(Type of report and inclusive dates)*

Final Report, December 1965-December 1966

5. AUTHOR(S) *(First name, middle initial, last name)*

Daniel A. Boryta
Eugene W. Dezmelyk

6. REPORT DATE
October 1967

7a. TOTAL NO. OF PAGES
144

7b. NO. OF REFS
13

8a. CONTRACT OR GRANT NO.
AF 33(615)-3382

b. PROJECT NO. 6373

c. Task No. 637302

d.

9a. ORIGINATOR'S REPORT NUMBER(S)

Foote Mineral Company Research
Report No. FOOTE-1266

9b. OTHER REPORT NO(S) *(Any other numbers that may be assigned this report)*

AMRL-TR-67-62

10. DISTRIBUTION STATEMENT

Distribution of this document is unlimited. It may be released to the Clearinghouse, Department of Commerce, for sale to the general public.

11. SUPPLEMENTARY NOTES

12. SPONSORING MILITARY ACTIVITY

Aerospace Medical Research Laboratories
Aerospace Medical Div., Air Force Systems
Command, Wright-Patterson AFB, Ohio 45433

13. ABSTRACT

The bulk density of lithium oxide shapes and granules has been increased substantially while retaining good reactivity. Absorbent forms of the oxide can be prepared in the bulk density range of 0.18 to 0.28 g/cc. For granular oxide, results indicate a reasonable compromise between reactivity and absorbent volume efficiency is about 0.20 g/cc in passive systems and 0.26 to 0.28 g/cc in semipassive or dynamic systems. The improvement results from use of high (about 18 m^2/g) surface area lithium peroxide raw material and techniques in processing the peroxide to oxide. Tests indicate the oxide forms developed can equal (passive exposure) or exceed (semipassive or dynamic exposur) the 0.8 g CO_2/g LiOH capacity of granular lithium hydroxide before 2% breakthrough. Dusting of the granular oxide form was reduced by controlled abrasion and fabric encasement techniques. Tests at one-third and normal atmospheres indicated higher carbon dioxide absorption rates at the lower pressure. A marked improvement was found in oxygen-helium as compared to oxygen and oxygen-nitrogen atmospheres. Atmospheric moisture conditions required for efficient absorption were defined. Exploratory work indicates partial hydration of the oxide is one method for initiating absorption under low humidity conditions. Gravimetric analysis work, which confirmed that density limitations are presently imposed by reaction product-substrate molar volume relations, should provide useful guidelines for absorbent design and further experimentation.

DD FORM 1 NOV 65 **1473**

Security Classification

Security Classification

14. KEY WORDS	LINK A		LINK B		LINK C	
	ROLE	WT	ROLE	WT	ROLE	WT
Environmental control						
Configuration investigation						
Lithium oxide						
Carbon dioxide control						
Life support						
Alkali metal oxides						
Carbon dioxide absorption						
Space vehicles						
Passive absorption						
Semipassive absorption						
Dynamic absorption						

Security Classification